# ADVANCES IN PHYSICS

## A QUARTERLY SUPPLEMENT of the PHILOSOPHICAL MAGAZINE



VOLUME 5 APRIL 1956 NUMBER 18

PRICE per part £1
PRICE per annum £3 15*s.* 0*d.* post free

PRINTED AND PUBLISHED BY TAYLOR & FRANCIS, LTD.
RED LION COURT, FLEET ST., LONDON E.C.4

# CONTENTS

ADVANCES IN PHYSICS

A QUARTERLY SUPPLEMENT
of the
PHILOSOPHICAL MAGAZINE

VOLUME 5 APRIL 1956 NUMBER 18

# *The Study of Epitaxy in Thin Surface Films*

By D. W. PASHLEY†
Physics Department, Imperial College, London, S.W.7

CONTENTS



† Now at Tube Investments Research Laboratories, Hinxton Hall, Cambridge.

## § 1. Introduction

The term epitaxy ('arrangement on') was introduced by Royer (1928) to denote the phenomenon of the oriented growth of one crystal upon another. The first examples of such growth were observed to have occurred naturally on minerals; two crystals of different species grow together with some definite and unique orientation relationship between their crystal axes. Many such cases of oriented intergrowths have been observed, and comprehensive lists of the examples have been given by Wallerant (1902) and by Mugge (1903).

Such observations led to experiments designed to bring about oriented growth in the laboratory. The first successful attempt appears to be that of Frankenheim (1836), the previous claims of Wakkernagel (1825) having been disputed. Frankenheim found that sodium nitrate grew from solution in parallel orientation on the surface of a calcite crystal, and also found that potassium iodide, bromide and chloride were oriented when crystallized from solution on to a mica cleavage surface. The first systematic experiments in which a series of related structures are grown upon each other were made by Barker (1906, 1907, 1908), who studied, amongst other things, the growth of alkali halides upon each other. Barker found that some alkali halides oriented upon each other, while others did not. It was noticed that oriented growth is more likely to occur if the molecular volumes of the two alkali halides are nearly equal. Royer (1928) repeated much of the work of Barker, and extended it to cover many other examples of growth from solution. In the meantime, the discovery of x-ray diffraction had greatly increased knowledge of the structure of crystals. On the basis of his results, Royer put forward three rules of epitaxy, the most important of which is that oriented growth occurs only when it involves the parallelism of two lattice planes which have networks of identical or quasi-identical form and of closely similar spacings. The difference between the network spacings is usually expressed in terms of the percentage misfit, which is defined as $100(b-a)/a$. $a$ and $b$ are the corresponding network spacings in the substrate and overgrowth respectively. The experiments indicated that the misfits should be no more than about 15%, this limit being most strikingly illustrated by the growth of alkali halides both upon alkali halides and upon a mica cleavage surface.

The discovery of electron diffraction at about the time when Royer carried out his experiments greatly increased the scope of studies of epitaxy. Whereas previous work had to be carried out by means of optical microscopy, with its inherent limitation on the types of layers which can be studied, the electron diffraction technique provided a means of studying very thin surface films. It was now possible to examine deposits other than those grown from solution, and to study earlier stages of growth. Although the early development was slow, it soon became apparent that epitaxy occurs with a wide variety of deposits on single crystal surfaces. Very thin chemically grown layers (Aminoff and Broome

1936, 1938, Wilman 1940), electrodeposited metal films (Cochrane 1936, Finch and Sun 1936) and metal layers condensed from the vapour phase (Bruck 1936) are all found to be oriented in some cases. One of the most striking features of the results of these new experiments is that Royer's rule concerning a good numerical fit between the substrate and the overgrowth is not always obeyed. This applied particularly to the case of metals condensed on to heated rocksalt surfaces (Bruck 1936), for which misfits as big as 38% were observed. Attempts were made to explain the occurrence of these large misfits by consideration of the formation of initial layers which are oriented with a low misfit, and upon which other orientations formed at a later stage. A mechanism of this kind, in which the occurrence of twinning played a vital role, was considered in detail by Menzer (1938 a, b, c) for the case of silver and nickel on rocksalt.

A further concept which was introduced by Finch and Quarrell (1933, 1934) as a result of electron diffraction studies is that of 'basal plane pseudomorphism'. This involves the formation of an initial oriented film which has an abnormal crystal structure. The bulk structure of the deposit material is constrained so that the lattice plane parallel to the surface is identical in size to that of substrate. Frank and van der Merwe (1949 a, b, c) followed up this concept, and developed a theory of epitaxy which involves, as a necessary condition of orientation, the formation of an initial pseudomorphic layer. This theory predicts limiting misfits of the same order of magnitude as those observed by Royer. However, certain difficulties arise concerning the stability of such layers (Smollet and Blackman 1951), and more recent experiments have failed to confirm the necessity of a small misfit (e.g. Schulz 1951 b, 1952 a). In addition, these more recent experiments have included the examination of extremely thin layers (mean thickness less than 10 Å), and this has provided much needed evidence of the structure of the initial nuclei of an oriented deposit. No support for the concept of basal plane pseudomorphism is found.

The main purpose of this article is to give an account of the electron diffraction evidence concerning the formation of an oriented overgrowth, and to consider the relation of this evidence to existing theories. This will include a discussion of the uses and limitations of electron diffraction as a technique in such studies. It has not been possible to include a detailed review of the results obtained by other methods, but such results have been included and discussed where they are directly related to the electron diffraction work. Comprehensive reviews containing most of the results obtained by optical microscopy, together with the few results obtained by other methods such as x-ray diffraction will be found elsewhere (Neuhaus 1950–51, 1952, van der Merwe 1949, Seifert 1953). Any consideration of the growth of deposits on amorphous substrates, upon which fibrous orientations are often observed has also been omitted.

## § 2. The Methods of Studying Epitaxy

### 2.1. *The Optical Microscope Method*

The optical microscope has been used almost exclusively for the study of growth from solution. The essential requirements of the method are that the crystallites of the deposit should be sufficiently big, and should have a well-defined external form so that the nature of the boundary faces can be determined. The orientation of each crystallite is then determined separately, and any preference can be established.

### 2.2. *The X-ray Diffraction Method*

The x-ray method involves a direct determination of the orientation of the overgrowth crystallites, independent of their external form. A composite diffraction pattern from a large number of crystallites is obtained, and any preferred orientation can be directly established. Various techniques are possible, but it is usually necessary to use a rotation method, so that any orientation of the overgrowth will give rise to observable patterns. Almost any type of layer can be examined in this way, provided that it has sufficient thickness.

### 2.3. *The Electron Diffraction Method*

A great deal of work has been carried out during the last twenty-five years on the application of electron diffraction to the study of epitaxy. Most of the comments in this paper refer to the use of fast electrons (30 to 100 kev), most of the work having been carried out in this energy range.

The most common and more generally useful method is the reflection method, in which the overgrowth is examined *in situ* on the substrate. The transmission method may also be used; there are two distinct techniques. Firstly, a single crystal substrate in the form of a thin film may be used, and the overgrowth formed on this film (see, for example, Wilman (1940) or Finch and Sun (1936)). Secondly, the overgrowth is formed on a single crystal substrate and then detached (e.g. by dissolving away the substrate) so as to form a thin film which can be examined by transmission (see, for example, Bruck (1936) or Shirai (1937)).

In most cases, the electron beam illuminates a specimen area of at least 0·1 mm × 0·1 mm, so that the diffraction pattern arises from a large number of overgrowth crystallites. In some electron diffraction instruments, particularly those combined with electron microscopes, much finer and more intense electron beams are used. The number of crystallites irradiated may then be much smaller, and in certain cases of high resolution examination it would be possible to study the individual crystallites. This technique has not yet been applied to study of epitaxy.

Electron diffraction has one considerable advantage over other methods. Even quite thin surface films (see § 2.3.6) give very intense patterns,

which are clearly visible on a fluorescent screen. A thorough visual examination of the overgrowth can therefore be made at various crystal settings, and photographs can be readily obtained at all appropriate settings.

Further details of the general technique of electron diffraction may be found elsewhere (Beeching 1936, Finch and Wilman 1937, Pinsker 1953, Raether 1951, Thomson and Cochrane 1939).

### 2.3.1. *Types of Specimen Suitable for Examination*

In the case of transmission specimens, the thickness of the films must not be more than a few hundred ångströms. This limit arises because of the inelastic scattering processes, which give rise to a continuous background on the diffraction patterns. Since studies of epitaxy necessitate the use of single crystal substrates, this thickness condition provides a very severe limitation. There are two possible ways of increasing the maximum specimen thickness. Firstly, the energy of the electrons can be increased. According to Mollenstedt (1946), a tenfold increase in film thickness is possible, for polycrystalline aluminium, if the energy is increased from 80 to 500 kev. Secondly, the inelastically scattered electrons may be filtered from the diffraction pattern. Boersch (1953) has shown that this results in a considerable improvement in the contrast of the pattern, but no data are available concerning the application of the technique to the examination of thick films.

For reflection work, the substrate should have a macroscopically flat surface, preferably parallel to a definite lattice plane. Cleavage faces of a crystal are very convenient, particularly since they usually provide surfaces which are fairly flat on an atomic scale, at least over a limited area. It is often necessary, particularly in the case of metal substrates, to use surfaces prepared by some form of etching. Only in very rare cases does the etching process produce surfaces as flat as a cleavage face; generally the surface is rough on an atomic scale. The suitability of such a surface as a substrate depends upon various factors such as the extent to which the contact planes may be determined (see §§ 2.3.2 and 2.3.3).

The overgrowths may be prepared by any method which provides crystals which give sufficiently bright diffraction patterns.

### 2.3.2. *Examination of the Surface Form of the Substrate*

Any theoretical discussion of the mode of orientation of an overgrowth must involve a consideration of how the two lattices are joined together. Hence it is important to establish the planes of contact between the two lattices. It has been shown by several experimenters (see, for example, Pashley (1952 a) that the relative orientation does depend upon these contact planes. The first step in their determination involves the investigation of the topography of the substrate.

The ideal type of substrate to use is one which has an atomically smooth surface. The contact planes can then be deduced immediately from the relative orientation. In practice, the nearest approach to such a surface is a cleavage face of a good single crystal. These usually have a step structure, the regions between the steps consisting of surface which is fairly flat on an atomic scale. Observations for mica are given by Tolansky (1948, p. 122) and for sodium chloride by Schulz (1952 a).

A substrate which cannot be prepared in the form of a cleavage surface is usually quite rough on an atomic scale. It is important that the topography of such a surface be examined. The only methods of much value are electron microscopy or electron diffraction, although optical techniques such as the Bridgman (1925) method can be used to identify well-developed crystal facets. Electron microscopy has not so far been used very much in this field. This is partly because the limit of resolution of replica techniques has been, until recently, no better than about 100 Å. There now exists the carbon replica technique which has been developed by Bradley (1954), and which is claimed to have a much higher resolution. It is to be hoped that more extensive use of electron microscopy will follow, although contrast limits might well prove to be serious.

Fig. 1

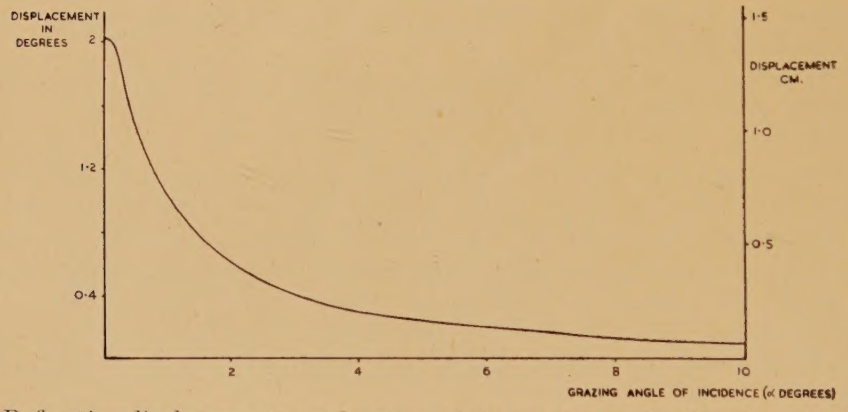


Refraction displacement as a function of the grazing angle of incidence ($\alpha$). $\mu = 1{\cdot}0002$ ; camera length 40 cm.

Electron diffraction is capable of supplying a certain amount of information about surface topography, which can be quite detailed in favourable cases. The degree of flatness of a surface can be judged from the amount of displacement caused by the refraction effect. For fast electrons (30 to 100 kv) the refractive indices of materials varies approximately from 1·00005 to 1·0004. Because of this low value the refractive displacement is measurable only if the electron beam enters the surface at a small glancing angle $\alpha$. The variation of the displacement with $\alpha$ is given in fig. 1, for a value of $\mu = 1{\cdot}0002$. The displacement is

expressed both in degrees and in terms of the shift obtained on a photographic plate at a typical distance of 40 cm from the specimen. In normal circumstances this shift can be detected only if it is greater (at best) than about 0·2 mm. The value of $\alpha$ is usually no more than about 5°, so that a measurable refractive displacement is observed if the surface is perfectly flat (see fig. 2 (*a*)). If the surface is rough on an atomic scale, the electron beam enters the actual surface at a large glancing angle, and no appreciable refractive displacement results (see fig. 2 (*c*)). An intermediate effect occurs with a surface which is fairly smooth, but which contains shallow undulations (see fig. 2 (*b*)). If the mean slope of the undulations is less than about 5°, then observable displacements occur. For a parallel incident electron beam, the glancing angle of entry $\alpha$ will vary according to the part of the surface entered ; a range of refractive displacements occurs, causing the diffraction spots to be tailed down

Fig. 2

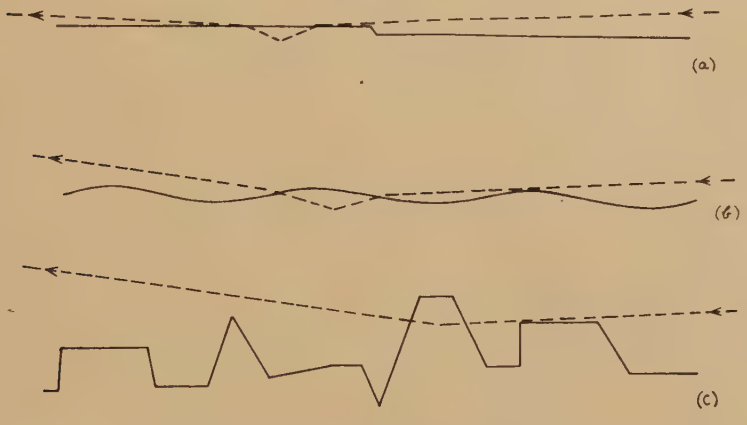


Refraction effects and surface form.
(*a*) Atomically flat surface ; (*b*) wavy surface ; (*c*) rough surface.

towards the shadow edge of the surface. Such patterns are commonly found from electrolytically polished surfaces (Kranert, Leise and Raether 1944). The refractive displacement therefore gives useful information concerning surface flatness. Some confusion occurs in the literature concerning the meaning of the terms ' atomically smooth ' and ' atomically flat '. Surfaces, such as that of fig. 2 (*a*), which show the full refraction effect are usually considered to be flat to the extent that their boundary is made up of an almost completely filled atomic plane, although the extent to which this need be so is unknown. In this article the term ' atomically flat ' will only be used to denote surfaces which fulfil this condition of full refraction. Surfaces which give rise to tailing (fig. 2 (*b*)) will not be included in this category, although some authors refer to these and similar surfaces as ' atomically smooth '. Some authors also deduce that surfaces are ' atomically smooth ' from the fact that sharp

Kikuchi lines are observed. This conclusion is, in the writer's opinion, completely unjustified because the formation of the Kikuchi lines has no direct relationship to the surface form.

The electron diffraction technique cannot be used to determine the area of the 'atomically flat' patches (e.g. areas between cleavage steps) on a surface; it can only be used to provide an approximate lower limit to this area. The relevant condition to be fulfilled is that the electron beam should both enter and leave the surface through the atomically flat region. Since the path length of the electrons in the material is limited, this will certainly be fulfilled if the patches are more than a few hundred angströms in extent in the direction of the electron beam. Thus the minimum requirement of a surface, such that it fulfils the definition of 'atomically flat' given above, is that it should be made up of a large number of regions which are flat enough to give rise to the full refraction displacement, the linear size of these regions being a few hundred ångströms.

When the substrate surface is of the type shown in fig. 2 (*c*), it is of some importance to establish whether there are any well-developed facets, since any overgrowth will be formed upon these facets. If a surface is bounded by a large number of similar facets, these can be identified in favourable cases. There are two distinct effects.

Firstly, if the incident beam is so directed that electrons can enter or leave the surface via these facets at a small glancing angle, a refractive displacement will occur. This will shift the diffraction spots on the photographic plate in a direction normal to the plane of the facet, so that identification is possible. Such discrete shifts are not often observed. Instead, diffraction spots are 'tailed' along the inwards normal to a particular set of facets, and such 'tailing' is usually attributed to refraction effects. Several difficulties arise in this interpretation (Pashley 1951 a); in particular, some effect such as a wavy facet surface has to be postulated, in order to account for the observation of tailing rather than discrete spot displacements.

The second effect concerns the form of the diffraction spots. The theory has been developed by Laue (1936, 1937 a, 1948) and Laue and Riewe (1936). If a small crystallite has well-developed boundary faces, the reciprocal lattice points corresponding to the crystallite will be extended in directions normal to those boundary faces. These extensions or 'stacheln' give rise to the splitting of diffraction spots, so that several spots appear instead of one. Each subsidiary spot arises from an intersection of the Ewald sphere with the 'stacheln' through the corresponding reciprocal lattice point. From the form and magnitude of the splitting the boundary facets may be identified. For a given system of facets, the pattern may be calculated from a formula derived by Pashley (1951 a).

The application of this theory to observed practical cases involves certain interpretative difficulties. The first examples of such effects were for the growth of silver layers on rocksalt (Lassen 1934, Kirchner

and Lassen 1935) and for the growth of cobalt layers on copper (Cochrane 1936). In both of these cases Laue (1936, 1937 a) deduced, from the observed diffraction patterns, that the (111) type planes were the prominent boundary planes. From the geometrical viewpoint this interpretation was satisfactory, since the observed patterns were consistent with the occurrence of extensions along the [111] directions in the reciprocal lattice. However, Kirchner and Rudiger (1937) have criticized the facet interpretation, and disagreement with Laue was expressed (Kirchner 1937, Laue 1937 b). There are three main points : (1) The splitting was accompanied by features which indicated the occurrence of repeated (111) twinning in the layers. The splitting effects can be associated, at least in part, with this twinning (Cochrane 1936). (2) Kirchner and Rudiger (1937) maintain, from other electron diffraction features, that the cube planes and not the (111) planes, form the boundaries. (3) The observed effects correspond to ' stacheln ' which are longer and more intense than those to be expected from Laue's theory, for crystals of a reasonable size.

More recently (Pashley 1951 a) splitting effects have been observed from etched silver crystals, for cases where twinning was definitely absent. The length and intensity of the ' stacheln ' were more near to the theoretical prediction, but the ' stacheln ' were found to be asymmetrical about the centres of the reciprocal lattice points. No satisfactory explanation for this has been found, although surface deformations of a special type might be responsible.

To summarize, there exists, in theory, a method of detecting small, numerous surface facets by means of a study of the form of diffraction spots. This method usually gives rise to certain difficulties of interpretation, which make the identification of facets not completely certain. More work on the interpretation of fine structure features is necessary ; in particular, correlation with electron microscope observations might prove to be helpful.

### 2.3.3. *The Determination of Contact Planes*

When a rough single crystal surface is used as a substrate, an overgrowth will often occur in several orientations, corresponding to deposition on the various surface facets. It is then necessary to determine which of these planes is giving rise to a particular overgrowth orientation. In favourable cases, unambiguous interpretations may be arrived at (Pashley 1952 a) as a result of electron diffraction examination. A careful study is made of the surface at different azimuth settings. When a facet is set approximately perpendicular to the electron beam, the growth on that facet gives rise to a prominent secondary diffraction pattern, which results from scattering by both the substrate and the overgrowth. When the same facet is set nearly parallel to the electron beam, only a primary pattern is obtained from the overgrowth. These differences depend upon whether or not the electron beam traverses a substrate projection in

entering or leaving a thin deposit on a facet surface. By correlating information of this kind obtained at different crystal settings, the number of possible contact planes can be reduced considerably. This number is further reduced by considering as possible contact planes only those pairs of lattice planes in the substrate and overgrowth which are parallel. The extent to which this restricts the choice depends considerably upon the symmetry of the two structures, and upon their relative orientation.

By means of this method, the true contact planes have been deduced with certainty for silver halides on etched silver crystal surfaces (Pashley 1952 a) and for cadmium oxide on electropolished cadmium crystal surfaces (Lucas 1952).

2.3.4. *Spacing Measurements and their Limitations*

Since it is difficult to measure the electronic wavelength directly, accurate spacing measurements are often carried out with the aid of a calibration specimen. This technique can be successfully employed for both reflection and transmission specimens; provided adequate precautions are taken, the inaccuracy of calibration need be no greater than about 0·1% for reflection and can be much less for transmission. The choice of a standard calibration material is of importance. Thallium chloride prepared by deposition *in vacuo* is very suitable and reliable (Boswell 1950, 1951).

The accuracy of measurement is, in most cases, limited by the lack of sharpness of the diffraction spots. This restriction becomes particularly serious in the reflection case, where effects due to surface form and lack of penetration are often considerable. Diffraction spots are broadened or elongated, sometimes in an asymmetrical manner, so that the point to which measurements should be made is ill-defined. An absolute accuracy of about 1% is usually possible for spacings of planes perpendicular to the surface, but for the planes parallel to the surface the spacings can sometimes be measured only to a much poorer accuracy. Only in a comparatively few, although sometimes vital, cases is it impossible to distinguish between the spacings of the substrate and the overgrowth (further discussion is given in § 4.4).

2.3.5. *Continuous Examination during the Growth of a Layer*

When an oriented layer is formed *in situ* in the evacuated diffraction camera, it is possible to obtain a continuous record of the change of the diffraction pattern during the growth. This technique has been applied mainly to the study of the growth of layers from the vapour phase. Two distinct methods are used. In the first (Schulz 1951 b, 1952 a), a number of different specimens are prepared in the evacuated camera and these are then examined. Further deposits on the same specimens may be also examined. In the second (Uyeda 1942) a single specimen is used and deposition is carried out while the electron beam is being used for the examination of the surface. The advantage of this latter method is that all stages of growth are studied in one experiment, and that the same

area of one specimen is examined. Effects due to specimen patchiness or variation from one specimen to another, are avoided. The disadvantage however, is that in some cases the electron beam is known to influence the growth of the deposit (Collins and Heavens 1952). We have found, in this laboratory, that growth upon several alkali halides is seriously influenced by the electron beam. The effect seems to be due to some permanent damage to the substrate, probably arising from a partial decomposition at the surface. In such cases, the first method must be used.

The importance of these techniques is that the growth may be carried out in a very controllable manner, so that the very early stages of an oriented layer may be studied. The value of the techniques depends upon the extent to which electron diffraction can be used in the examination of extremely thin layers.

### 2.3.6. *The Limit of Detection of a Surface Film*

Since a transmission specimen of only 100 Å in mean thickness will yield a bright diffraction pattern, it is to be expected that a uniform film of thickness $t$ on a flat substrate surface will give an observable pattern if the path of the beam traversing the film is at least 100 Å. For a grazing angle of incidence $\alpha$, this condition becomes $t/\sin\alpha > 100$ Å, which reduces, for a typical value of $\sin\alpha = 0{\cdot}02$, to $t > 2$ Å. A single uniform atomic layer should therefore be observable. The precise limit of detection would depend upon the deposit material used, and would be a function of both the angle $\alpha$ and the incident electron energy $E$. The dependence upon $E$ is difficult to predict, since it is controlled by an intensity balance between the inelastic scattering from both the substrate and the overgrowth, which causes a general background, and the elastic scattering from the overgrowth. For a rough substrate, the sensitivity of detection is lower because the electron path length in the overgrowth is smaller for a uniform deposit of a given thickness (see Raether 1949, 1950). A non-uniform film is also less easy to detect than a uniform layer.

Any experimental investigation concerning these conclusions is difficult because it involves independent measurements of film thickness in the range 1 to 10 Å. Weighing methods are too insensitive, and most other recognized methods are also unsuitable. Various authors have attempted to measure the thickness of evaporated films by methods involving an estimation of the amount of material which leaves the source. In several cases bright diffraction patterns have been reported from layers of only a few ångströms in thickness. Schulz (1951 b, 1952 a) has used such a method, to an estimated accuracy of about 20%. As a result, he was able to show that oriented layers of alkali halides as thin as 1 or 2 Å give observable patterns.

This aspect has been studied in more detail (Newman and Pashley 1955) with the aid of a radioactive tracer technique. Atomically flat silver crystal surfaces were used as substrates, and two types of layer were

investigated : (1) radioactive metallic copper deposited from the vapour ; (2) silver bromide formed by the chemical attack of radioactive bromine vapour. The $\beta$-activity of the specimens was used to give thickness measurements for deposits as thin as 0·1 Å. The results showed that layers of mean thickness less than 1 Å gave observable diffraction patterns, the limit of detection being about 0·8 Å for the copper and 0·4 Å for the silver bromide, for electrons of energy about 45 kev. Detailed qualitative information concerning the effect of the grazing angle of incidence $\alpha$ was obtained.

An important feature of these latter experiments is that in neither case did the deposits grow as uniform layers, but in the form of separated crystallites distributed over the surface. This aggregation has little effect upon the limit of detection, provided the crystallites are sufficiently small, as they are in this case. If the crystallite size is such that the incident coherent electron intensity is considerably reduced as the beam traverses it, the sensitivity of detection is reduced. Since the sensitivity of detection is greatest for a uniform deposit, it follows from the results with copper and silver bromide that for substances of average atomic number, and for atomically flat substrate surfaces, partial as well as complete atomic monolayers may be detected and examined.

In cases where growth occurs in the form of a large number of isolated crystallites, detection may be possible only after the crystallites have reached several atomic layers in thickness, although the average thickness of the deposit material may still be less than that of one atomic layer. The mode of growth of such crystallites cannot be studied in detail during the early stages.

### 2.3.7. *The Form of the Overgrowth Crystallites*

Although electron diffraction can be used to provide useful information concerning the form (e.g. size and shape) of the overgrowth crystallites, great caution is necessary in the interpretation of the results because of the limited penetrating power of the electrons. For this reason, it is also difficult to make any reliable deductions, unless the overgrowth is formed on an atomically flat surface. Even in this latter case, the overgrowth must be sufficiently thin to ensure that the diffraction arises from the whole of the layer. This normally implies that the layer must be no more than about 10 Å in average thickness. If the thickness of the individual crystallites exceeds about 10 Å, the information will be further limited when the lateral extent of the crystallites exceeds about 100 Å.

When layers of only a few ångströms in mean thickness are studied by the methods outlined in § 2.3.5, the mode of nucleation of the deposit may be investigated. If the layer spreads over the surface so as to form a coherent film of almost uniform thickness, the diffraction pattern consists of spots which are considerably elongated in a direction perpendicular to the surface. In the limiting case of a single atomic layer, this

elongation results in the formation of continuous streaks, corresponding to diffraction by a two-dimensional grating. If the layer forms as a number of separated crystallites, the pattern consists of distinct spots. The detailed structure of these spots is related to the size and shape of the crystallites. The interpretation of the effects is exactly similar to that used for the determination of surface form (see § 2.3.2). A check upon this kind of electron diffraction evidence has recently been made, in one isolated example. Miyake (1938) deduced that antimony oxide ($Sb_2O_3$) grew on a heated stibnite surface in the form of well-defined prisms which were oriented in a regular manner. Ito, Ito and Watanabe (1954) have since studied the same tarnishing reaction by electron microscopy, and confirm Miyake's result, which had been based entirely upon electron diffraction evidence. More work of this kind would be very helpful, in view of the various sources of uncertainty.

If the crystallites of the deposit grow such that they are partially embedded below the surface of the substrate, the size and shape of the primary diffraction spots correspond to the part of the crystallite protruding above the surface. The embedded part might, however, contribute to the secondary diffraction patterns. It is possible for measured sizes of crystallites to be false because of crystal irregularities (e.g. stacking faults) which reduce the size of good coherent crystal.

## § 3. The Observed Cases of Epitaxy

As a result of the many studies which have been made, a large number of cases of epitaxy has been observed. A comprehensive list of examples has been given by van der Merwe (1949) and further data will be found in the other reviews quoted in § 1. A survey will now be given of all of the cases of epitaxy which have been observed by electron diffraction methods, and these results will be compared with the corresponding observations which have been carried out with other techniques, mainly optical microscopy.

### 3.1. *Alkali Halides upon Themselves*

The first extensive experiments on the growth of alkali halides upon each other were carried out by Barker (1906, 1907, 1908). His results are included in table 1, and refer to growth from aqueous solution on to cleavage surfaces. No x-ray structure data were available at the time, but Barker noticed that absence of orientation was always associated with large discrepancies between the molecular volumes of the substrate and the deposit. The work was subsequently repeated by Royer (1928). His results (see table 1) indicated that orientation occurs provided the misfit is less than about $\pm 14\%$. Some of Barker's results were attributed to mixed crystal formation. When orientation occurred it did so not only on the (100) cleavage surface, but also on any other surface which was used.

Table 1 (*a*). Alkali Halides upon Alkali Halides

| Deposit \ Substrate | | LiF | | | MnS | | NaCl | | | | | | | | PbS | | | | NaBr | | | KCl | | | | | | |
|---|---|---|---|---|---|---|---|---|---|---|---|---|---|---|---|---|---|---|---|---|---|---|---|---|---|---|---|---|
| | $a_0$ Å | 4·02 | | | 5·21 | | 5·63 | | | | | | | | 5·92 | | | | 5·96 | | | 6·28 | | | | | | |
| | | V | VI | M | II | M | I | II | III | IV | V | VI | VII | M | II | III | IV | M | I | VI | M | I | II | III | IV | V | VI | M |
| LiF | 4·02 | | | | | | | | | | O | O | | −29 | | | | | | | | | | | | | | |
| NaF | 4·62 | O | | +15 | R | −11 | | R | R | | | | | −18 | R | R | | −22 | | | | | | | | O | O | −36 |
| LiCl | 5·13 | O | | +27 | O | −3 | | O | O | | O | | | −9 | R | R | | −13 | | | | | R | R | | O | | −26 |
| KF | 5·34 | O | | +33 | O | +3 | | O | O | | O | | | −5 | R | R | | −10 | | | | | R | R | | | | −18 |
| LiBr | 5·49 | | | | O | +6 | | O | O | | | | | −3 | R | R | | −7 | | | | | O | O | | | | −15 |
| AgCl | 5·55 | | | | O | +7 | | O | O | | | | O | −2 | O | O | | −6 | | | | | | O | | | | −13 |
| NaCl | 5·63 | O | O | +40 | O | +8 | | | | | | | | | O | O | | −5 | | | | O | O | O | | O | O | −12 |
| RbF | 5·64 | | | | R | +8 | | O | | | | | | 0 | O | | | −5 | | | | | O | | | | | −10 |
| AgBr | 5·77 | | | | R | +11 | | O | O | | | | O | +2 | O | O | | −2 | | | | | O | O | | | | −9 |
| NaCN | 5·83 | | | | | | | | O | | | | | +4 | | O | | −1 | | | | | | O | | | | −8 |
| PbS | 5·92 | | | | | | | O | O | | | | | +5 | | | | | | | | | | O | | | | −7 |
| NaBr | 5·96 | O | | +48 | R | +15 | O | O | O | | O | | | +6 | O | O | | +1 | | | | O | | O | | O | | −6 |
| LiI | 6·00 | | | | R | +15 | | O | | | | | | +7 | O | | | +1 | | O | +1 | | O | | | | | −5 |
| CsF | 6·01 | | | | R | +15 | | O | | | | | | +7 | O | | | +2 | | | | | O | | | | | −5 |
| KCl | 6·28 | O | O | +56 | R | +21 | O | O | O | | O | O | | +11 | O | O | | +6 | | | | | | | | | | −5 |
| TlCl | 6·30 | | | | | | | | | | | | | | | | | | | | | | | | | | | |
| NaI | 6·46 | | | | R | +24 | O | R | O | | | | | +15 | O | O | | +9 | O | | +9 | O | | O | | | | +3 |
| KCN | 6·51 | | | | R | +25 | O | | O | | | | | +16 | | O | | +10 | | | | O | | O | | | | +4 |
| RbCl | 6·54 | | | | R | +26 | O | R | R | O | | | | +16 | R | O | | +11 | O | | +10 | O | O | O | | | | +4 |
| TlBr | 6·58 | O | | +63 | | | | | | | O | | | +17 | | | | | | | | | | | | | | |
| KBr | 6·59 | O | O | +64 | R | +27 | O | R | O | | O | O | | +17 | R | O | | +11 | | | | O | | O | | O | O | +5 |
| RbCN | 6·82 | | | | | | O | | | | | | | +21 | | | | | | | | O | | | | | | +9 |
| RbBr | 6·85 | | | | R | +32 | R | R | R | O | | | | +22 | R | O | | +16 | O | | +15 | O | | O | | | | +9 |
| TlI | 6·94 | O | | +72 | | | | | | | O | | | +23 | | | | | | | | | | | | | | |
| CsCl | 6·94 | O | | +72 | | | | | | | O | | | +23 | | | | | | | | | | | | | | |
| KI | 7·05 | | O | +75 | R | +35 | O | R | O | | O | O | | +25 | R | R | O | +19 | O | | +18 | R | R | R | O | | O | +12 |
| CsBr | 7·23 | O | | +80 | | | | | | | O | | | +28 | | | | | | | | | | | | | | |
| $NH_4I$ | 7·24 | | | | R | +39 | R | R | R | O | | | | +28 | R | R | | +22 | | | | R | R | R | O | | | +15 |
| RbI | 7·33 | O | | +82 | R | +41 | R | R | R | O | O | | | +30 | R | R | | +24 | O | | +23 | R | R | R | O | O | | +17 |
| CsI | 7·66 | O | | +90 | | | | | | | O | | | +36 | | | | | | | | | | | | | | |

## Table 1 (*b*). Alkali Halides upon Alkali Halides

| Deposit \ Substrate | | KCN | | RbCl | | | KBr | | | | | | RbCN | | RbBr | | | KI | | | | $NH_4I$ | | | RbI | | |
|---|---|---|---|---|---|---|---|---|---|---|---|---|---|---|---|---|---|---|---|---|---|---|---|---|---|---|---|
| | $a_0$ Å | 6·51 | | 6·54 | | | 6·59 | | | | | | 6·82 | | 6·85 | | | 7·05 | | | | 7·24 | | | 7·33 | | |
| | | I | M | I | II | M | I | II | V | VI | VII | M | I | M | I | II | M | I | II | VI | M | I | II | M | I | II | M |
| LiF | 4·02 | | | | | | | | O | O | | −39 | | | | | | | | | | | | | | | |
| NaF | 4·62 | | | | R | −29 | | R | | | | −30 | | | | R | −32 | | R | O | −43 | | | | | | |
| LiCl | 5·13 | | | | R | −22 | | R | O | | | −22 | | | | R | −25 | | R | | −27 | | R | −44 | | R | −37 |
| KF | 5·34 | | | | R | −18 | | R | O | | | −19 | | | | R | −22 | | R | | −24 | | R | −29 | | R | −30 |
| LiBr | 5·49 | | | | R | −16 | | R | | | | −17 | | | | R | −20 | | R | | −22 | | R | −26 | | R | −27 |
| AgCl | 5·55 | | | | | | | | | | O | −16 | | | | | | | | | | | R | −24 | | R | −25 |
| NaCl | 5·63 | | | O | R | −14 | O | R | O | O | | −15 | | | R | R | −18 | O | R | O | −20 | R | R | −22 | R | | −23 |
| RbF | 5·64 | | | | R | −14 | | R | | | | −14 | | | | R | −18 | | R | | −20 | | R | −22 | | R | −23 |
| AgBr | 5·77 | | | | | | | | | | O | −12 | | | | | | | | | | | | | | | |
| NaCN | 5·83 | | | | | | | | | | | | | | | | | | | | | | | | | | |
| PbS | 5·92 | | | | | | | | | | | | | | | | | | | | | | | | | | |
| NaBr | 5·96 | | | O | | −9 | O | O | O | | | −9 | | | O | R | −13 | O | | | −15 | | R | −18 | O | | −19 |
| LiI | 6·00 | | | | R | −8 | | O | | | | −9 | | | | R | −12 | | R | | −15 | | R | −17 | | R | −18 |
| CsF | 6·01 | | | | R | −8 | | R | | | | −9 | | | | R | −12 | | R | | −15 | | R | −17 | | R | −18 |
| KCl | 6·28 | O | −4 | | O | −4 | O | | O | O | | −5 | O | −8 | O | | −8 | R | R | O | −11 | | R | −13 | R | R | −14 |
| TlCl | 6·30 | | | | | | | | O | | O | −4 | | | | | | | | | | | | | | | |
| NaI | 6·46 | O | −1 | O | | −1 | O | | | O | | −2 | | | O | | −6 | O | O | | −8 | O | R | −11 | | R | −12 |
| KCN | 6·51 | | | O | | 0 | O | | | | | −1 | | | | | | O | | | −8 | O | | −10 | O | O | −11 |
| RbCl | 6·54 | O | 0 | | | | O | | | O | | −1 | O | −4 | O | | −5 | O | O | | −7 | | R | −10 | R | R | −11 |
| TlBr | 6·58 | | | | | | | | O | | | 0 | | | | | | | | | | | | | | | |
| KBr | 6·59 | O | +1 | O | | +1 | | | | | | | O | −3 | O | O | −4 | O | O | O | −6 | | O | −9 | O | O | −10 |
| RbCN | 6·82 | O | +5 | O | | +4 | O | | | | | +4 | | | O | | 0 | O | | | −3 | | | | | | |
| RbBr | 6·85 | | | | | | O | O | | | | +4 | O | 0 | | | | O | O | | −3 | | O | −5 | O | O | −7 |
| TlI | 6·94 | | | | | | | | O | | | +5 | | | | | | | | | | | | | | | |
| CsCl | 6·94 | | | | | | | | O | | | +5 | | | | | | | | | | | | | | | |
| KI | 7·05 | O | +8 | | O | +8 | O | O | | O | | +7 | O | +3 | O | O | +3 | | | | | | | | O | O | −4 |
| CsBr | 7·23 | | | | | | | | O | | | +10 | | | | | | | | | | | | | | | |
| $NH_4I$ | 7·24 | O | +11 | R | R | +11 | O | O | | | | +10 | O | +6 | O | O | +6 | O | | | +3 | | | | O | O | −1 |
| RbI | 7·33 | | | R | R | +12 | O | O | O | | | +11 | O | +7 | O | O | +7 | O | O | | +4 | O | | +1 | | | |
| CsI | 7·66 | | | | | | | | O | | | +16 | | | | | | | | | | | | | | | |

O indicates parallel orientation.

R indicates random orientation.

Headings to columns :

I Results of Barker (1906, 1907, 1908).
II Results of Royer (1928).
III Results of Sloat and Menzies (1931) for growth from aqueous solution.
IV Results of Sloat and Menzies (1931) for growth from solvents listed in table 2.
V Results of Schulz (1951 c, 1952 a) for growth from vapour.
VI Results of Ludemann (1954) for growth from vapour.
VII Results of Pashley (1952 b) for growth from vapour.
M Percentage misfit.

Sloat and Menzies (1931) examined the effect of using various solvents and were able to show that in some cases orientation is obtained with misfits larger than 14%. All of their results are included in table 1 ; the effect of different solvents is shown in table 2. It was pointed out that reduction in the dielectric constant of the solvent improves the probability of orientation, the limiting case being growth from the vapour phase (dielectric constant of unity). This was interpreted as showing that the solvent interferes with the orientation process and that the higher the polarizability of the solvent, the greater is its influence. In these experiments, the limiting misfit was extended to +30% (RbI on NaCl).

Table 2. Effects of Solvent upon Orientation

(Results of Sloat and Menzies 1931)

| Substrate | Deposit | Solvent and dielectric constant | | | | | |
|---|---|---|---|---|---|---|---|
| | | Water 81 | Furfural 39 | Methyl alcohol 32 | Ethyl alcohol 25 | Acetone 21 | From vapour 1 |
| NaCl | KBr | O | O | O | O | | |
| | RbCl | R | | O | O | | |
| | RbBr | R | O | O | O | | |
| | KI | O | O | O | O | | |
| | $NH_4I$ | R | R | R | R | R | O |
| | RbI | R | R | R | R | O | |
| KCl | KI | R | R | O | O | O | |
| | $NH_4I$ | R | O | O | O | O | O |
| | RbI | R | O | O | O | O | |

R indicates random orientation. O indicates parallel orientation.

As an extension of these studies, Schulz (1951 c, 1952 a) has examined, by electron diffraction, thin alkali halide deposits condensed *in vacuo* from the vapour phase. He finds (table 1) that, for all substrate–deposit combinations examined, a parallel-oriented growth occurs, independent of the misfit. Misfits varying from −39% (LiF on KBr) to +90% (CsI on LiF) are tolerated. Ludemann (1954) has carried out similar experiments and confirms the results of Schulz. Elleman and Wilman (1948) find other orientations of lead sulphide condensed on to heated rocksalt surfaces.

Schulz attempted to include an examination of growth from solution in his work, by allowing the condensed alkali halide layers to come into contact with moist air. Recrystallization occurred when the specimen was returned to the vacuum of the diffraction camera. In all cases except lithium fluoride substrates, the results were complicated by mixed crystal formation.

The growth of alkali halides which normally have the caesium chloride structure is complicated by polymorphic effects, which are discussed in § 5.4.

### 3.2. *Alkali Halides upon Mica*

The growth of alkali halides upon muscovite mica has been studied extensively. The first systematic work was by Royer (1928), who examined growth from solution. The most commonly observed orientation has a (111) plane of the halide parallel to the (001) mica cleavage surface, with the [1$\bar{1}$0] or [$\bar{1}$10] directions in the halide parallel to the mica [100]. The oriented crystallites are easily visible under the optical microscope, and appear as (111) based triangular pyramids. The results are presented in table 3. Only salts with a lattice constant of greater than 6·2 Å are oriented.

Table 3 (*a*). Alkali Halides with the Rocksalt Structure on Mica
(Orientation as shown in fig. 3)

| Deposit | $a_0$ Å | I | II | III | IV | V | VI | M |
|---|---|---|---|---|---|---|---|---|
| LiF | 4·02 | | | | | | | −45 |
| NaF | 4·62 | R | | | | | | −37 |
| LiCl | 5·13 | R | | | | | | −30 |
| KF | 5·34 | R | | | | O | | −27 |
| LiBr | 5·49 | R | | | | | | −25 |
| AgCl | 5·55 | R | | | | | O | −24 |
| NaCl | 5·63 | R | O | O | | O | | −23 |
| RbF | 5·64 | R | | | | | | −23 |
| AgBr | 5·77 | R | | | | | O | −21 |
| NaBr | 5·96 | R | | O | | O | | −19 |
| LiI | 6·00 | R | | | | | | −18 |
| CsF | 6·00 | R | | | | | | −18 |
| KCl | 6·28 | O | O | O | | O | | −14 |
| NaI | 6·46 | O | | O | O | O | | −12 |
| RbCl | 6·54 | O | | O | | | | −11 |
| KBr | 6·59 | O | O | O | O | O | | −10 |
| RbBr | 6·85 | O | | O | | | | − 7 |
| CsCl | 6·94 | | | | | O | | − 6 |
| KI | 7·05 | O | O | O | O | O | | − 4 |
| CsBr | 7·23 | | | | | O | | − 1 |
| $NH_4I$ | 7·24 | O | | O | | O | | − 1 |
| RbI | 7·33 | O | | O | O | O | | 0 |

O indicates orientation of fig. 3. R indicates random orientation.

Column headings :

I Results of Royer (1928) for growth from solution.
II Results of Deicha (1946, 1947 a, b, c) for growth from solution.
III Results of Lisgarten (1954) for growth from solution.
IV Results of West (1945) for growth from the melt.
V Results of Schulz (1951 b) for growth from the vapour and solution.
VI Results of Pashley (1952 b) for growth from the vapour.
M Percentage misfit.

Royer considered this in terms of the fit between the (111) face of the halide and the potassium ion sites in the mica cleavage surface. The fit for the case of potassium bromide is shown in fig. 3, the two parallel networks

Fig. 3

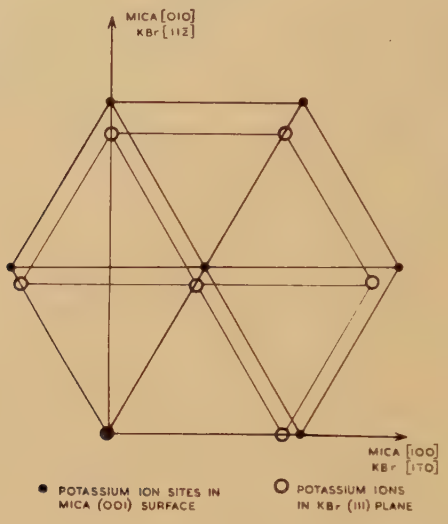


The fit of the main potassium bromide orientation upon mica.

Table 3 (*b*). Alkali Halides with the Caesium Chloride Structure on Mica (Orientation as shown in fig. 3)

| Deposit | $a_0$ Å | I | II | III | M |
|---|---|---|---|---|---|
| TlCl | 3·83 | | | O | +5 |
| $NH_4Cl$ | 3·87 | O | O | | +6 |
| $NH_4Br$ | 4·05 | O | | | +11 |
| CsCl | 4·11 | R | | | +12 |
| CsBr | 4·29 | R | O | | +17 |
| CsI | 4·56 | R | O | O | +25 |

O indicates orientation of fig. 3. R indicates random orientation.

Column headings :

I Results of Royer (1928) for growth from solution.
II Results of Lisgarten (1954) for growth from solution.
III Results of Schulz (1951 c) for growth from the vapour.

each having a hexagonal arrangement. As shown in table 3, the misfit is always less than 14% where orientation occurs. The significance of the fit is emphasized by the behaviour of potassium chloride, which is a limiting case. A misfit of only −1% occurs if the (111) plane is twisted through 90°

(see fig. 4) so as to make the [1$\bar{1}$0] or [$\bar{1}$10] directions of the potassium chloride parallel to the mica [010] direction. This abnormal (111) orientation was in fact observed, in addition to the above. However, other alkali halides which could adopt this orientation with a small misfit failed to do so.

Fig. 4

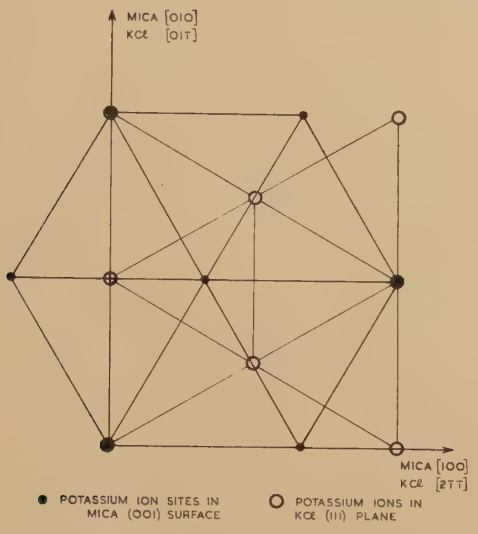


The fit of the subsidiary potassium chloride orientation upon mica.

Table 4. Alkali Halides with the Rocksalt Structure on Mica (Orientation as shown in fig. 4)

| Deposit | $a_0$ Å | I | II | III | M |
|---|---|---|---|---|---|
| NaCl | 5·63 | N | | O | −11 |
| NaBr | 5·96 | N | | O | −6 |
| KCl | 6·28 | O | O | O | −1 |
| NaI | 6·46 | N | | O | +2 |
| RbCl | 6·54 | N | | O | +3 |
| KBr | 6·59 | N | | O | +4 |
| RbBr | 6·85 | N | | N | +8 |
| KI | 7·05 | N | | N | +11 |
| $NH_4I$ | 7·24 | N | | N | +14 |
| RbI | 7·33 | N | | N | +16 |

O indicates orientation as for fig. 4. N indicates no orientation as for fig. 4.

Column headings :

I Results of Royer (1928).
II Results of Deicha (1947 b).
III Results of Lisgarten (1954).

Lisgarten (1954) has re-examined these results of Royer. By using very clean conditions, he was able to extend the range of orientation

(see table 3). Thus sodium chloride is oriented with a misfit of $-23\%$, the crystallites having hexagonal bases as shown in fig. 5. This latter case had previously been observed by Deicha (1946, 1947 a, c), who took precautions to avoid formation of crystallites in solution, so as to ensure that nucleation occurred on the mica surface. In addition, Lisgarten observed the abnormal (111) orientation for salts other than potassium chloride (see table 4), although this was less frequently observed than the normal orientation.

Fig. 7

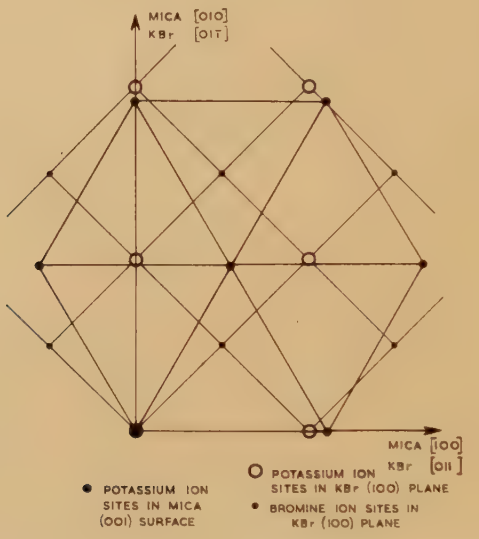


The fit of the potassium bromide cube orientation upon mica.

West (1945) has obtained large oriented sections of certain alkali halides by crystallizing them from the melt on a mica cleavage surface. In this way, crystals as large as 4 cm diameter by 0·4 cm thick have been obtained; the results are included in table 3. The salts are all within the Royer range of orientation: West apparently did not try to grow salts outside this range.

Schulz (1951 b) has deposited alkali halides from the vapour phase *in vacuo*, and finds oriented growth up to misfits of $-27\%$, almost double that of Royer (see table 3). He also employed his recrystallization method (see § 3.1) for studying growth from solution and found that the results were essentially the same as growth from the vapour phase. It has also been observed that silver chloride and silver bromide orient from the vapour phase on mica with large misfits (Pashley 1952 b, see table 3).

Deicha (1946, 1947 b, c, 1948, 1949) and Lisgarten (1954) have found that certain of the halides give rise to square-based crystallites on the mica (see fig. 6). These have (100) planes parallel to the mica surface.

Royer (1948 a, b) has criticized Deicha's results, suggesting that the cubes from in solution and then fall on to the mica. Both Deicha and Lisgarten interpret their results in terms of nucleation on the mica. Two main orientations occur, either the [011] or [001] halide directions being parallel to the mica [100] axis. In addition, Lisgarten occasionally finds other angular positions. The first of the two orientations is illustrated in fig. 7, and the misfits involved are given in table 5.

Table 5. Misfit Values for Observed Cases of the Orientation shown in fig. 7 (Lisgarten 1954)

| Deposit | % misfits | | % misfit along mica [010] when two deposit ion distances are fitted with one substrate distance |
|---|---|---|---|
| | Along mica [100] | Along mica [010] | |
| RbBr | −6 | −46 | +8 |
| KBr | −10 | −48 | +4 |
| RbCl | −10 | −48 | +4 |
| NaI | −12 | −49 | +2 |
| KCl | −14 | −51 | −1 |
| NaBr | −19 | −53 | −6 |
| NaCl | −23 | −56 | −11 |

### 3.3. *Alkali Halides upon Calcite and Sodium Nitrate*

Several workers have studied the growth of alkali halides upon cleavage surfaces of calcite and sodium nitrate, which are both rhombohedral structures. The crystal axes used in the following description are those which define the cleavage rhomb. Heintze (1937) obtained oriented

Table 6. Misfit Values for Observed Orientations of Alkali Halides upon Calcite and Sodium Nitrate

| Deposit | % misfit on calcite (Royer 1937) | % misfit on sodium nitrate (Heintze 1937) |
|---|---|---|
| LiCl | | −21 |
| LiBr | | −15 |
| NaCl | | −13 |
| NaBr | −7 | −8 |
| KCl | −2 | −3 |
| NaI | +1 | 0 |
| RbCl | +2 | |
| KBr | +3 | +2 |
| RbBr | +7 | |
| KI | +10 | +9 |

growth of several halides from solution on to sodium nitrate, and Royer (1937) obtained similar results with calcite (table 6). The principle orientation observed is illustrated in fig. 8 ; the cleavage plane of the substrates consists of an oblique network of ions which are arranged as in a rocksalt cleavage face. There is only one set of parallel lattice rows, along the substrate [001] or [010] directions, there being two geometrically equivalent orientations. The misfits quoted in table 6 refer to these parallel rows. Van der Merwe (1949) also defines an angular misfit between the two contact planes. In addition to these orientations, Heintze obtained growth with (110) halide planes parallel to the sodium nitrate cleavage face with NaCl, KCl, KBr, KI and LiCl.

Fig. 8

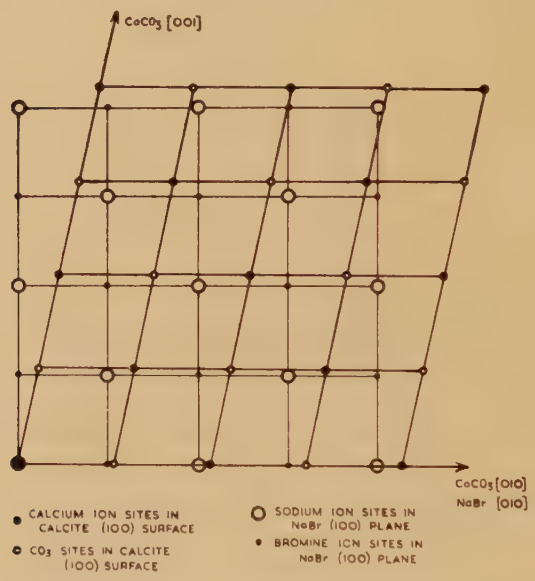


The fit of sodium bromide on calcite (Royer 1937).

Schulz (1952 b) has studied thin evaporated layers of a number of halides upon both substrates, by means of electron diffraction. Growth from solution was examined also. The types of orientation which he observed are given in table 7, and table 8 lists the cases for which they occurred. Again, the contact planes do not have lattice networks of the same form and the misfits quoted in table 8 refer to the fit along the [011] and [01$\bar{1}$] directions in the substrate surface. The fit of the main orientation is shown in fig. 9. A surprising feature of these results is that the observed growths from solution do not have the same orientation as those found by Heintze and Royer. The reason for this is not clear.

The observed misfits are fairly small in most cases. Although there is the general tendency for an electrically neutral plane of low indices to form parallel to the substrate surface, this condition is not always fulfilled (Schulz 1952 b).

Table 7. Observed Orientations of Alkali Halides upon Calcite and Sodium Nitrate (Schulz 1952 b)

| Orientation | Overgrowth plane parallel to substrate (100) cleavage surface | Overgrowth axis parallel to substrate [011] axis |
|---|---|---|
| I | (100) | [011] |
| II*a* | (110) | [001] |
| II*b* | (110) | [1$\bar{1}$0] |
| III*a* | (111) | [1$\bar{1}$0] |
| III*b* | (111) | [$\bar{1}$10] |
| IV | (741) | [$\bar{1}$13] |

Table 8. Observed Orientations and Misfits for Alkali Halides upon Calcite and Sodium Nitrate (Schulz 1952 b)

| Deposit | Structure type | Orientation (see table 7) | | | | % misfits | | | |
|---|---|---|---|---|---|---|---|---|---|
| | | Growth from vapour | | Growth from solution | | $CaCO_3$ | | $NaNO_3$ | |
| | | $CaCO_3$ | $NaNO_3$ | $CaCO_3$ | $NaNO_3$ | Along [011] | Along [01$\bar{1}$] | Along [011] | Along [01$\bar{1}$] |
| NaCl | A | I | I | I | I | −1 | −20 | −2 | −21 |
| KCl | A | I | I | I | I | +10 | −11 | +9 | −12 |
| KBr | A | I | I | I | I | +16 | −7 | +15 | −8 |
| CsCl | A | I | I | | | +22 | −2 | +21 | −3 |
| CsBr | A | I | I | | | +27 | +2 | +26 | +1 |
| CsCl | B | | | II*b* | II*b* | +2 | +16 | +1 | +21 |
| CsBr | B | | | II*b* | II*b* | +6 | +15 | +6 | +20 |
| RbI | A | I | I | | | +29 | +4 | +28 | +2 |
| RbI | A | | | III*a* | III*a* | | +4 | | +2 |
| KI | A | I | I | | | +24 | 0 | +23 | −1 |
| KI | A | | | III*a*, *b* | III*a*, *b* | | 0 | | −1 |
| NaF | A | I | I | | I | −19 | −35 | −20 | −35 |
| NaF | A | | | II*a* | | −19 | −7 | | |
| KF | A | | | II*a* | | −6 | +7 | | |
| LiF | A | IV | IV | IV | IV | | | | |
| CsF | A | III | | | | | −15 | | |

A ≡ Rocksalt type structure. B ≡ Caesium chloride type structure.

Table 9. Observed Orientations of Alkali Halides upon Metals

| Substrate | Type of surface | Deposit | Mode of growth | Method of observation | Plane parallel to surface | Parallel axes | | % misfit | Reference | Remarks |
|---|---|---|---|---|---|---|---|---|---|---|
| | | | | | | Deposit | Substrate | | | |
| Ag | C | NaCl | S | E.D. | (001) | [100] | [110] | −3 | (1), (2) | Bruck's (1) interpretation of extra spots |
| Ag | A | NaCl | V | E.D. | (111) | [1$\bar{1}$0] | [100] | −3<br>+69 | (1) | Substrate at 340° c |
| Ag | A | NaCl | S | M | (001) | [100] | [110] | −3 | (3), (4), (5) | See correction to ref. (4) in ref. (6) |
| Ag | B | NaCl | S | M | (111) | [1$\bar{1}$0] | [110] | +38 | (3), (4), (5) | Do. |
| Cu | A | NaCl | S | M | (001) | [100] | [110] | | (5) | |
| Cu | B | NaCl | S | M | (111) | [1$\bar{1}$0] | [110] | | (5) | |
| Au | B | NaCl | S | M | (111) | [1$\bar{1}$0] | [1$\bar{1}$0] | +38 | (5) | |
| Ag | A | KCl | S | M | (001) | [100] | [110] | +9 | (5) | |
| Ag | B | KCl | S | M | (111) | [110] | [110] | +54 | (5) | |
| Zn | F | NaCl | S | M | | | | | (5) | Good orientation on individual grains |
| Pb | D | NaCl | S | M | | | | | (5) | Well-defined orientations ; not determined |
| Bi | E | NaCl | S | M | (111) | [1$\bar{1}$0] | [1$\bar{1}$0] | | (5) | |
| Bi | E | KCl | S | M | (111) | [1$\bar{1}$0] | [1$\bar{1}$0] | | (5) | |
| Bi | E | RbCl | S | M | (111) | [1$\bar{1}$0] | [1$\bar{1}$0] | | (5) | |
| Sb | E | NaCl | S | M | (111) | [1$\bar{1}$0] | [1$\bar{1}$0] | | (5) | |
| Fe | F | CsCl | S | M | | | | | (5) | Good orientation on individual grains |
| Ag | A | CsCl | V & S | E.D. | (001) | [100] | [100] | +1 | (7) | |
| Ag | A | CsBr | V & S | E.D. | (001) | [100] | [100] | +5 | (7) | |
| Ag | A | NaCl | V | E.D. | (111) | [1$\bar{1}$0] | [100] | −3<br>+69 | (7) | |
| Ag | A | NaCl | S | E.D. | (001) | [100] | [110] | −3 | (7) | |
| Ag | A | NaBr | V | E.D. | (111) | [1$\bar{1}$0] | [100] | +3<br>+79 | (7) | |

Table 9—*cont.*

| Substrate | Type of surface | Deposit | Mode of growth | Method of observation | Plane parallel to surface | Parallel axes | | % misfit | Reference | Remarks |
|---|---|---|---|---|---|---|---|---|---|---|
| | | | | | | Deposit | Substrate | | | |
| Ag | A | NaBr | S | E.D. | (001) | [100] | [110] | +3 | (7) | |
| Ag | A | KCl | V | E.D. | (111) | [1$\bar{1}$0] | [100] | +9<br>+88 | (7) | |
| Ag | A | KCl | S | E.D. | (001) | [100] | [110] | +9 | (7) | |
| Ag | A | RbBr | V | E.D. | (111) | [1$\bar{1}$0] | [100] | +18<br>+105 | (7) | |
| Ag | A | RbBr | S | E.D. | (001) | [100] | [110] | 0 | (7) | Has abnormal CsCl structure |
| Ag | B | CsCl | V | E.D. | (001) | Fibrous | | | (7) | |
| Ag | B | CsCl | S | E.D. | (111) | [2$\bar{1}\bar{1}$] | [1$\bar{1}$0] | −42 | (7) | |
| Ag | B | CsBr | V | E.D. | (001) | Fibrous | | | (7) | |
| Ag | B | CsBr | S | E.D. | (111) | [2$\bar{1}\bar{1}$] | [1$\bar{1}$0] | −39 | (7) | |
| Ag | B | LiF | V | E.D. | (111) | [1$\bar{1}$0] | [1$\bar{1}$0] | −1 | (7) | |
| Ag | B | NaCl | V & S | E.D. | (111) | [110] | [2$\bar{1}\bar{1}$] | −20 | (7) | Trace of other orientations with growth from solution |
| Ag | B | NaBr | V & S | E.D. | (111) | [1$\bar{1}$0] | [2$\bar{1}\bar{1}$] | −16 | (7) | Do. |
| Ag | B | KCl | V & S | E.D. | (111) | [1$\bar{1}$0] | [2$\bar{1}\bar{1}$] | −11 | (7) | Do. |
| Ag | B | KI | V & S | E.D. | (111) | [1$\bar{1}$0] | [2$\bar{1}\bar{1}$] | −1 | (7) | Do. |

Types of surface :

A (001) oriented film on rocksalt. C (001) transmission film. E (111) cleavage surface.
B (111) oriented film on mica. D Etched single crystal. F Polycrystalline surface.

S = growth from solution. V = growth from vapour. M = optical microscope. E.D. = electron diffraction.

References :

(1) Bruck (1936). (2) Goche and Wilman (1939). (3) Johnson (1950 b).
(4) Johnson (1950 c). (5) Johnson (1951). (6) Johnson (1950 d).
(7) Schulz (1952 c).

### 3.4. *Alkali Halides upon Metals*

Bruck (1936) and Goche and Wilman (1939) found extra spots on transmission patterns from oriented layers of silver stripped from rocksalt surfaces. Bruck interpreted these as due to oriented rocksalt which had crystallized from solution on the silver film ; when rocksalt was condensed *in vacuo* on to heated silver, a different orientation was found (table 9).

Fig. 9

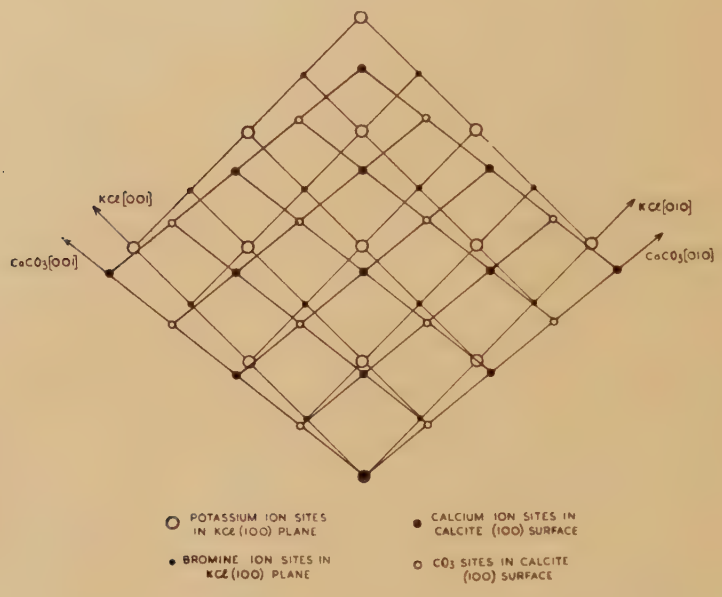


The fit of potassium chloride on calcite (Schulz 1952 c).

Johnson (1950 b, c, d, 1951) has used the optical microscope to study the growth from solution of halides upon metal substrates, which were in various forms : (1) etched polycrystalline surfaces ; (2) etched massive single crystal surfaces ; (3) oriented metal layers formed on other single crystal substrates. His results are included in table 9. The misfit for many of the results is not quoted because it is likely that the halides were growing not on the metal surface but on an oxide surface film (Johnson 1951). The orientation of the halides on (111) silver surfaces is stated to be parallel to the substrate ; hence the data given in table 9. However, it is also stated that this corresponds to a misfit of 73% in the case of rocksalt. This is consistent neither with the parallel orientation, nor with the orientation observed by Schulz (see below) for which the misfit is −20%.

Deposits of alkali halides upon silver have been studied in detail by Schulz (1952 c), who has examined both growth from the vapour phase and growth from solution. The substrates were formed by depositing the metal on to hot rocksalt to give (100) silver surfaces, and upon hot mica to give (111) silver surfaces. The results, given in table 9, show that the different methods of growth do not always give the same orientation. A wide range of misfits is observed. In all of the experiments listed in

table 9 the topography of the substrate surfaces was not well known; the contact planes have been assumed parallel to the surface for the purpose of calculating the misfits.

### 3.5. *Metals upon Metals*

Most studies of the oriented growth of metals upon metals have been made on electrodeposits. x-ray work (Wood 1930, 1935) first indicated that epitaxy could occur in such cases. Later, electron diffraction methods confirmed this for several substrate–deposit combinations. Cochrane (1936) used etched single crystal copper surfaces, and found that some metals were oriented on them. Finch and Sun (1936) used beaten foils of platinum, palladium and gold as substrates. The results are given in table 10. Further data were obtained by Finch, Wilman and Yang (1947), who studied deposits on etched copper and iron single crystals.

Table 10. Electrolytically Deposited Metals

| Substrate | Type of surface | Deposit | Parallel planes | | Parallel axes | | % misfit | Reference |
|---|---|---|---|---|---|---|---|---|
| | | | Deposit | Substrate | Deposit | Substrate | | |
| Cu | B | Ni | (110) | (110) | [001] | [001] | −3 | (1) |
| Cu | A | Ni | (001) | (001) | [100] | [100] | −3 | (3) |
| Cu | B | β−Co | (110) | (110) | [001] | [001] | −2 | (1) |
| Cu | A | β−Co | (001) | (001) | [100] | [100] | −2 | (3) |
| Cu | B | Ag | (110) | (110) | [001] | [001] | +13 | (1), (3) |
| Cu | A | Ag | (001) | (001) | [100] | [100] | +13 | (3) |
| Cu | C | Ag | (111) | (111) | [1$\bar{1}$0] | [1$\bar{1}$0] | +13 | (1) |
| Cu | C | Au | (111) | (111) | [1$\bar{1}$0] | [1$\bar{1}$0] | +13 | (3) |
| Cu | C | Cr | (110) | (111) | [001] | [1$\bar{1}$0] | +13<br>−8 | (1) |
| Fe | B | Au | (001) | (110) | [100] | [001] | +42<br>+1 | (3) |
| Fe | B | Ag | (001) | (110) | [100] | [001] | +42<br>+1 | (3) |
| Pt | D | Cu | (110) | (110) | [001] | [001] | −8 | (2) |
| Pt | D | Ni | (110) | (110) | [001] | [001] | −10 | (2) |
| Pt | D | β−Co | (110) | (110) | [001] | [001] | −9 | (2) |
| Pd | E | Cu | (001) | (001) | [100] | [100] | −7 | (2) |
| Pd | E | Fe | (001) | (001) | [110] | [100] | +5 | (2) |
| Au | E | Fe | (001) | (001) | [110] | [100] | −1 | (2) |
| Au | E | β−Co | (001) | (001) | [100] | [100] | −13 | (2) |
| Au | E | Ni | (001) | (001) | [100] | [100] | −14 | (2) |
| β-brass | F | Cu | (211) | (211) | [1$\bar{1}\bar{1}$] | [01$\bar{1}$] | 0<br>+50 | (4) |
| β-brass | F | Cu† | (10$\bar{1}$0) | (211) | [0001] | [01$\bar{1}$] | 0 | (4) |

† Abnormal hexagonal close-packed structure.

Type of surface:

A Etched (001).
B Etched (110).
C Etched (111).
D (110) foil.
E (001) foil.
F Electropolished (211).

References:

(1) Cochrane (1936).
(2) Finch and Sun (1936).
(3) Finch, Wilman and Yang (1947).
(4) Takahashi (1952, 1953).

A study of copper deposits on an electrolytically polished (211) surface of β-brass has been made by Takahashi (1952, 1953). In addition to the occurrence of oriented face-centred cubic copper, it is found that a deposit

with a hexagonal structure also occurs. This fits with a close-packed hexagonal copper lattice and corresponds to a remarkably good fit on the $\beta$-brass surface, as shown in fig. 10. With all of the oriented electrodeposits the misfits are fairly small. Where a bad misfit occurs, it is accompanied by a low misfit in the perpendicular direction.

Fig. 10

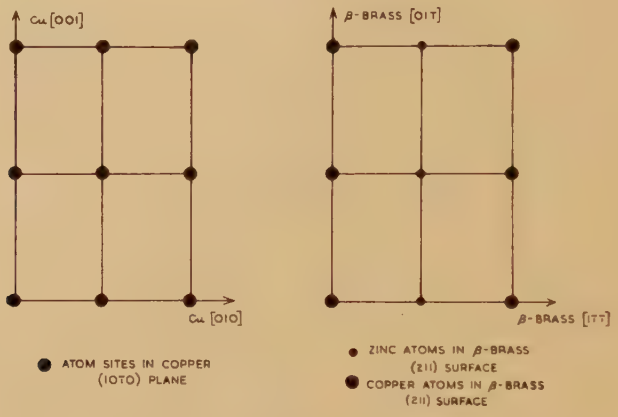


The fit of hexagonal copper on a $\beta$-brass (211) surface.

Bruck (1936) deposited silver and gold upon each other, from the vapour phase, the substrates being oriented metallic films formed by deposition on to rocksalt (see § 3.6). He found that oriented growth occurred when the substrate was heated above a certain temperature.

Table 11. Metals Condensed on to a Silver (111) Surface (Newman, results to be published)

| Metal | Structure | Orientation | | % misfit |
|---|---|---|---|---|
| | | Thin layer | Thick layer | |
| Cu | A | P | R | −11 |
| Au | A | P | R | 0 |
| Ni | A | R+P | R | −14 |
| Pb | A | P | R+P | +21 |
| Tl | B | P | R+P | +19 |
| Sn | C | A | S+R | +101<br>−36 |

Structures :

A, face-centred cubic. B, hexagonal close-packed. C, face-centred tetragonal.

Orientations :

P Hexagonal planes parallel.
S (011) Sn parallel to (111) Ag with [100] Sn parallel to [1$\bar{1}$0] Ag.
R Random.
A Amorphous.

More recently, Newman (results to be published) has studied the growth of extremely thin metallic deposits condensed on to atomically flat (111) silver surfaces maintained at room temperature. His results are given in table 11. The orientations were mostly prominent during the growth of the first approximately 10 Å in average thickness (thin layer) and predominantly random orientation occurred with thicker deposits.

### 3.6. *Metals upon Non-Metals*

The epitaxy of metals upon non-metals has been studied almost entirely by electron diffraction. The first evidence of orientation was obtained by Lassen (1934). Silver was deposited from the vapour phase *in vacuo*, on to a rocksalt cleavage surface and the resulting metal film was detached and examined by the transmission method. A parallel orientation of silver was indicated. This was immediately followed by an account by Lassen and Bruck (1935 a) of the preparation of good single crystal films of silver obtained by deposition on to heated rocksalt. The observed orientation corresponds to a misfit of $-27\%$. This caused Royer (1935) to challenge the observations and to point out that a misfit of only $+3\%$ would result from the orientation (100) silver parallel to (100) rocksalt, with the [011] of silver parallel to the [001] of rocksalt, which would therefore be expected to occur. However, Lassen and Bruck (1935 b) confirmed that their original claim was correct and that the latter orientation is not observed, despite the small misfit. This was confirmed by Kirchner and Lassen (1935), who used the reflection technique. The same result has since been obtained by many workers including Finch and Wilman (1937), Kirchner and Cramer (1938), Goche and Wilman (1939), Uyeda (1942), Shirai (1943 b), Johnson (1950 a) and Goswami (1954). Bru and Gharpurey (1951 a, b) and Raether (1951) also find parallel orientation of silver on (110) and (111) surfaces, where misfits are also $-27\%$.

Bruck (1936) has studied the growth of a number of metals on rocksalt and finds a marked dependence upon the temperature of the substrate. Above a certain critical temperature (the epitaxial temperature) good orientation was obtained ; below this temperature, the growth included at least some randomly oriented deposit. Bruck's results for the face-centred cubic metals are given in table 12. A characteristic of many of the above experiments is the occurrence of pronounced twinning on the (111) planes. This is discussed further in §§ 5.1 and 6.1.

The results for body-centred cubic metals are given in table 13. This includes data by Shirai, who has carried out many experiments by means of the transmission technique. In several cases the substrates were preheated to a temperature of several hundred degrees Centigrade before the deposition was carried out at some lower temperature. This appeared to influence the results. In addition to the orientations quoted by Bruck (1936), Shirai found that orientations with (111), (210) and (331) planes parallel to the surface occurred, the results being erratically dependent

Table 12. Observed Cases of Parallel Orientation of Face-Centred Cubic Metals upon Alkali Halides

| Substrate | Deposit | Epitaxial temperature (°C) | % misfit | References |
|---|---|---|---|---|
| NaCl | Ni | 370 | −38 | (1), (4), (2) |
| | $\beta-C_0$ | >540 | −37 | (1) |
| | Cu | 300 | −36 | (1) |
| | Pd† | 250 | −31 | (1), (5) |
| | Al‡ | 440 | −28 | (1) |
| | Au‡ | 400 | −28 | (1), (2), (6) |
| | Ag | 150 | −28 | (1), (3) |
| KCl | Ni | 410 | −44 | (1) |
| | Pd | 250 | −38 | (1) |
| | Ag | 150 | −35 | (1), (3) |
| | Pt | | −38 | (7) |
| KBr | Ag | 115 | −38 | (3) |
| KI | Ag | 80 | −42 | (3) |
| NaBr | Ag | 80 | −32 | (3) |

References :

(1) Bruck (1936).
(2) Shirai (1943 a).
(3) Shirai (1943 b).
(4) Collins and Heavens (1954).
(5) Fordham and Khalsa (1939).
(6) Trillat, Terao, Tertian and Gervais (1955).
(7) Thirsk (1950).

† (100) Pd parallel to (100) NaCl, with [011] Pd parallel to [001] NaCl, observed also (ref. (5)).

‡ (111) metal parallel to (100) NaCl, with [1$\bar{1}$0] metal parallel to [011] NaCl, observed at lower temperatures (refs. (1) and (2)).

Table 13. Observed Cases of Orientation of Body-Centred Cubic Metals upon Alkali Halides

| Substrate | Deposit | % misfit | | Reference |
|---|---|---|---|---|
| | | Orientation I | Orientation II | |
| NaCl | Fe | −28 | −28<br>−49 | (1), (2), (6) |
| | Cr | −28 | −28<br>−49 | (1), (3) |
| | Mo | −21 | −21<br>−44 | (4), (5) |
| KCl | Fe | −36 | −36<br>−54 | (6) |
| KBr | Fe | −38 | −38<br>−57 | (6) |
| KI | Fe | −43 | −43<br>−59 | (6) |

References :

(1) Bruck (1936).
(2) Shirai (1938).
(3) Shirai (1939).
(4) Shirai (1941 a).
(5) Shirai (1941 b).
(6) Shirai (1937).

Orientations :

I (100) metal ‖ (100) halide, with [011] metal ‖ [001] halide.
II (110) metal ‖ (100) halide, with [001] metal ‖ [001] halide.

Table 14. Metals upon Mica

| Metal | Epitaxial temperature (°C) | Plane parallel to surface | Axis parallel to mica [100] | % misfit | References |
|---|---|---|---|---|---|
| Ag | 150 | (111) | [1$\bar{1}$0] | −44 | (1), (2) |
| | | (111) | [2$\bar{1}\bar{1}$] | −68<br>−4 | (1), (2) |
| | 250 | (100) | [001] | −21<br>−54 | (2) |
| Au | 450 | (111) | [1$\bar{1}$0] | −44 | (1) |
| | | (111) | [2$\bar{1}\bar{1}$] | −68<br>−4 | (1) |
| Pd | 470 | (111) | [1$\bar{1}$0] | −47<br>−70 | (1) |
| | | (111) | [2$\bar{1}\bar{1}$] | −9 | (1) |

References :

(1) Rudiger (1937). (2) Thirsk (1950).

Table 15. Metals upon Calcite (Rudiger 1937)

| Metal | Epitaxial temperature (°C) | Plane parallel to calcite (100) surface | Axis parallel to calcite [001] | % misfit |
|---|---|---|---|---|
| Ag | 470 | (111) | [1$\bar{1}$0] | −10 |
| | 470 | (111) | [2$\bar{1}\bar{1}$] | −22 |
| | 510 | (100) | [011] | −10 |
| Au | 360 | (111) | [1$\bar{1}$0] | −10 |
| | 360 | (111) | [2$\bar{1}\bar{1}$] | −22 |
| | 470 | (100) | [011] | −10 |
| | 510 | (110) | [1$\bar{1}$2] | −22 |
| Pd | 400 | (111) | [1$\bar{1}$0] | −15 |
| | 400 | (111) | [2$\bar{1}\bar{1}$] | −26 |
| | 420 | (100) | [011] | −15 |
| | 490 | (110) | [1$\bar{1}$2] | −26 |

Table 16. Metals upon Fluorspar (Rudiger 1937)

| Metal | Epitaxial temperature (°C) | % misfit | |
|---|---|---|---|
| | | Orientation I | Orientation II |
| Ag | >500 | −25 | +30<br>−57 |
| Au | 380 | −25 | +30<br>−57 |
| Pd | 400 | −29 | +23<br>−59 |

Orientations :

I (111) metal ‖ (111) $CaF_2$ with [1$\bar{1}$0] metal ‖ [1$\bar{1}$0] $CaF_2$

II (111) metal ‖ (111) $CaF_2$ with [2$\bar{1}\bar{1}$] metal ‖ [1$\bar{1}$0] $CaF_2$

upon temperature. This behaviour was found for chromium (Shirai 1939), molybdenum (Shirai 1941 a, b) and iron (Shirai 1937, 1938), which was found to behave similarly upon KCl, KBr and KI.

Oriented growth of metals upon mica, calcite and fluorspar has also been found (see tables 14, 15, 16). These are characterized, in general, by the occurrence of mixtures of orientations which are temperature dependent. The misfits are often quite high, but can be considered as smaller if two deposit atom distances are compared with one corresponding substrate distance. The misfits quoted in table 15 refer to the calcite [001] direction only, since no other parallel lattice rows occur. In addition to the results quoted in table 14, Votava (1953) has found oriented growth on mica of platinum formed by a method due to Pigeon (1890). The metal crystallites in the form of hexagonal plates were visible under the optical microscope.

Table 17. Metals upon Mineral Sulphides

| Substrate | Deposit | Temperature conditions (°c) | Parallel planes | | Parallel axes | | % misfit | References |
|---|---|---|---|---|---|---|---|---|
| | | | Sub. | Dep. | Sub. | Dep. | | |
| $MoS_2$ | Pt | $\geqslant 250$ | (0001) | (111) | $[10\bar{1}0]$ | $[1\bar{1}0]$ | +4 | (6) |
| | Ag | $\geqslant 20$ | (0001) | (111) | $[10\bar{1}0]$ | $[1\bar{1}0]$ | +9 | (1), (2), (6) |
| | Cu | $\geqslant 50$ | (0001) | (111) | $[10\bar{1}0]$ | $[1\bar{1}0]$ | −3 | (6) |
| | Ni | $\geqslant 120$ | (0001) | (111) | $[10\bar{1}0]$ | $[1\bar{1}0]$ | −6 | (6) |
| | Au | $\geqslant 80$ | (0001) | (111) | $[10\bar{1}0]$ | $[1\bar{1}0]$ | +9 | (6) |
| PbS | Cu | 100 to 250 | (100) | (110) | [011] | $[1\bar{1}1]$ | −49<br>+6 | (4) |
| | Ag | $\geqslant 100$ | (100) | (100) | [001] | [001] | −31 | (1), (5) |
| ZnS | Au | $\geqslant 120$ | (110) | (110) | [001] | [001] | −25 | (3) |
| | Ag | $\geqslant 80$ | (110) | (110) | [001] | [001] | −25 | (1), (2) |
| | Ni | $\geqslant 120$ | (110) | (111) | [001] | $[1\bar{1}0]$ | −54<br>+12 | (3) |
| | Cu | $< 190$ | (110) | (310) | $[1\bar{1}0]$ | [001] | −6<br>+49 | (3) |
| | Cu | 190 to 350 | (110) | (110) | [001] | [001] | −33 | (3) |
| | Cu | 350 to 500 | (110) | (111) | [001] | $[1\bar{1}0]$ | −53<br>+15 | (3) |
| $FeS_2$ | Ag | $\geqslant 150$ | (100) | (100) | [001] | [001] | −24 | (1) |

References:

(1) Uyeda (1940).
(2) Uyeda (1942).
(3) Miyake and Kubo (1947 a).
(4) Miyake and Kubo (1947 b).
(5) Kubo and Miyake (1948).
(6) Kainuma (1951).

The deposition of metals on to mineral sulphide surfaces obtained by cleavage has been studied by a number of workers. Uyeda (1940, 1942) has studied silver on galena, molybdenite and zinc blende, and Miyake and Kubo (1947 a, b) have studied deposits upon galena. In the latter experiments the results were complicated by effects attributed to the diffusion of the metal into the galena, and to the occurrence of chemical reactions which lead to the formation of oxides and sulphides of the deposit metal, as well as of metallic lead. The orientation of these reaction products is considered in § 3.7. Where oriented metallic deposits were formed, the results are given in table 17. Kubo and Miyake (1948) have

also studied the growth of metals upon zinc blende. No misfit is quoted for the orientation of gold given in table 17, because it is stated that the (110) gold planes were not exactly parallel to the surface. For the growth of metals upon molybdenite (Kainuma 1951), a (111) plane of the metal is parallel to the hexagonal basal plane of the substrate ; mostly there is double positioning, but in the case of nickel and gold, single positioning occurs under some conditions.

### 3.7. *Chemically Grown Layers*

With the exception of a few x-ray studies, all of the results for the occurrence of preferred orientation in chemically grown layers have been obtained by electron diffraction. These results are given in table 18. Several types of reactions are included. In some cases the contact planes between the substrate and the overgrowth are not known, so that a significant value of the misfit cannot be determined. In other cases, the contact planes have been determined by special techniques (see § 2.3.3), or are fairly certain as a result of the type of substrate used. For these, a significant misfit value can be calculated, and has been included in table 18. These values vary between wide limits.

Fig. 12

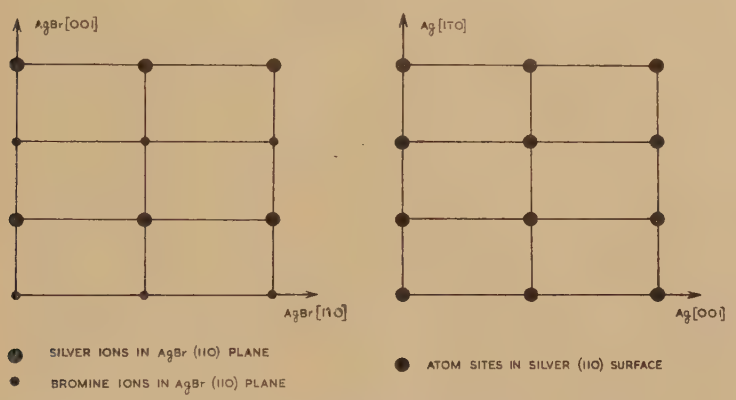


The fit of silver bromide on a silver (110) surface.

The chemically grown deposits have provided several clear examples of the dependence of the orientation upon the contact planes. Thus for silver halides upon silver, the orientation on the (100), (110) and (111) faces are quite different. It was originally found that silver bromide on the (111) face of a massive silver crystal is mainly in a fibrous orientation (Pashley 1952 a). However, more recently the author has carried out many experiments with substrates consisting of atomically flat highly oriented silver layers on mica, which have (111) planes parallel to the surface. When fresh surfaces are used, the orientation is not fibrous, but is very well defined, with the (111) planes of the bromide parallel to the

## Table 18. Orientation in Chemically Grown Layers

| Substrate | Type of surface | Deposit | Growth process | Parallel planes | | Parallel axes | | % misfit | References | Comments |
|---|---|---|---|---|---|---|---|---|---|---|
| | | | | Dep. | Sub. | Dep. | Sub. | | | |
| Cu | Etched | $Cu_2O$ | In air | (100) | (100) | [001] | [001] | +18 | (1), (3) | |
| | Etched (111) | $Cu_2O$ | Electrolytic | (111) | (111) | $[1\bar{1}0]$ | $[1\bar{1}0]$ | +18 | (2) | |
| | Electropolished | $Cu_2O$ | Immersion in boiling water | (100) | (100) | [001] | [001] | +18 | (4) | |
| | (100) foil | $Cu_2O$ | In air | (100) | (100) | [001] | [001] | +18 | (5), (31) | Other orientations in ref. (31) |
| | Etched (111) | $Cu_2O$ | In air | (111) | (111) | $[1\bar{1}0]$ | $[1\bar{1}0]$ | +18 | (6) | |
| | Etched (100) | $Cu_2O$ | 1000 c in air | (100) | (100) | [001] | [001] | +18 | (7) | Other orientations also |
| Fe | Etched | FeO | Heated to 700°c | (100) | (100) | [011] | [001] | +6 | (3) | |
| Fe | Evaporated film | $Fe_3O_4$ | | | | | | | (8) | A definite orientation not completely specified |
| Ba | Evaporated film | BaO | | | | | | | (9) | Do. |
| Ni | (100) foil | NiO | Heated in air | (111) | (100) | $[1\bar{1}0]$ | [011] | | (30) | |
| Pd | Thin foil | PdO | Annealed in air | (100) | (100) | [011] | [011] | | (10) | |
| Zn | (0001) cleavage | ZnO | In air | (0001) | (0001) | $[10\bar{1}0]$ | $[10\bar{1}0]$ | +22 | (11), (12) (13), (14) | |
| | (0001) electropolished | ZnO | Heated in air | (0001) | (0001) | $[10\bar{1}0]$ | $[10\bar{1}0]$ | +22 | (12), (15) | |
| | $(10\bar{1}0)$ electropolished | ZnO | Do. | $(10\bar{1}0)$ | $(10\bar{1}0)$ | [0001] | [0001] | +22<br>+5 | (12) | |
| | $(10\bar{1}0)$ etched | ZnO | Do. | (0001) | (0001) | $[10\bar{1}0]$ | $[10\bar{1}0]$ | +22 | (12) | Growth on facets |
| | $(10\bar{1}1)$ etched | ZnO | Do. | $(10\bar{1}1)$ | $(10\bar{1}1)$ | $[21\bar{3}\bar{2}]$ | $[21\bar{3}\bar{2}]$ | +22<br>+8 | (12) | Also facet growth |
| | | ZnO | Do. | $(10\bar{1}1)$ | $(10\bar{1}1)$ | $[1\bar{1}00]$ | $[21\bar{3}\bar{2}]$ | +22<br>+3 | (12) | |
| Cd | (0001) electropolished | CdO | Do. | (111) | (0001) | $[1\bar{1}0]$ | $[10\bar{1}0]$ | +12 | (12) | Also facet growth |
| | $(10\bar{1}1)$ electropolished | CdO | Do. | (111) | $(10\bar{1}1)$ | $[2\bar{1}\bar{1}]$ | $[21\bar{3}\bar{2}]$ | +12<br>+3 | (12) | |
| | $(10\bar{1}0)$ electropolished | CdO | Do. | (111) | $(10\bar{1}0)$ | $[1\bar{1}0]$ | $[01\bar{1}0]$ | +12<br>−7 | (12) | |
| CuZn | (100 foil | $Cu_2O$ | Water attack | (100) | (100) | [001] | [001] | | (16) | |

Table 18 (*continued*)

| Substrate | Type of surface | Deposit | Growth process | Parallel planes | | Parallel axes | | % misfit | References | Comments |
|---|---|---|---|---|---|---|---|---|---|---|
| | | | | Dep. | Sub. | Dep. | Sub. | | | |
| CuZn | (100) foil | ZnO | 450°c *in vacuo* | (0001) | (100) | [11$\bar{2}$0] | [011] | | (16) | Facet growth |
| Cu | Etched (111) | CuI | Electrolytic | (111) | (111) | [2$\bar{1}\bar{1}$] | [1$\bar{1}$0] | | (2) | |
| Cu | Etched (111) | CuBr | Electrolytic | (111) | (111) | [2$\bar{1}\bar{1}$] | [1$\bar{1}$0] | | (2) | |
| Cd | (10$\bar{1}$0) etched | $\beta$—CdS | Do. | (111) | (0001) | [1$\bar{1}$0] | [10$\bar{1}$0] | +39 | (12) | Facet growth |
| Cd | Do. | $\alpha$—CdS | Do. | (0001) | (0001) | [10$\bar{1}$0] | [10$\bar{1}$0] | +39 | (12) | |
| Ag | (100) foil | AgBr | Bromine attack | (100) | (100) | [011] | [001] | 0 | (17) | |
| | Do. | AgBr | Do. | (111) | (100) | [1$\bar{1}$0] | [001] | 0<br>+73 | (17) | |
| | Do. | AgCl | Chlorine attack | (100) | (100) | [011] | [001] | −4 | (17) | |
| | Do. | AgCl | Do. | (111) | (100) | [1$\bar{1}$0] | [001] | −4<br>+66 | (17) | |
| | Do. | hex. AgI | Iodine attack | (0001) | (100) | [10$\bar{1}$0] | [001] | +12<br>+95 | (17) | |
| | Do. | Cubic AgI | Do. | (111) | (100) | [1$\bar{1}$0] | [001] | +12<br>+95 | (17) | |
| | Do. | Cubic AgI | Do. | (100) | (100) | [011] | [001] | +13 | (17) | |
| | (100) facet or flat surface | AgBr | Bromine attack | (100) | (100) | [011] | [001] | 0 | (6) | |
| | | AgBr | Do. | (111) | (100) | [1$\bar{1}$0] | [001] | 0<br>+73 | (6) | |
| | | AgBr | Do. | (211) | (100) | [01$\bar{1}$] | [001] | 0<br>+23 | (6) | |
| | (110) facet or flat surface | AgCl | Chlorine attack | (100) | (100) | [011] | [001] | −4 | (6) | |
| | | AgBr | Bromine attack | (110) | (110) | [1$\bar{1}$0] | [001] | 0 | (6) | |
| | | AgCl | Chlorine attack | (110) | (110) | [1$\bar{1}$0] | [001] | −4 | (6) | |
| | | AgBr | Bromine attack | (111) | (111) | [1$\bar{1}$0] | [1$\bar{1}$0] | +41 | (6) | Also much fibrous growth |
| | (111) flat surface | AgCl | Chlorine attack | (111) | (111) | [1$\bar{1}$0] | [1$\bar{1}$0] | +36 | (6) | |
| | | Cubic AgI | Iodine attack | (111) | (111) | [2$\bar{1}\bar{1}$] | [1$\bar{1}$0] | −8 | (6) | |
| | | Cubic AgI | Do. | (111) | (111) | [1$\bar{1}$0] | [1$\bar{1}$0] | +59 | (6) | |
| | | Hex. AgI | Do. | (0001) | (111) | [1$\bar{1}$00] | [1$\bar{1}$0] | −8 | (6) | |
| | | Hex. AgI | Do. | (0001) | (111) | [10$\bar{1}$0] | [1$\bar{1}$0] | +59 | (6) | |
| $MoS_2$ | (0001) cleavage | $MoO_3$ | Heated in air | (010) | (0001) | [101] | [01$\bar{1}$0] | | (18) | |
| $Sb_2S_3$ | (010) cleavage | $Sb_2O_3$ | 270–440°c in air | (110) | (010) | [001] | [100] | −1<br>+2 | (19) | |

**Table 18** (*continued*)

| Substrate | Type of surface | Deposit | Growth process | Parallel planes | | Parallel axes | | % misfit | References | Comments |
|---|---|---|---|---|---|---|---|---|---|---|
| | | | | Dep. | Sub. | Dep. | Sub. | | | |
| ZnS | (110) cleavage | ZnO | Heated in air | $(10\bar{1}3)$ | (110) | $[01\bar{1}0]$ | $[1\bar{1}0]$ | | (20), (21), (24) | For further data see refs. (23) and (25) |
| ZnS | (100) natural | ZnO | Do. | $(20\bar{2}3)$ | (100) | $[01\bar{1}0]$ | [011] | | (22) | |
| ZnS | (110) natural | ZnO | Do. | $(10\bar{1}3)$ | (110) | $[01\bar{1}0]$ | $[1\bar{1}0]$ | | (22) | |
| ZnS | (111) natural | ZnO | Do. | (0001) | (111) | $[10\bar{1}0]$ | $[1\bar{1}0]$ | | (21), (22) | |
| PbS | (100) cleavage | $PbSO_4$ | Do. | (001) | (100) | [100] | [011] | | (26) | |
| PbS | Do. | $PbSO_4$ | Do. | (210) | (100) | [001] | [001] | | (26) | |
| PbS | Do. | $Pb_2SO_5$ | Do. | (210) | (100) | [001] | [001] | | (26) | |
| AgBr | (111) etched | Cubic AgI | Reaction in KI solution | (111) | (111) | $[1\bar{1}0]$ | $[1\bar{1}0]$ | | (27) | |
| AgBr | Do. | Hex. AgI | Do. | (0001) | (111) | [1000] | $[1\bar{1}0]$ | | (27) | |
| AgBr | Do. | Hex. AgI | Do. | (0001) | $(11\bar{1})$ | [1000] | $[1\bar{1}0]$ | | (27) | |
| PbS | (100 cleavage | Pb | Copper deposited on to heated base | (100) | (100) | [001] | [001] | −17 | (28) | |
| PbS | Do. | $Cu_2O$ | Do. | (100) | (100) | [001] | [001] | −28 | (28) | |
| PbS | Do. | $Cu_2O$ | Do. | (111) | (100) | $[1\bar{1}0]$ | [001] | 50<br>−12 | (28) | |
| PbS | Do. | FeS | Iron Deposited on to heated base | (100) | (100) | [011] | [001] | | (28) | |
| PbS | Do. | $\gamma-Fe_2O_3$ | Do. | (111) | (100) | $[1\bar{1}0]$ | [001] | | (28) | |
| PbS | (100) layer on rocksalt | $PbCl_2$ | Heated in air | (010) | (100) | [100] | [011] | | (29) | Mode of contact not clear |
| | | | | (012) | (100) | [100] | [011] | | (29) | |
| | | | | (110) | (100) | [001] | [011] | | (29) | |

References :


(1) Thomson (1948).
(2) Usmani (1941).
(3) Mehl, McCandless and Rhines (1934).
(4) Frisby (1947).
(5) Bruck (1936).
(6) Pashley (1952 a).
(7) Yamaguti (1938).
(8) Nelson (1937).
(9) Burgers and van Amstel (1936).
(10) Fordham and Khalsa (1939).
(11) Lucas (1951).
(12) Lucas (1952).
(13) Raether (1950).
(14) Ehlers and Raether (1952).
(15) Ehlers (1953).
(16) Takahashi (1954).
(17) Wilman (1940).
(18) Uyeda (1938).
(19) Miyake (1938).
(20) Yamaguti (1935).
(21) Aminoff and Broomé (1936).
(22) Aminoff and Broomé (1938).
(23) Uyeda, Takagi and Hagihara (1940).
(24) Evans and Wilman (1950).
(25) Uyeda, Takagi and Hagihara (1941).
(26) Hagihara (1952).
(27) Berry (1949).
(28) Miyake and Kubo (1947 a).
(29) Elleman and Wilman (1949).
(30) Shirai (1943 c).
(31) Shirai (1947).

surface and [1$\bar{1}$0] or [$\bar{1}$10] bromide directions parallel to the silver [110] axis (double positioning). In some cases preferred single positioning occurs ([1$\bar{1}$0] AgBr only parallel to Ag [1$\bar{1}$0]). This is illustrated in fig. 11 ; double positioning would give the same array of spots, but the intensity distribution in the pattern would be symmetrical about the central line. These orientations correspond to a +41% misfit between two parallel hexagonal networks. The exact nature of the orientation appears to depend upon thickness and is still being investigated. In contrast, the orientations on the (100) and (110) silver surfaces correspond to a zero misfit (see fig. 12).

An interesting effect is found for the growth of zinc oxide on a heated zinc blende surface. The hexagonal zinc oxide always grows with its [0001] axis nearly parallel to a [111] type axis of the sulphide, the exact orientation being slightly adjusted so that a particular lattice plane is exactly parallel to the surface, which has in all cases been parallel to a closely packed plane of the sulphide lattice. Since there are four distinct [111] type axes in the zinc blende, there are four possible orientations on any surface. Not all of these possibilities occur on a given face, the results depending upon the direction of the piezo-electric axis (Uyeda, Takagi and Hagihara 1940, 1941).

An effect which appears to be unique in studies of growth on single crystal substrates has been observed by Frisby (1948). Various electro-polished copper surfaces which contain a [110] axis, but which are not necessarily parallel to any lattice plane, have been oxidized in water at 100°C. It is found that a (110) plane of the cuprous oxide always grows parallel to the surface, with the [1$\bar{1}$0] direction parallel to the copper [110] axis. This appears to be the only known case, excepting ' fibrous ' orientations, where the arrangement cannot be defined in terms of two parallel lattice networks which have at least one pair of parallel lattice rows.

Most of the x-ray work has been carried out by Schwab (1942, 1947 a, b, c). Because of the uncertainty of the determination of the contact planes in this work, the results are not included in table 18. Oriented growths have, however, been established for a number of reactions, including halides upon silver, and silver and thallium halides upon each other by 'exchange' reactions.

According to the table published by van der Merwe (1949), magnesium oxide is oriented upon magnesium. The reference quoted is that of Finch and Quarrell (1933). This is an incorrect interpretation of the observed facts, and only followed from an unconfirmed remark concerning pseudomorphic growth (see § 4.2). There appears to be no valid evidence that the magnesium oxide is oriented upon magnesium.

### 3.8. *Orientation during Decomposition*

In addition to the occurrence of epitaxy in thin chemically grown layers, it is also found that orientation can occur during decomposition processes.

Berry (1949) and Berry and Griffith (1950) irradiated single crystals of silver bromide with ultra-violet. x-ray diffraction examination showed that silver in parallel orientation (two parallel cubic lattices) grows well inside the silver bromide, while electron diffraction examination showed that other orientations occur at the surface. Pashley (1951 b, 1952 c) has decomposed thin oriented layers of silver halide by electron bombardment in the electron diffraction camera (reflection technique). He finds that the silver is in a well-defined parallel orientation when the chloride and bromide are used, but that less marked orientation occurs with the iodide. Prominent (111) twinning is also observed. Although Trillat (1951, 1952) failed to find such orientation when thin oriented silver bromide films were examined by the transmission technique, Pashley (1952 d) has obtained orientation with such specimens of both chloride and bromide. The pattern of fig. 13 illustrates this. The square array of very intense spots is due to unchanged silver chloride, and the other weaker spots arise from silver in parallel orientation, including extra spots due to secondary diffraction. The absence of orientation in Trillat's films was explained as due to a gradual disorientation of the bromide, before decomposition, resulting from heating effects.

The decomposition of small crystals of silver azide has been studied by Sawkill (1955), who finds that much silver is formed with its cube planes parallel to the (100) plane of the azide, which has a body-centred orthorhombic structure. A [110] silver direction is parallel to the azide [001] direction.

## § 4. Spacing Measurements and 'Basal Plane Pseudomorphism'

### 4.1. *The Early Work and its Original Interpretation*

The term 'basal plane pseudomorphism' was introduced by Finch and Quarrell (1933) in the explanation of certain of their results concerned with sputtered metal films. It was found that zinc deposited on to a quartz substrate rapidly became covered with an oxide layer. Measurement of the electron diffraction rings obtained by the reflection technique revealed that a certain number of the rings fitted with neither metallic zinc nor zinc oxide. These extra rings were interpreted as arising from a new structure of the oxide, which is of the normal ZnO type, but which has a modified cell shape. The $a$-axis is reduced to equal that of the hexagonal metallic zinc lattice, while the $c$-axis is increased so as to maintain an approximately unchanged cell volume. The occurrence of the new cell was attributed to the influence of the metallic zinc structure. It was considered that the oxide grew in contact with the basal (0001) planes of the zinc and in parallel orientation, such that its basal plane was constrained to fit that of the zinc. This 'pseudomorphic' structure was believed to grow to a considerable thickness before recrystallization produced the normal structure. Later, Finch and Quarrell (1934) studied

by the transmission technique thin skins of zinc oxide which had been lifted on a gauze from the surface of molten zinc exposed to air. It was claimed that the resulting ring patterns also indicated the presence of this pseudomorphic structure.

Other similar cases have been reported. Finch and Quarrell (1933) deposited a layer of aluminium on to a previously sputtered layer of platinum, and concluded that the aluminium had formed in a new tetragonal structure. The basal plane of the new cell is supposed to fit the cube plane of the platinum. A layer of magnesium oxide (Finch and Quarrell 1933) formed by oxidation of sputtered magnesium was found to have abnormal spacings which were also attributed to pseudomorphic effects.

Cochrane (1936) found evidence for modified spacings in electrodeposited layers of nickel and cobalt on single crystals of copper. With a fast rate of deposition he obtained randomly oriented films of nickel, which gave rise to a pattern of rings which passed through the diffraction spots attributed to the underlying copper. It was concluded that all the spacings of the nickel lattice were abnormal and equal to that of the copper. With slow rates of deposition, Cochrane found that parallel orientation of nickel and cobalt occurred, and that this was accompanied by repeated twinning on the (111) planes, which gave rise to extra features on the diffraction patterns. Measurements indicated that the nickel and cobalt had spacings equal to that of the copper. Although there was no change in cell shape in these cases, it did appear to suggest some form of influence of the substrate on the lattice spacings of the overgrowth.

Miyake (1938) obtained anomalies in the spacing of $Sb_2O_4$ formed on stibnite ($Sb_2S_3$) which he has attributed to the influence of the stibnite substrate.

Clark, Pish and Weeg (1944) have studied the electroplating of several metals on to various metal sheets. In some cases, the absence of x-ray diffraction patterns from the thinnest layers is interpreted as due to a three-dimensional pseudomorphic effect.

### 4.2. *The Validity of the Early Results*

Despite the above evidence for the occurrence of basal plane pseudomorphism, many studies of even thinner layers of well-oriented deposits have failed to produce further evidence. Since the concept of ' basal plane pseudomorphism ' is frequently put forward in textbooks and reviews, it is of importance that the position should be thoroughly examined, in an attempt to discover why more evidence of the effect is not obtained. It is natural that this investigation should start with an examination of the validity of the earlier results.

With the exception of the work of Cochrane (1936) and Miyake (1938), none of the early experiments was carried out on single crystal substrates. Thus, in the case of the oxide on zinc, it was not even established that the

oxide was oriented, although this was an implicit assumption. In addition, only growth on hexagonal (0001) planes of the zinc was considered, although other types of facets, upon which the occurrence of different pseudomorphic structures would be expected, would certainly be present on a polycrystalline surface. More recently, therefore, other workers have investigated this aspect. Raether (1950), Lucas (1951, 1952), Ehlers and Raether (1952) and Ehlers (1953) have studied the growth of zinc oxide on single crystals of zinc. The first two papers deal with the growth which occurs upon a freshly cleaved surface, as soon as it is exposed to air. The oxide forms almost instantaneously, so that examination of the surface by electron diffraction gives rise to oxide diffraction patterns, but no patterns from the underlying metal. It is always found that the zinc oxide is oriented parallel to the zinc, and that it has its normal structure and lattice spacings. No evidence was found for the pseudomorphic structure. Attempts have been made to study the initial stages of oxidation, but the extreme affinity between zinc and oxygen has so far limited this aspect. Raether estimates that his oxide film is at least 20 to 40 Å in thickness. By cleaving a specimen and immediately plunging it into benzene, Lucas (1951) was able to reduce the thickness of the oxide sufficiently to allow the zinc substrate pattern to be obtained. The specimen was mounted with its surface still covered by benzene, which evaporated as the diffraction camera was evacuated. The film thickness under these conditions was estimated to be certainly less than 25 Å, it being difficult to make any accurate determination. Again the oxide had its normal structure. Although thinner layers could probably be studied if controlled growth were carried out on a specimen cleaved in a vacuum the main conclusion follows quite clearly without such experiments. The most favourable condition for the growth of the pseudomorphic form reported by Finch and Quarrell would undoubtedly be on the cleavage (0001) face of the metal. The experiments of Lucas and Raether show that such a structure does not occur, except possibly during the growth of the first two or three atomic layers only. But if the structure did occur in the first two or three layers only, it would not have been observed by Finch and Quarrell, since their experimental conditions would not have allowed the detection of such thin layers as readily as in the experiments of Raether (1950) and Lucas (1951). It therefore follows that the extra rings observed by Finch and Quarrell were not due to a pseudomorphic form of zinc oxide occurring as a result of epitaxy. Thus the existence of such a pseudomorphic growth is reduced to that of theoretical speculation and has no valid experimental foundation.

Experimental checks of the case of aluminium on platinum are not so easy. Although subsequent reports of this experiment have described it as growth on to ' a crystalline platinum substrate in (100) orientation ' (Quarrell 1941), this is an unjustified description. The actual substrate consisted of a layer of platinum sputtered on to a quartz surface. This layer was randomly oriented. A layer of aluminium was then evaporated

on to the platinum from a filament, the heating from which caused recrystallization of the platinum during the deposition, to give an oriented film (see Finch and Quarrell 1933, p. 413). A repeat of this experiment under more controlled conditions has probably not been carried out because of the difficulty of preparation of a suitable substrate. However, a close examination of the evidence of Finch and Quarrell (1933) reveals a completely different interpretation of the observations.

Finch and Quarrell appear to have treated their a pattern as one of continuous rings and to have used only the radii of the rings for the assignment of indices. They do not appear to have correlated the indexing with the distribution of the arcs of the pattern (see their fig. 9). However their published pattern is a contact print of the actual photograph and sufficiently accurate measurements can be made on this print to allow the unambiguous identification of the original measurements for almost every arc. In this way, the assignment of indices by Finch and Quarrell can be studied. This indexing is found to be inconsistent, as has already been pointed out by Shishakov (1952).

During the recrystallization process, the platinum substrate film orients in a fibrous manner, with its (100) planes parallel to the surface (see Finch and Quarrell 1933, fig. 12). There are two possible ways for the growth of the tetragonal aluminium.

Firstly, the (001) aluminium planes are parallel to the platinum surface (100) planes. This would give an (001) aluminium fibrous pattern, which would be a slightly distorted form of the published platinum pattern (see Finch and Quarrell 1933, fig. 12). This is clearly not the case, since the pattern obtained after the deposition of the aluminium shows pairs of arcs in place of the single arcs given by the platinum. The second possibility is that the aluminium (001) planes are parallel to either the (100), (010) or (001) platinum planes. This would correspond to the aluminium growing in a ' pseudomorphic ' manner on all of the cube-type platinum facets. This type of growth would give rise to the pattern plotted in fig. 14. It will be seen that the pattern is of the same basic form as a simple (001) fibrous pattern, but that many of the spots now become split into pairs or triplets. Part of this splitting would be obscured by the arcing of the patterns, but some of it would still remain observable. Comparison with Finch and Quarrell's pattern shows certain differences in form and many differences in indexing. Although the absence of triplets (e.g. the (420), (402) and (204) set) can possibly be explained as due to insufficient resolution (e.g. (402) and (420) unresolved), the observation of a doublet where a single arc is predicted (e.g. the (222) set) cannot be explained in this way. Also, the variation in the spot separations from pair to pair does not agree. Thus, in accord with the conclusions of Shishakov (1952), it is necessary to reject Finch and Quarrell's interpretation of the pattern.

The pattern may be completely and satisfactorily interpreted as due to a mixture of platinum and aluminium with their normal cubic structure

and lattice spacings. This interpretation is illustrated in fig. 15. The form of the pattern appears to be identical with the observations. The

Fig. 14

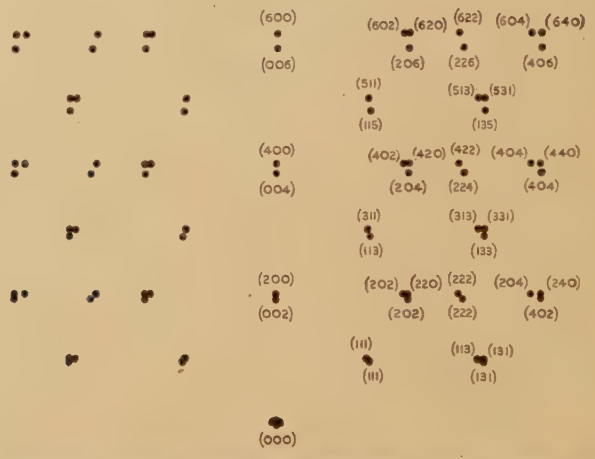


The indexed pattern which would be obtained from Finch and Quarrell's (1933) supposed pseudomorphic tetragonal aluminium layer. A superposition of (100) and (001) fibrous patterns.

Fig. 15


The indexed pattern which would be obtained from a mixture of normal aluminium and platinum in (001) fibrous orientation.

agreement with measurements is given in table 19. Finch and Quarrell's measurements have been used, but their calculated spacing values have been changed by $+2{\cdot}8\%$, corresponding to a wavelength error of $+2{\cdot}8\%$, to give the best agreement with the normal aluminium and platinum spacings. This adjustment is justified because Finch and Quarrell claim

an absolute accuracy of only about 2% for their measurements of the wavelength. This reinterpretation agrees with that put forward by Shishakov (1952), except for a few minor differences in indexing. However, it is considered that Shishakov's further deduction that the platinum has a slightly abnormal spacing is unjustified in view of the limited accuracy of the measurements.

Table 19. Interpretation of Pattern from Aluminium–Platinum Layer

| Data from Finch and Quarrell (1933) | | | Reinterpretation of the results | | | | |
|---|---|---|---|---|---|---|---|
| | | | | Aluminium | | Platinum | |
| $r$ (cm) | ($hkl$) tetragonal aluminium | $d$ Å ($\lambda$=0·0564) | $d$ Å ($\lambda$=0·0580) | ($hkl$) | $d$ Å | ($hkl$) | $d$ Å |
| 1·17 | (111) | 2·29 | 2·35 | (111) | 2·33 | (111) | 2·26† |
| 1·33 | (002) | 2·01 | 2·07 | (200) | 2·02 | (200) | 1·96† |
| 1·95 | (220) | 1·37 | 1·41 | (220) | 1·42 | (220) | 1·38† |
| 2·25 | (113) | 1·19 | 1·22 | (311) | 1·22 | | |
| 2·31 | (131) | 1·16 | 1·19 | | | (311) | 1·18 |
| 2·36 | (222) | 1·14 | 1·16 | (222) | 1·16 | | |
| 2·41 | | | 1·14 | | | (222) | 1·13 |
| 2·75 | (400) | 0·98 | 1·00 | (400) | 1·01 | (400) | 0·98† |
| 2·98 | (133) | 0·90 | 0·92 | (331) | 0·93 | | |
| 3·05 | (204) | 0·88 | 0·90 | (420) | 0·90 | (331) | 0·90 |
| 3·12 | (240) | 0·86 | 0·88 | | | (420) | 0·88 |
| 3·34 | (224) | 0·80 | 0·82 | (422) | 0·82 | | |
| 3·41 | (242) | 0·79 | 0·81 | | | (422) | 0·80 |
| 3·54 | (333), (115) | 0·76 | 0·78 | (511) | 0·78 | | |
| 3·61 | (151) | 0·74 | 0·76 | | | (511) | 0·76 |
| 3·90 | (440) | 0·69 | 0·71 | (440) | 0·71 | | |
| 3·97 | (135) | 0·67 | 0·69 | | | (440) | 0·69 |
| 4·08 | (153), (244), (351) | 0·66 | 0·68 | (531) | 0·68 | | |
| 4·15 | (600), (442) | 0·65 | 0·66 | | | (531) | 0·66 |
| 4·35 | (260) | 0·62 | 0·63 | (620) | 0·64 | | |
| 4·41 | (335), (226) | 0·61 | 0·62 | | | (620) | 0·62 |
| 4·50 | (353) | 0·60 | 0·61 | (622) | 0·61 | | |
| 4·60 | (262) | 0·58 | 0·60 | | | (622) | 0·59 |
| 4·89 | (406) | 0·55 | 0·56 | (711) | 0·56 | | |
| 5·00 | (460) | 0·54 | 0·55 | | | (711) | 0·55 |

†Aluminium and platinum arcs unresolved.

This interpretation of the pattern is perfectly reasonable. The aluminium is deposited on to randomly oriented platinum, which recrystallizes during the deposition because of heating effects. A mixture of aluminium and platinum is to be expected. It is therefore concluded that the evidence for a ' pseudomorphic ' tetragonal form of aluminium is false.

The experiments of Cochrane (1936) concerning nickel and cobalt deposits have been repeated in this laboratory by Newman (1956). He finds no change in spacing of nickel deposited at a fast rate (see § 4.1). The pattern interpreted by Cochrane as due to nickel rings passing through copper spots was, in fact, a pattern of nickel rings passing through nickel spots. Apparently some of the nickel was oriented,

even at the faster rates of deposition, giving rise to a nickel spot pattern, and sufficient nickel had been deposited to obscure the copper pattern.

For the slow rates of deposition, Newman confirmed Cochrane's result that the spacing of the deposited layer was that due to copper and not that of either nickel or cobalt. The electrolytic bath was being run under conditions for which no deposition would be expected, because the cell voltage was not above the overpotential. However, both Cochrane (private communication) and Newman obtained blackish-looking deposits. This deposition occurred because of unclean anodes and it was found by Newman that no deposition occurred when a carefully cleaned anode was used. This was checked, in the case of the cobalt bath, by the use of a radioactive cobaltous sulphate solution. It was found, by a tracer technique, that less than 1 A of cobalt was deposited, no matter how long the cell was left running, for the low current densities. However, an interesting result followed. The specimens treated in this way often showed considerably changed diffraction patterns, although no cobalt had been deposited. The patterns were very similar to those obtained from the specimens which showed the blackish deposits, prominent twinning spots and streaks being observed. This has been interpreted as resulting from the dissolution and subsequent redeposition of copper on to the specimen. This evidence gives a very plausible explanation of the spacing measurements on the deposited layers (Newman, to be published). The cobalt deposition occurs at a very slow rate, and is accompanied by the redeposition of copper. This latter would tend to deposit preferentially on the specks of deposited nickel or cobalt. This would result in the deposited nickel or cobalt being covered by a layer of copper, which would prevent its being observed by electron diffraction. It is also possible that small regions of nickel–copper or cobalt–copper alloy are formed. Even if these alloy regions did contribute to the diffraction pattern, their spacings would be indistinguishable from that of copper, unless they contained more than about 20% of the nickel or cobalt. Such an explanation of the observed spacing measurements seems far more plausible than that of the formation of metallic nickel or cobalt with lattice spacings equal to that of copper.

The other remaining supposed evidence of pseudomorphic growth (see § 4.1) is even less convincing. Miyake's (1938) identification of an $Sb_2O_4$ layer on $Sb_2S_3$ is complicated by the possibilities of other oxide formation. Finch and Quarrell's (1933) magnesium oxide layer gave a pattern of a few rather broad rings. If a wavelength error is allowed, most of these rings may be fitted to cubic magnesium oxide. The weakness of the evidence of Clark, Pish and Weeg (1944) is that their evidence is of a negative character. Certain electrodeposited layers of about 500 Å mean thickness gave no X-ray patterns, whereas 1000 Å layers did. There are several other possible interpretations of these results, besides the 'pseudomorphic' one. In any case, it is difficult to visualize (to quote one example) how a pseudomorphic zinc structure could be identical, as regards all

spacings, with that of steel. In view of the lack of detailed evidence in these three cases, they are rejected in that they do not supply conclusive evidence in favour of the hypothesis that ' pseudomorphic ' growths occur.

From the above examination of all of these early results it follows that in no case is the claim of the existence of a pseudomorphic structure justified. None of these experiments supports the model of pseudomorphic growth in epitaxy.

### 4.3. *The Extent to which Pseudomorphism can be Investigated Experimentally*

Since the early evidence on pseudomorphism is invalid, it is necessary to consider to what extent the phenomenon can be investigated experimentally. Many investigations of oriented layers which are less than 10 Å in average thickness have been carried out in this laboratory and elsewhere (see, for example, Schulz 1951 b, 1952 a, Uyeda 1942). In none of these experiments has positive evidence of pseudomorphism been found.

Electron diffraction can be used to analyse single atomic layers on flat surfaces, if the growth occurs in the form of monolayers (see § 2.3.6). The experiments which most nearly fulfil these conditions are those of Schulz (1951 b, 1952 a) concerning the growth of alkali halides upon other alkali halides and upon mica. When the misfit between overgrowth and substrate is less than about 10%, a deposit of less than one atomic layer in average thickness does not form independent widely separated nuclei, but collects into patches of some unknown size, but not more than an atom or two in thickness. Although Schulz (1951 b) originally suggested that the ' monolayer ' patches had spacings equal to that of the substrate, he appears to have modified his views, and has since stated (Gomer and Smith 1953, p. 375) : " . . . There was no evidence to show that the natural bulk spacing of the deposit changed to match that of the substrate ; the evidence (what there was) would suggest that the deposit always retained its natural bulk spacing. . . ". In addition, Blackman (1952) has pointed out that (111) alkali halide monolayers (on mica) would be of a special type, whose natural spacing would not be that of the bulk material. The detailed interpretation of the almost monolayer patterns is made difficult by their diffuse nature, which limits the accuracy of measurement to a few per cent. Further ambiguities could also arise as a result of secondary diffraction, which could shift the centre of a broad diffuse streak. This latter effect is illustrated in fig. 16. In addition to the primary diffuse streaks from the deposit (assumed, for this argument, to have its natural bulk spacing), secondary streaks could arise as a result of the substrate diffractions acting as new sources. The spots along the central line would give secondary patterns coincident with the primary patterns. The spots along the rows A of the substrate pattern, for example, would, if they acted as secondary sources, give rise to the extra diffuse

streaks indicated. These would merge along the lines B with the primary streaks to give broad diffuse streaks which would appear to have the same spacing as those of the substrate. In this way, a deposit which is a few per cent different in spacing from that of the substrate could give a diffuse streak pattern which would erroneously suggest a conformity in spacing. We have made some attempts in this laboratory to investigate in more detail the monolayer region found by Schulz, by using the continuous examination technique described in § 2.3.5. However, no further evidence has been obtained. With mica substrates, the substrate pattern is not sufficiently well defined to allow a conclusive study of the cases of small misfit (10% and less), because of charging effects with the mica. With alkali halide substrates it has been found that the continuous examination technique is not very successful because the electron beam affects the substrate in some manner which seriously influences the growth of the deposit. Our general experience so far would support the conclusion of Schulz which is quoted above. There is certainly no doubt that, once the deposit becomes more than about one atomic layer in average thickness separated crystallites are formed and that these have their natural bulk spacing.

Fig. 16

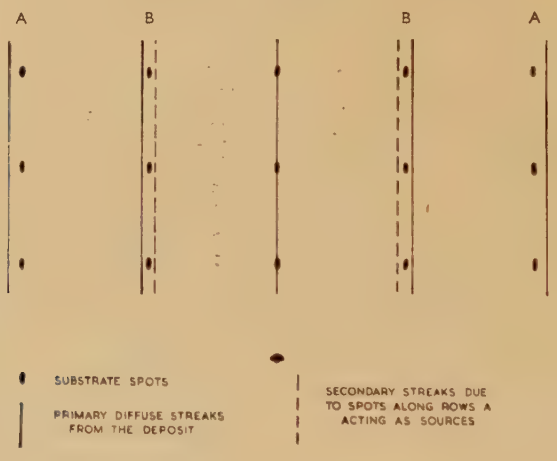


A possible effect of secondary diffraction upon spacing measurements of monolayers.

When the deposit grows in such a manner that it has formed widely separated crystallites when it first gives an observable pattern, the natural bulk spacing is always observed. At this stage, most of the crystallites will already have grown to a certain thickness, which will vary considerably from case to case. The value of the deposit lattice spacings at any earlier stage of their growth cannot be measured.

### 4.4. *Conclusions*

From the evidence available to date, it seems reasonable to conclude that pseduomorphism, in the sense in which it was first postulated by Finch and Quarrell, does not occur. Whether it occurs in a much more restricted sense is open to speculation, but certainly no positive evidence of this has been found.

## § 5. Experimental Evidence concerning the Mode of Growth of an Oriented Layer

Before any comprehensive theory of epitaxy can be formulated, a certain amount of knowledge of the mode of growth of an oriented layer is essential. Although optical microscope studies can give useful information, most of the existing direct evidence concerning the earliest stages of growth has resulted from electron diffraction studies.

### 5.1. *Monolayers and Nucleated Deposits*

One of the most important questions is whether the initial deposit grows in the form of a two-dimensional monolayer, or whether three-dimensional nuclei or crystallites are formed initially. It is possible to obtain the most systematic evidence in the case of growth *in vacuo* from the vapour phase, because this may be carried out inside a diffraction camera. For reliable results, it is necessary that an atomically flat substrate surface be used. Schulz (1951 b, 1952 a) has studied the growth of alkali halides upon other alkali halides and upon mica. He finds that the initial deposits are in the form of three-dimensional crystallites when the atomic misfit is greater than a certain value (20% for alkali halide substrates and 10% for mica substrates), but that the growth of ' monolayers ' occurs for smaller misfits. The evidence for these ' monolayers ' derives from the observation of streak patterns from deposits which are less than one molecular layer in average thickness. Because of the weakness and diffuse nature of these streaks, detailed interpretation is difficult. Schulz deduces that the deposits occur in patches of not more than an atom or two in thickness, but of unknown lateral extent (see Gomer and Smith 1953, p. 375). It is certainly quite clear that the deposit material spreads over the substrate surface far more in these cases than it does for cases of larger misfit. This kind of effect was observed as long ago as 1907 by Barker (1907, 1908), who obtained so-called zonal growths (Schichtkrystall) for certain cases of low misfits with growths of alkali halides upon each other.

In the majority of cases which are studied by electron diffraction, growth occurs in the form of three-dimensional crystallites, independent of the misfit. This applies, for example, to the growth of alkali halides

upon silver, calcite and sodium nitrate (Schulz 1952 b, c). Metallic deposits from the vapour mostly grow in this way, although it has been found by Newman (results to be published) that lead and thallium deposited on to an atomically flat (111) silver surface at room temperature spread considerably (perhaps even as monolayers) during the growth of the first few angströms in average thickness. This is illustrated by the diffraction pattern of fig. 17. The continuous streaks arise from the lead, or from secondary scattering involving lead and silver, and the few elongated spots from the silver substrate. This pattern should be compared with fig. 18, which shows the pattern obtained from the same thickness (2 Å) of copper on a similar silver surface (Newman and Pashley 1955). Separate nuclei of copper have formed, giving rise to a pattern of distinct, although diffuse, elongated spots. It is estimated that these nuclei are in the form of plates which are about 12 Å high and about 60 Å across. Seifert (see Gomer and Smith 1953, p. 361) has expressed doubts concerning the electron diffraction evidence on nucleation effects; he suggests that a real monolayer exists in addition to the separated nuclei, and that this monolayer might remain undetected by electron diffraction. This is certainly not the case in most experiments, since any monolayer would give an observable streak pattern. In the case of copper on silver quoted above, it was found that separated nuclei were formed when the average thickness of the deposit was only about one-third of that of a single atomic layer, as determined by a radioactive tracer method. There was not enough copper present to form a monolayer of appreciable area, in addition to the nuclei. This is also true of the deposits of alkali halides studied by Schulz, although his thickness estimates were less accurate.

The study of layers grown by methods other than from the vapour phase is difficult in the thickness range below 10 Å, because of the lack of control which results from the inability to examine the layers during their growth. What evidence there is, suggests that separated nuclei are formed in most cases. Oriented chemically grown layers of silver bromide on silver form independent crystallites (see fig. 19), the size of which is estimated to be 40 Å high by 70 Å across in a particular case (Newman and Pashley 1955). There appear to be no examples of studies of very thin layers of metals electrodeposited on to atomically flat substrates. In most examples of oriented growth from solution, microscope observations reveal that large isolated crystallites form on the substrate, but the average thickness of the deposit is always high. It is not usually known whether any of the deposit in the form of monolayers or otherwise, remains between the crystallites which are visible under the microscope. For one or two examples of alkali halides grown from solution on to mica, specimens have been examined both by optical microscopy and by electron diffraction (Lisgarten 1954). The appearance of strong mica diffraction patterns shows that a large part of the mica surface has not been covered by the deposit, and that aggregation into large crystallites is complete.

### 5.2. *The Mechanism of Formation of a Nucleus*

The occurrence of separated crystallites in a layer evaporated on to a flat substrate surface must result from the mobility of the deposit atoms. The manner in which this mobility leads to nucleation is not well understood, but from the various remarks which have been made in the literature, it may be said that there are two distinct possibilities. These may be termed as ' gradual nucleation ' and ' spontaneous nucleation '.

In a ' gradual nucleation ' mechanism the deposit atoms are mobile over the substrate until they lose sufficient thermal energy and become trapped on the surface, either at a random lattice site or at some preferred place such as a hole, edge or step. Once trapped, the deposit atom acts as a preferential point for the trapping of other deposit atoms, so that a nucleus, which it is assumed can be oriented, is built up. By this mechanism both the number and size of the nuclei would increase with any increase in the deposit thickness.

In a ' spontaneous nucleation ' mechanism crystallization occurs via an intermediate stage, which could be one of an amorphous or liquid state. When the amount of deposit material is increased to a certain value a crystallization process occurs, and nuclei are spontaneously formed. Again it is assumed that the nucleus can be oriented. This type of process might form a large number of nuclei of almost the same size, so that for a certain period of the growth the number of the nuclei would increase, but their sizes would not increase appreciably.

What evidence there is tends to favour some kind of ' spontaneous crystallization ' mechanism in some cases. According to Schulz (1952 a), the nucleated deposits of alkali halides upon alkali halides first give observable diffraction patterns for average thicknesses as low as 2 Å. The linear size of the nuclei at this stage is already at least 100 Å. As the thickness of the layer is increased to about 100 Å, no marked change occurs in the size of the nuclei, but the increase in pattern intensity indicates a large increase in the number of the nuclei. Newman and Pashley (1955) find similar effects with copper deposited on to silver (111) surfaces. The diffraction pattern is observed continuously during the growth of the copper, which takes place at a rate of only about 0·5 Å/min in average thickness. No visible change occurs on the diffraction pattern during the deposition of the first 0·8 Å ; a pattern of spots due to oriented copper nuclei of about 60 Å across then appears and these spots rapidly increase in intensity for further small increases in the deposit thickness. The number of nuclei increases, but their apparent size remains the same. This seems to be inconsistent with a ' gradual nucleation ' mechanism, but could perhaps be reconciled with some kind of ' spontaneous nucleation ' process. It is necessary to consider what form the deposit could take before appreciable nucleation occurs (i.e. at 0·8 Å) and why it gives rise to no observable diffraction pattern. Since very bright spot patterns are obtained from layers of

1·0 Å thickness, it would be expected that if the layers of 0·5 Å were of the same form and different only in amount, an observable pattern would be obtained from them. Only tentative suggestions can be offered at this stage. One possibility is that a large proportion of the first 0·8 Å of the deposit becomes trapped in holes, cracks or grain boundaries, where it will be shielded from the electron beam. Alternatively, all the copper may be contributing to the diffraction pattern, but this contribution is either (*a*) spread over the background of the pattern, or (*b*) coincides with the silver pattern. (*a*) would result from an almost random distribution of the copper atoms ; (*b*) would arise from regular arrays (perhaps two-dimensional) of the copper atoms, matching in form and spacing that of the silver substrate. In view of the results discussed in the next paragraph, (*a*) seems the more likely.

There is further evidence that, for a given substrate temperature, nucleation will not occur until sufficient material is deposited to form nuclei larger than a certain critical size. The solidification temperature of very small droplets is lower than the value for the bulk material. Turnbull (1950) has made measurements on the solidification temperature of droplets, 50 $\mu$ in diameter, of various metals and finds pronounced supercooling effects. Takagi (1954) has observed similar effects by

Fig. 20

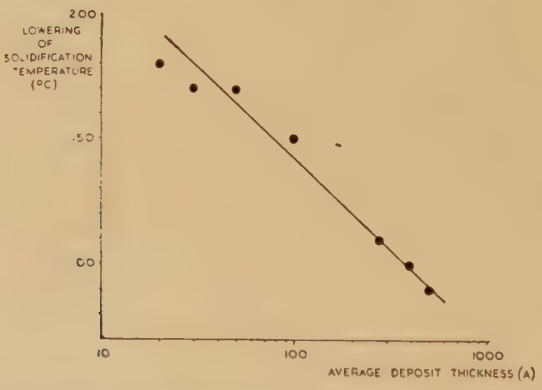


The solidification temperature of thin lead deposits (Takagi 1954).

electron diffraction with thin films of lead, bismuth and tin on a substrate surface. The solidification temperature is found to decrease as the average thickness of the deposit decreases. The results, for the case of lead, are given in fig. 20. When the layer is cooled below the solidification temperature, the diffraction pattern changes from one due to an amorphous or liquid state to one due to a crystalline deposit, which is oriented in some cases. With a behaviour of this kind, a layer condensed on to a substrate at a given temperature would be in a liquid or amorphous state until a thickness is reached at which the solidification temperature

of the layer equals the temperature of the substrate. Nucleation would then occur. This kind of behaviour has, in fact, been observed by Newman (work to be published) for the growth of tin on a silver (111) face at room temperature, the nucleation occurring at an average thickness of about 10 Å, to give a partially oriented layer.

### 5.3. *Influence of the Substrate Surface Topography*

When an atomically flat substrate surface is used, the orientation of any deposit will be controlled, in general, by the type of lattice plane parallel to the surface. When the substrate surface is rough on an atomic scale, it will influence the orientation of any overgrowth in a more complicated manner. The simplest case occurs when the substrate is bounded by well-defined facets ; for the growth of silver halides on silver (Pashley 1952 a) and of oxides on cadmium and zinc (Lucas 1952) it has been shown that the orientations which occur on such facets are the same as those which occur on flat surfaces of the same lattice type. In other cases, the interpretation of the observations is less obvious. It is possible that any form of surface irregularity, ranging from that which results from the termination of a dislocation line to larger features such as steps or cracks in the surface, might influence an overgrowth orientation. Such effects would be particularly marked if the growth were to occur preferentially at surface irregularities. Unfortunately, it is extremely difficult to determine experimentally whether any such surface features are of importance. Optical microscope evidence often shows that overgrowth crystallites are preferentially located at steps or other irregularities on the surface, as shown in fig. 21. However, there is usually no evidence to suggest that the irregularities have been responsible for the observed orientation. Thus, in fig. 21, a number of crystallites have formed along a curved step on the surface, but the orientation of the crystallites has not been influenced by the curvature of the step. Wilman (1951) has stated that rotational slip results show that the existence of angles or edges or cleavage steps is quite unnecessary for epitaxial orientation to occur. This deduction is far from convincing, since it is based upon data concerning the way in which two crystallites of the same substance are locked together, when they are misoriented with respect to one another by a small amount. This is, in the author's opinion, irrelevant to any general rules of epitaxy ; the latter involves the growth of one substance upon the surface of another.

Although no direct evidence of the effect of small-scale irregularities is available, there are indications that such effects are operative in some cases. The oriented growth of silver bromide on variously prepared silver surfaces (Pashley 1952 a) provides some evidence. Although the main orientations observed were not attributed to surface irregularity effects, some subsidiary orientations were interpreted in this way. This applied, in particular, to an orientation in which a (211) plane of silver bromide is parallel to a (100) plane of silver. The evidence that this is

initiated by surface irregularities (probably steps) is the following: (1) the (211) orientation does not occur on atomically flat (100) silver surfaces, but does occur on electropolished (100) surfaces, which are known to contain irregularities; (2) the (211) orientation occurs on (010) and (001) facets on an etched (100) surface, but not all equivalent orientations occur simultaneously; this can only be explained by asymmetries in the fine structure of the facet surfaces. It is interesting to note that this (211) orientation corresponds to a good fit only along the direction of the step at which it is supposed to form.

### 5.4. *Polymorphism in Thin Layers*

The measurement of the lattice spacings of small nuclei has been considered in § 4.3, it being shown that all evidence suggests that these spacings are nearly normal and are not constrained to fit that of the substrate. The structure of small oriented nuclei is not, however, always the same as that found for the bulk material. Rubidium bromide, which normally crystallizes with the rocksalt structure, is found to have the caesium chloride structure when deposited on to a silver substrate (Schulz 1951 a), the misfit being then zero; thallium chloride has a rocksalt structure instead of its normal caesium chloride structure when deposited on to potassium bromide (Pashley 1952 b).

Schulz (1951 c) has studied deposits of caesium and thallium halides on various substrates. Although these salts normally occur in bulk with the caesium chloride structure, the thin surface deposits often have the rocksalt structure. The complete results are summarized in table 20, which includes the values of the percentage misfits involved for both structures. The rocksalt type structures orient on the rocksalt type substrates in parallel orientation; the caesium chloride type structures grow with their (110) planes parallel to the substrate (001) surface, and their [001] direction parallel to the [110] or [1$\bar{1}$0] direction of the substrate.

It is clearly shown that the substrate has some influence upon the type of structure which occurs in the deposit, but the effect does not seem to be associated with a small misfit. In some cases (e.g. CsI upon mica), the normal structure is observed although a smaller misfit (+5% instead of +25%) would occur for the abnormal structure, which is observed upon other substrates.

No other systematic evidence of the occurrence of abnormal structures in oriented layers has been reported. A close-packed hexagonal structure has been observed in an oriented copper layer electrodeposited on to a single crystal of $\beta$-brass (Takahashi 1952, 1953), the normal copper structure being face-centred cubic. This case corresponds to a zero misfit (see fig. 10), but it is possible that the transition is influenced by the presence of small amounts of some impurity (particularly zinc) in the electrolytic bath.

Table 20. Observations on Polymorphism in Caesium and Thallium Halides (Schulz 1951 c)

| Substrate | LiF | | | NaCl | | | KBr | | | Mica | | |
|---|---|---|---|---|---|---|---|---|---|---|---|---|
| Deposit | I | II | III | I | II | III | I | II | III | I | II | III |
| CsCl | A | +72 | +44<br>+104 | A | +23 | +3<br>+45 | A | +5 | −12<br>+25 | A | −5 | +12 |
| CsBr | A | +80 | +51<br>+114 | A | +28 | +8<br>+52 | A | +10 | −8<br>+30 | A | −1 | +17 |
| CsI | A | +90 | +60<br>+127 | A | +36 | +15<br>+62 | A | +16 | −2<br>+38 | B | +5 | +25 |
| TlCl | | | | B | +12 | −3<br>+36 | A | −4 | −17<br>+17 | B | −14 | +5 |
| TlBr | A | +63 | +40<br>+98 | A | +17 | 0<br>+41 | A | 0 | −15<br>+21 | | | |
| TlI | A | +72 | +48<br>+109 | A | +23 | +6<br>+49 | A | +5 | −10<br>+28 | | | |

Column headings :
I, Observed structure. II, % misfit for structure A. III, % misfit for structure B.
A ≡ Rocksalt type structure. B ≡ Caesium chloride type structure.

### 5.5. *Variations with Thickness*

An oriented layer will usually persist only up to a certain thickness, after which further deposition gives rise to less regular growth. In some cases the transition occurs when the average thickness is only about 10 Å, while in other cases layers of several thousand ångströms are well oriented.

Most of the evidence concerning thickness effects has been obtained for the growth of metal films, for which pronounced temperature effects are observed (see § 3.6). For metals (silver has been studied in most detail) deposited from the vapour phase on to various heated substrates (rocksalt, mica, etc.) three main effects can occur during thickness increase : (1) twinning ; (2) changes in orientation ; (3) changes in surface topography.

Twinning on all four (111) planes occurs with most of the face-centred cubic metals. Where systematic tests have been carried out, it is found that the twinning does not occur in the thinnest deposits, but only develops as the thickness is increased above a certain value (Kirchner and Cramer 1938, Kehoe (results to be published)). One point of interest is that there is no conclusive evidence of the occurrence of second (or higher) twinning, i.e. twinning occurring on one set of (111) planes to give a new orientation (first-twin) which, at a later stage, twins on another set of (111) planes to produce a further orientation (second-twin). Such an effect produces sixteen orientations in addition to the initial or parent orientation. ' First-twinning ' gives rise to just four of these extra orientations. The orientations which arise may be readily deduced from the following expressions. A first-twin on the (111) plane has its $(hkl)$ plane parallel to the $(-h+2k+2l,\ 2h-k+2l,\ 2h+2k-l)$ plane of the parent, and for a first-twin on a $(11\bar{1})$ plane the corresponding plane is the $(-h+2k-2l,\ 2h-k-2l,\ -2h-2k-l)$. If a first-twin on the (111) plane is subsequently twinned on its (111) plane, the resulting second-twin has its $(hkl)$ plane parallel to the $(h-8k-4l,\ -8h+k-4l,\ 4h+4k-7l)$ plane of the substrate ; there are corresponding expressions for other combinations of twin planes.

Goswami (1954) claims to have observed second-twins with silver layers on a heated (001) rocksalt cleavage surface. When first-twinning occurs, it is often accompanied by the appearance of orientations involving a (211) type silver plane parallel to the (001) rocksalt surface. Extra spots due to these orientations are visible on fig. 4 of a paper by Kirchner and Cramer (1938), and the same orientation is found by Kehoe (results to be published). Goswami points out that some of the second-twins have a (211) type plane nearly parallel to the surface and so concludes that these orientations are due to second-twinning. However, the application of the above formula shows that it is the (447) plane which is exactly parallel to the (001) surface. The (112) plane makes an angle of $3\frac{1}{2}°$ with the surface. The observations are not consistent with a difference as large as this. It is therefore difficult to reconcile the (211) type orientation with second-twinning, although it does seem to have

some relation to the first-twinning, since it only appears when the twinning is present. In terms of the rocksalt substrate, this orientation is (211) Ag parallel to (001) NaCl, with the [01$\bar{1}$], [0$\bar{1}$1], [$\bar{1}$11] or [1$\bar{1}\bar{1}$] Ag directions parallel to the NaCl [110]. The four positions are geometrically equivalent.

There is evidence, in some cases, that the orientation of a deposit improves as it is built up. Randomly oriented material is formed during the early stages of growth, but the material deposited at a later stage is all well oriented. Rudiger (1937) has illustrated the effect quite clearly. Gold was deposited on to a thin sheet of mica at 380°c and examined by both reflection and transmission. The transmission pattern consisted mainly of rings, indicating that the bulk of the film had a fibrous structure, whereas the reflection pattern indicated complete orientation of the gold on its upper surface. Other evidence has not always been so decisive. When stripping methods are used as a means of study of thickness variations, spurious results can be obtained because the thin layers ($<$200 Å) become randomly oriented as a result of the stripping process (Bruck 1936). Further, the dependence upon thickness can be influenced by rises in temperature which can occur during the deposition as a result of radiant heat from the source or as a result of the thermal energy carried by the molecules. Because of these factors, the behaviour of the deposits depends considerably upon the experimental conditions. If a slow rate of deposition is used, and the radiation effect is reduced to a minimum by the insertion of suitable shields, any temperature rises can be made negligible. In some circumstances, the rises in surface temperature can be as high as a few hundred degrees Centigrade (Wilman 1955).

In view of the uncertainties involved, the majority of evidence concerning orientation improvements with thickness is not decisive. Even where the improvement is established as being a genuine effect of an increase in the thickness of the deposit, it is usually not possible to decide whether it has resulted from some kind of preferential growth on to the better oriented nuclei, or whether a complete recrystallization of the film has occurred at a certain stage of the deposition. More experiments on this aspect of oriented growth are necessary before any further conclusions can be drawn.

Since, in most cases, the metal is deposited in the form of separated crystallites, the initial layers are rough on an atomic scale. As the crystallites grow together to form a coherent film, there is often a tendency to form a fairly smooth surface. Silver on heated rocksalt behaves in this manner; in extreme cases, an atomically flat surface may be formed (Tull 1951). The author has studied in detail (results to be published) the growth of silver on mica heated to about 250°c. With a rate of deposition of a few hundred Å/min the deposit starts off as partly oriented in (111) double positioning ([1$\bar{1}$0] and [$\bar{1}$10] Ag parallel to mica [010]), and partly random. This is followed by twinning on all (111) planes and the disappearance of random orientation in the surface layers. As the thickness reaches several hundred ångströms, the twinning

becomes less pronounced and the surface starts to become smooth. The surface orientation gradually changes from double to single positioning ([110] Ag only parallel to mica [010]). With a thickness of more than about 1000 Å the surface is atomically smooth and it is oriented with complete single positioning.

### 5.6. *Perfection of Orientation*

The perfection of orientation varies considerably from case to case. Sometimes the deposits give rise to diffraction spots which are appreciably arced, indicating that the individual crystallites are aligned to an accuracy of only a few degrees. In other cases, the bright sharp Kikuchi line patterns from the deposit show that the alignment is much more accurate. Figure 22 shows a high angle Kikuchi pattern from a layer of silver on mica. The sharpness of the lines indicates that the variation in alignment of the silver crystallites is less than about one-fifth of a degree.

Some interesting misorientation effects are sometimes observed. It is found that a layer studied by the reflection technique gives a pattern of fairly sharp spots at one azimuth, but appreciably arced spots at the perpendicular azimuth (cf. figs. 23 and 24). Clearly, a misorientation has occurred as a result of a partial rotatory degree of freedom about one preferred axis parallel to the surface. This effect has been observed by Evans and Wilman (1950), with a layer of zinc oxide obtained by heating a cleavage (110) surface of zinc blende. The oxide is oriented with its (10$\bar{1}$3) plane parallel to the surface. When the electron beam is sent along the oxide [010] direction, the diffraction spots are prominently arced ; along the perpendicular azimuth, the diffraction spots are comparatively sharp. Their interpretation is that a disorientation of initially well aligned nuclei occurs as a result of rotational slip on the (12$\bar{1}$0) planes which are perpendicular to the [010] direction, so that an 'epitaxial strain' is relieved. This strain is supposed to result from the initial layers of the deposit having a pseudomorphic structure. There is no other evidence to support this hypothesis of the pseudomorphism of the zinc oxide layer. The explanation of Evans and Wilman does not seem very likely, since a similar effect has been observed (Pashley 1952 a) in a case where the misfit is zero and no epitaxial strain can possibly exist. This example is illustrated in figs. 23 and 24, which are patterns obtained from an oriented silver bromide layer on a (110) surface of silver. Along the |110] AgBr direction the diffraction spots are prominently arced (fig. 23) ; at the [001] azimuth, the spots are sharp. Misorientation occurs about the [1$\bar{1}$0] axis.

The origin and significance of these misorientation effects are still, therefore, a matter of speculation.

## § 6. Theories of Epitaxy

All theoretical considerations of the occurrence of epitaxy have been based upon the concept of the geometrical fitting between the lattices of the substrate and of the overgrowth. As a result of his extensive

studies, Royer (1928) put forward the three following rules for epitaxy : (1) That there exist lattice planes with networks, elementary or multiple, which are identical in form and of nearly the same dimension in the two structures. It is implied that these two networks grow parallel to one another. (2) That, where ionic crystals are involved, the ions of the overgrowth should take up positions which corresponding ions of the substrate of the same polarity would have occupied had the substrate continued to grow. (3) That the substrate and overgrowth crystals should have the same type of bonding.

The extensive data on epitaxy which has been accumulated since Royer's early work have shown quite definitely that the third rule is unnecessary. Thus, for example, ionic and metallic crystals can be mutually oriented (see § 3.4). In accord with the later views of Royer (1954), this rule must be rejected, at least in its original form.

The oriented growth of various metals on heated rocksalt (see § 3.6) could not be explained directly in terms of Royer's rules, since the orientation predicted by rule (1) did not occur. Bruck (1936) attempted to explain the results by saying that the orientation is such as to make the sum of the distances of the substrate ions from the deposit atoms a minimum when considered over one unit cell only. This rule has been criticized by Thomson and Cochrane (1939), who point out that what would be a favourable orientation for the first cell might be an unfavourable one for nuclei of greater lateral extent. Also, the effect of both positive and negative ions being present was not considered, and Engel (1953) has attempted to develop the rule to take this into account.

Dankov (1946, see also Pinsker 1953, p. 220) has attempted to establish the condition for the growth of an oriented crystal nucleus, strained to fit the substrate, by considering the energy of deformation which results from the misfit. However, this calculation cannot be carried out in most cases, because of the absence of the necessary lattice data. A calculation based upon the hypothetical growth of sodium chloride on sodium, under the action of chlorine gas, was carried out, but this led to no satisfactory application to other cases.

### 6.1. *The Menzer Mechanism*

Some attempts at explanation of the occurrence of large misfits have been based upon the idea that an oriented layer corresponding to a good fit occurs during the initial stages of growth and that subsequent growth gives rise to different orientations. The most notable of these mechanisms is that put forward by Menzer (1938 a, b, c) for the growth of nickel and silver on rocksalt. This is based upon the data of Bruck (1936), which showed that such layers are prominently twinned on their (111) planes when the film thickness is several hundred ångströms. Since the twinned lattices have (221) planes parallel to the rocksalt surface, Menzer suggested that the initial nuclei of the deposit grow with (221) planes parallel to the surface of the rocksalt, there being four geometrically equivalent positions for these nuclei (fig. 25). As deposition continues,

these nuclei are supposed to twin on their (11$\bar{1}$) planes and grow together to form an interpenetrating lattice which eventually develops into the parallel orientation. Goche and Wilman (1939) considered this mechanism to be consistent with their observations on silver films on rocksalt. The reciprocal lattice corresponding to the observed pattern consists of a body-centred cubic array of points (see fig. 6 of Goche and Wilman's paper) due to the parallel orientation, plus extra spots along the body diagonals ; these spots divide the diagonals into six equal parts. Only some of the extra spots arise directly from the (221) or twin orientations ; Menzer explained the remainder as due to the junction region between the parallel and twin lattices in which there is an incomplete filling of the (111) planes. This region is thus supposed to have a periodicity which is three times that of the normal lattice. The intensity of the extra spots indicated that the junction regions formed an appreciable part of the film.

Fig. 25

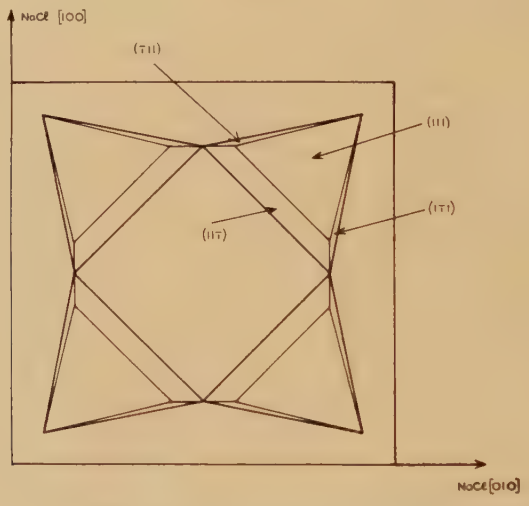


A plan view of four (221) silver nuclei on an (001) rocksalt surface. The boundary faces, all of (111) type, make the following angles with the rocksalt surface : (111), 15° 54′ ; (11$\bar{1}$), 54° 45′ ; ($\bar{1}$11) and ($\bar{1}$11), 78° 54′.

According to this mechanism, the misfit of the initial nuclei on the rocksalt substrate is only $-7\%$ for nickel and $+9\%$ for silver (see fig. 26). However, it should be pointed out that these misfits apply only if one silver (or nickel) distance is compared with two sodium distances along the silver (or nickel) [114] and if three silver (or nickel) distances are compared with two sodium distances along the silver (or nickel) [110]. This is really no better a fit than occurs for the parallel orientation, which is given in fig. 27. Along all of the principal directions the misfit can be regarded as $+9\%$ for silver (or $-7\%$ for nickel) if three silver (or nickel) distances are compared with two sodium distances.

It should also be pointed out that the mechanism only accounts for the twinning of the initial nuclei on their (11$\bar{1}$) planes. Twinning on the other (111) type planes, particularly the (111) (see fig. 25), of the (221) nuclei would give rise to orientations other than the parallel one ; these are not observed.

Fig. 26

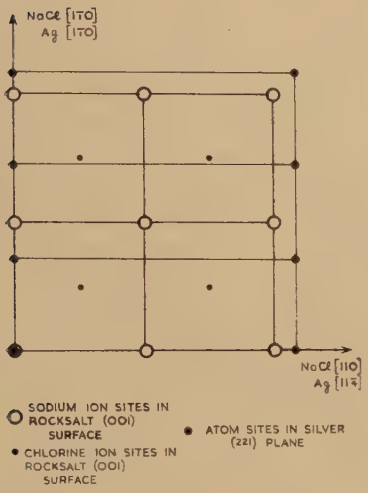


The fit of the (221) silver plane (Menzer hypothesis) on a rocksalt (001) surface.

Fig. 27

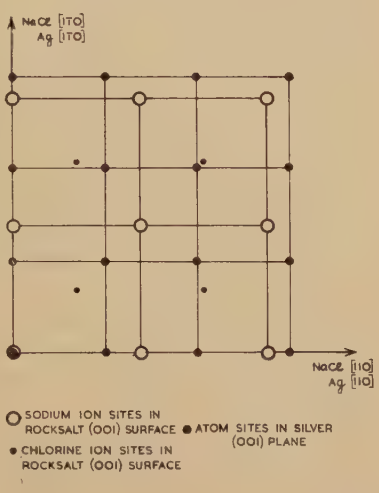


The fit of the (001) silver plane on a rocksalt (001) surface.

### 6.2. *The Engel Theory*

Engel (1952, 1953) has put forward a theory for the orientation of metals upon salt substrates, in which she attempts to explain both the observed fits and the dependence of the orientation upon the substrate temperature. This dependence (Bruck 1936) amounts to there being a minimum substrate temperature (the epitaxial temperature) for the occurrence of complete orientation. It is suggested that the first stage in the formation of an oriented film is that the atoms in the first layer become ionized, so that a two-dimensional chemical reaction occurs. A monolayer of the deposit–metal salt then exists at the interface between the substrate and the overgrowth. According to this theory, the occurrence of orientation depends upon the possibility of suitable ionization processes and upon the misfit of the intermediate salt with both the substrate and the deposit. An empirical approach indicates that an approximately linear relation exists between Bruck's observed epitaxial temperatures for various metals, and the ionization potential corresponding to the most commonly observed ionization state of the

metal. Engel suggests that this can be used to predict the epitaxial temperature for other metals.

As an illustration of the fits involved in this mechanism, the case of silver on rocksalt is quoted. The misfit of the silver chloride on rocksalt is only $-2\%$ and the misfit of the silver on the silver chloride is again only $-2\%$ if three cell lengths of the silver chloride lattice are compared to four cell lengths of the silver. However, this does not amount to any better fit than occurs without the silver chloride layer, since the application of this latter fitting procedure gives a misfit of only $-3\%$ for silver direct on to rocksalt.

### 6.3. *The Frank and van der Merwe Theory*

Van der Merwe (1949) and Frank and van der Merwe (1949 a, b, c) have put forward a theory of orientation, in which it is assumed that the initial stage of growth of an oriented deposit is the formation of an immobile monolayer of regular atomic pattern. This monolayer is considered to be homogeneously deformed to fit on to the substrate (i.e. have the same spacing), in order to form a suitable embryo. The theory is developed so as to lead to predictions regarding the necessary conditions under which such an embryo can be formed. A one-dimensional dislocation model is used, but reasons for justifying the extension of the results to two dimensions are given. The overgrowth is represented by a row of identical balls connected by a row of identical springs (force constant $\mu$); the substrate is represented by a periodic force acting on the balls, the first harmonic term ($\frac{1}{2}W$) of which is taken to represent the corresponding potential energy. It is shown that the lowest energy state of the system is the one with a monolayer constrained to fit the substrate, provided the misfit is less than a certain critical value given by $(b/a-1)_{\text{critical}}=2/\pi l_0$, where $a$ and $b$ are the natural spacings of the substrate and deposit respectively and $l_0^2=a^2/2W$. This critical misfit should be about $9\%$ in an average case, but would vary widely according to the relative values of $\mu$ and $W$ in a particular case. Above this critical misfit, dislocations will occur in the monolayer, but there remains an activation energy for their generation, which will be above zero for misfits less than a second critical misfit value of $1/l_0$, which will be about $14\%$ in an average case. Hence, below this second critical misfit, it is possible to form a metastable monolayer at sufficiently low temperatures.

Once this oriented monolayer has formed, a macroscopically thick oriented film can grow by repetition of the process. It was considered that this would give rise to an initially pseudomorphic film, which would undergo some transition process at a certain stage to give a strain free bulk deposit which remains oriented.

To summarize, according to this theory a necessary criterion for orientation is the formation of an initial pseudomorphic monolayer over the substrate surface. This will occur provided the misfit is less than a certain critical value, which is about $14\%$ in an average case.

### 6.4. *Discussion*

Since all of the theories involve the concept of good fitting between the substrate and overgrowth, the evidence concerning this will now be discussed.

Although many authors have explained the occurrence of a particular orientation as due to the existence of a small misfit, an examination of tables 1 to 18 shows that many cases of epitaxy involving large misfits are found. Any statistical analysis of all of the results is difficult, if not pointless. One of the best ways of considering the question is to examine cases where a series of similar deposits, with different spacings, has been studied on the same substrate. The results when both the substrates and the deposits are alkali halides are given in table 1. It is seen that although Royer and Sloat and Menzies found fairly well-defined misfit limits (e.g. $-13\%$ to $+9\%$ for a KCl substrate) for growth from aqueous solution, Schulz and Ludemann found no such limits for growth from the vapour phase. In these latter experiments, any alkali halide is found to orient on any other alkali halide and the complete results of these two authors indicate that epitaxy occurs for misfits covering the range $-43\%$ to $+90\%$. These are the limits set by the lattice constants available. Similar results followed from observations of the growth of alkali halides upon mica. Furthermore, it has been pointed out on several occasions (e.g. Thomson 1948) that the observed orientation is not always that which corresponds to the best fit. This applies particularly to the growth of metals upon alkali halides. The orientations corresponding to good fits are not observed, although they are observed when alkali halides are grown upon the metals (Johnson 1950 b, c, d, Schulz 1952 c).

Fig. 28


The regions of good fit introduced by the consideration of multiple fits.

In view of these conclusions, the concept of the need for a small misfit must be qualified considerably. The most obvious and most important conclusion is that the occurrence of a small misfit is not an essential condition for the appearance of orientation. Thus Royer's first law is invalid, at least in its original form.

When an orientation with a large misfit is observed, it is common practice to consider multiple fits, i.e. the fit of $m$ atom distances in the deposit with $n$ atom distances in the parallel direction in the substrate. This is, however, of dubious value, because a certain flexibility of application soon leads to an absurdity. If one allows only integral values of $m$ and $n$ of three or less, a misfit tolerance of $\pm 12\%$ would

allow almost all non-multiple misfits between $-70\%$ and $+130\%$ to be classed as good fits, as illustrated in fig. 28. The only appreciable gap is in the region of $20\%$ misfits and this would immediately be filled if $m$ and $n$ values of four were allowed. The significance of these remarks is illustrated by the fact that values as high as seven (Royer 1932) are sometimes put forward. Thus arguments concerning multiple fits must be treated with caution.

The Menzer mechanism (see § 6.1), which represents another attempt at explaining the occurrence of large misfits, is based upon the experiments of Lassen and Bruck (1935 a). In their work, silver films of several hundred ångströms in thickness were stripped from rocksalt substrates and examined by transmission; parallel orientation plus twinning was found. There was no direct evidence of the mode of growth of the initial nuclei. The growth of very thin layers of silver was studied by Kirchner and Cramer (1938), who used the reflection technique. They showed that twinning is not very prominent during the initial stags, but that it only becomes pronounced after the growth of the first 20 Å in average thickness. Similar results were found by Uyeda (1942). Later, Raether (1946, 1951) and Tull (1951) stripped layers of silver from rocksalt and examined, by the reflection technique, the silver which had been in contact with the rocksalt. Only silver in parallel orientation was observed. Raether (1951) concluded that Menzer's mechanism does not apply. Recently in this laboratory, Kehoe (results to be published) has examined the growth process in detail, by continuously studying the formation of deposits *in situ* in the diffraction camera. He finds that in the thinnest observable layers the silver is in parallel orientation and that twinning occurs only at a later stage. No (221) oriented nuclei occur as an initial stage of growth. These results are illustrated by figs. 29 to 31, which are from the same specimen at different stages of growth. In fig. 29, which corresponds to an average thickness of silver of only about 2 Å, the elongated spots are from the rocksalt substrate and the diffuse spots forming a centred rectangular pattern are from the silver in parallel orientation. Twin spots begin to appear at a thickness of about 10 Å and are clearly visible on fig. 30, which is from a layer of about 20 Å in thickness. This pattern is due entirely to the silver. At much greater thicknesses the silver surface becomes smoother, as indicated by the elongation of the main spots on fig. 31.

Further evidence concerning the Menzer hypothesis was obtained by Kehoe. He has studied growth of silver, copper and gold on several substrates and finds parallel orientation in all cases, at sufficiently high temperatures. Some of these cases (see table 21) would involve quite large misfits if they were interpreted in terms of the Menzer mechanism.

These results show, beyond all doubt, that the Menzer mechanism does not apply to the growth of a number of metals (including silver) upon alkali halides. The initial stage of growth is the formation of

nuclei in parallel orientation and twinning only occurs at a later stage of growth.

As a result of the data presented in tables 1 to 18, and on the basis of the above arguments, it is concluded that :

(1) A small misfit is not an essential condition for the occurrence of an oriented overgrowth.

(2) The orientation which occurs is not always that which corresponds to the best geometrical fit.

(3) Many cases of observed large misfits are not satisfactorily explained by the assumption of an intermediate orientation of smaller misfit, and the occurrence of very large misfits must be taken into account in any general theoretical treatment of epitaxy.

It follows from these conclusions that the Frank and van der Merwe theory (see § 6.3) cannot hold in general, since it predicts certain critical misfits for the occurrence of orientation. It is, however, necessary to consider whether this theory has a more limited application. Smollett and Blackman (1951) have criticized the theory on the basis that it predicts constrained monolayers which would not necessarily be stable. Certain examples of alkali halide monolayers in parallel orientation on

Table 21. Misfits for Observed Cases of Metals Oriented upon Alkali Halides (Kehoe, results to be published)

| Substrate | Deposit | % misfit for the parallel orientation | % misfit according to the Menzer mechanism |
|---|---|---|---|
| NaCl | Cu | −36 | −4 |
| NaCl | Au | −28 | +8 |
| NaCl | Ag | −28 | +9 |
| KBr | Cu | −45 | −18 |
| KBr | Ag | −38 | −7 |
| KCl | Cu | −42 | −14 |
| KI | Cu | −50 | −23 |

an alkali halide (100) surface were considered in detail. The effective elastic constants of the monolayers were found ; it was deduced that in some cases where oriented growth is known to occur, a monolayer constrained to fit on to the substrate would not be dynamically stable. It was therefore concluded that the orientation observed experimentally does not arise from an initial uniformly strained monolayer (for further comments on this point see Frank 1951 and Blackman 1951). Further, again with reference to the growth of alkali halides upon each other (see table 1), it is found that critical misfits are observed only in the case of growth from solution. However, it would be expected that the Frank and van der Merwe theory would apply to the vapour growth,

rather than growth from solution, since the theory did not take into account any possible influence of the solvent upon the growth. The results of Sloat and Menzies (1931) suggest that the presence of a solvent tends to reduce the chance of orientation rather than to increase it. Thus, in the case where the theory would be expected to be most applicable, there is no agreement with experiment. As is suggested by the calculations of Smollett and Blackman (1951), the discrepancy is probably due to the fact that the first stage of orientation is not the formation of a strained monolayer. The latest experimental evidence (see § 5.1) shows that in many cases, including some examples of growth of alkali halides upon each other, monolayers are not formed at all, but that surface migration of the deposit atoms leads to growth of small oriented three-dimensional nuclei. The Frank and van der Merwe theory would then not apply because it is based upon an initial mechanism which is not relevant to these cases.

The experiments of Kehoe which are quoted above also throw doubt upon Engel's theory (see § 6.2) of the effect of substrate temperature on the orientation of metals upon salts. Kehoe finds that good orientation occurs at temperatures appreciably lower than Bruck's (1936) epitaxial temperatures. Precautions were taken to ensure that no appreciable heating occurred during the deposition of the layers. The rates of deposition were lower than those used by Bruck, and smaller thicknesses were examined. The results suggest that the epitaxial temperatures observed by Bruck were a characteristic of the ability of the metal to orient upon itself, after the formation of initial oriented nuclei, rather than to orient upon the substrate. This is presumably controlled by an effect associated with surface mobility.

## § 7. Summary and Discussion

The electron diffraction method has contributed in two main ways to the subject of epitaxy. It has supplied many new examples of oriented growth and has provided certain information about the mode of growth of the initial nuclei of an oriented deposit. Although it has been concluded that a small misfit is not an essential criterion for the occurrence of epitaxy, it is not intended to imply that the misfit value has no significance. The results of Royer and of Sloat and Menzies (see tables 1, 2 and 3) provide very convincing evidence that the misfit value is significant under certain conditions. However, the writer is of the opinion that the concept of small misfit values has dominated the subject more than is justified by the experimental facts. Other approaches to the problem are needed.

The concept of basal plane pseudomorphism, which is linked with the small misfit criterion, has likewise been applied too widely, in view of the limited experimental backing. As is argued in § 4, none of the original evidence is valid, and more recent experiments have failed to supply any support for the concept.

The failure of existing theories in supplying a satisfactory explanation of epitaxy is that they are based upon unsuitable models for the growth of the initial nuclei of the deposit. In the case of the Menzer mechanism, the explanation was based upon effects (e.g. twinning) which are now known to occur only after the initial oriented nuclei have been formed. In the case of the Frank and van der Merwe theory, the concept of pseudomorphic monolayers was used. These monolayers certainly do not form in many cases. It therefore follows that the most important aspect of the study of epitaxy is the consideration of the mode of formation of the initial oriented nuclei. This is likely to vary considerably, according to the method used for the preparation of the deposit, as well as to other experimental conditions. Chemically grown deposits require special attention, because the substrate undergoes changes during the growth of a surface film.

Both experimental and theoretical studies of the nucleation problem are highly desirable. As a first step, it is necessary to determine the size and form of the smallest stable nuclei, under a given set of growth conditions. The energy of all possible arrangements of these nuclei must then be considered, so that the most probable orientation can be determined. This is a formidable task, and very little progress can be expected in the near future, because of the considerable lack of knowledge about the surface forces which are involved. However, from this point of view it might reasonably be expected that some form of preferred orientation will always occur provided the activation energies involved are not too high. Accordingly, as has already been pointed out by Schulz (see Gomer and Smith, 1953 p. 374), the actual problem should be to account for the failures to observe orientation.

Many failures may be due to the limitations of the method of observation. In particular, the study of extremely thin layers has shown that good orientation sometimes occurs only during the growth of the first hundred ångströms (e.g. Schulz 1952 a, for alkali halides upon themselves), or even just the first ten ångströms (e.g. Newman and Pashley 1955, for copper on silver). It is interesting to note that in both of these quoted examples, the poor orientation of the deposit occurs at a stage when the initial nuclei have just about covered the substrate surface. It is at this stage that the growth ceases to take place upon the flat substrate surface and starts to occur predominently on the existing deposit nuclei. Failure to observe orientation in these thicker films is therefore not directly related to growth of the deposit upon the substrate.

Acknowledgments

The author expresses his gratitude to Dr. M. Blackman, whose comments and discussions have stimulated many of the ideas presented in this article. He also wishes to thank Dr. R. B. Kehoe and Dr. R. C. Newman for allowing some of their unpublished results to be quoted and for supplying photographs. The article was written when the author was an I.C.I. Research Fellow in The University of London.

## References


Aminoff, G., and Broome, B., 1936, *Nature, Lond.*, **137,** 995 ; 1938, *Kungl. Svenska Vetensk. Handb.*, **16,** No. 7.

Barker, T. V., 1906, *J. Chem. Soc. Trans.*, **89,** 1120 ; 1907, *Mineral Mag.*, **14,** 235 ; 1908, *Z. Kristallogr.*, **45,** 1.

Beeching, R., 1936, *Electron Diffraction* (London : Methuen).

Berry, C. R., 1949, *Acta Cryst.*, **2,** 393.

Berry, C. R., and Griffith, R. L., 1950, *Acta Cryst.*, **3,** 219.

Blackman, M., 1951, *Proc. Phys. Soc.* A, **64,** 942 ; 1952, *Ibid.*, **65,** 1040.

Boersch, H., 1953, *Z. Phys.*, **134,** 156.

Boswell, F. W. C., 1950, *Phys. Rev.*, **80,** 91 ; 1951, *Proc. Phys. Soc.* A, **64,** 465.

Bradley, D. E., 1954, *Brit. J. Appl. Phys.*, **5,** 96.

Bridgman, P. W., 1925, *Proc. Amer. Acad. Arts Sci.*, **60,** 313.

Bru, L., and Gharpurey, M. K., 1951 a, *Proc. Phys. Soc.* A, **64,** 283.

Bru, L., and Gharpurey, K. G., 1951 b, *An. Soc. esp. Fis. Quim.* A, **47,** 101.

Bruck, L., 1936, *Ann. Phys.*, **26,** 233.

Burgers, W. G., and van Amstel, J. J. A. P., 1936, *Physica*, **3,** 1057.

Clark, G. L., Pish, G., and Weeg, L. E., 1944, *J. Appl. Phys.*, **15,** 193.

Cochrane, W., 1936, *Proc. Phys. Soc.*, **48,** 723.

Collins, L. E., and Heavens, O. S., 1952, *Proc. Phys. Soc.* B, **65,** 825.

Dankov, P. D., 1946, *Zhur. Fiz. Khim.*, **20,** 853.

Deicha, G., 1946, *C.R. Acad. Sci., Paris*, **223,** 1155 ; 1947 a, *Bull. Soc. franc. Mineral*, **70,** 177 ; 1947 b, *Ibid.*, **70,** 318 ; 1947 c, *La Nature*, No. 3143, 279 ; 1948, *C.R. Acad. Sci., Paris*, **226,** 412 ; 1949, *Nature, Lond.*, **164,** 68.

Ehlers, H., 1953, *Z. Phys.*, **136,** 379.

Ehlers, H., and Raether, H., 1952, *Naturwissenschaften*, **39,** 487.

Elleman, A. J., and Wilman, H., 1948, *Proc. Phys. Soc.*, **61,** 164 ; 1949, *Ibid.* A, **62,** 344.

Engel, O. G., 1952, *J. Chem. Phys.*, **20,** 1174 ; 1953, *J. Res. Nat. Bur. Stand., Wash.*, **50,** 249.

Evans, D. M., and Wilman, H., 1950, *Proc. Phys. Soc.* A, **63,** 298.

Finch, G. I., and Quarrell, A. G., 1933, *Proc. Roy. Soc.* A, **141,** 398 ; 1934, *Proc. Phys. Soc.*, **46,** 148.

Finch, G. I., and Sun, C. H., 1936, *Trans. Faraday Soc.*, **32,** 852.

Finch, G. I., and Wilman, H., 1937, *Ergebn. exakt. Naturw.*, **16,** 353.

Finch, G. I., Wilman, H., and Yang, L., 1947, *Disc. Faraday Soc.* A, **43,** 144.

Fordham, S., and Khalsa, R. G., 1939, *J. Chem. Soc.*, p. 406.

Frank, F. C., 1951, *Proc. Phys. Soc.* A, **64,** 941.

Frank, F. C., and van der Merwe, J. H., 1949 a, *Proc. Roy. Soc.* A, **198,** 205 ; 1949 b, *Ibid.*, **198,** 216 ; 1949 c, *Ibid.*, **200,** 125.

Frankenheim, M. L., 1836, *Ann. Phys.*, **37,** 516.

Frisby, H., 1947, *C.R. Acad. Sci., Paris*, **224,** 1003 ; 1948, *Ibid.*, **226,** 572.

Goche, O., and Wilman, H., 1939, *Proc. Phys. Soc.*, **51,** 625.

Gomer, R., and Smith, C. R. (Editors), 1953, *Structure and properties of solid surfaces* (Chicago : University Press).

Goswami, A., 1954, *J. Sci. Industr. Res.* B, **13,** 677.

Hagihara, H., 1952, *J. Phys. Chem.*, **56,** 610.

Heintze, W., 1937, *Z. Kristallogr.*, **97,** 241.

Ito, K., Ito, T., and Watanabe, M., 1954, *J. Electronmicroscopy*, **2,** 10.

Johnson, G. W., 1950 a, *J. Appl. Phys.*, **21,** 449 ; 1950 b, *Ibid.*, **21,** 1057 ; 1950 c, *J. Chem. Phys.*, **18,** 154 ; 1950 d, *Ibid.*, **18,** 560 ; 1951, *J. Appl. Phys.*, **22,** 797.

Kainuma, Y., 1951, *J. Phys. Soc. Japan*, **6,** 135.

KIRCHNER, F., 1937, *Ann. Phys.*, **30,** 619.
KIRCHNER, F., and CRAMER, H., 1938, *Ann. Phys.*, **33,** 138.
KIRCHNER, F., and LASSEN, H., 1935, *Ann. Phys.*, **24,** 113.
KIRCHNER, F., and RUDIGER, O., 1937, *Ann. Phys.*, **30,** 609.
KRANERT, W., LEISE, K. H., and RAETHER, H., 1944, *Z. Phys.*, **122,** 248.
KUBO, M., and MIYAKE, S., 1948, *J. Phys. Soc. Japan*, **3,** 114.
LASSEN, H., 1934, *Phys. Z.*, **35, 172.**
LASSEN, H., and BRUCK, L., 1935 a, *Ann. Phys.*, **22,** 65 ; 1935 b, *Ibid.*, **23,** 18.
LAUE, VON M., 1936, *Ann. Phys.*, **26,** 25 ; 1937 a, *Ibid.*, **29,** 211 ; 1937 b, *Ibid.*, **30,** 616 ; 1948, *Metariewellen und ihre Interferenzen* (Leipzig : Geest & Portig K.G.).
LAUE, VON M., and RIEWE, K. H., 1936, *Z. Kristallogr.*, **95,** 408.
LISGARTEN, N. D., 1954, *Trans. Faraday Soc.*, **50,** 684.
LUCAS, L. N. D., 1951, *Proc. Phys. Soc.* A, **64,** 943 ; 1952, *Proc. Roy. Soc.* A, **215,** 162.
LÜDEMANN, H., 1954, *Z. Naturforsch.*, **8a,** 252.
MEHL, R. F., M'CANDLESS, E. L., and RHINES, F. N., 1934, *Nature, Lond.*, **134,** 1009.
MENZER, G., 1938 a, *Naturwissenschaften*, **26,** 385 ; 1938 b, *Z. Kristallogr.*, **99,** 378 ; 1938 c, *Ibid.*, **99,** 410.
MERWE, J. H. VAN DER, 1949, *Disc. Faraday Soc.*, No. 5, p. 201.
MIYAKE, S., 1938, *Sci. Pap. Inst. Phys. Chem. Res. Japan*, **34,** 565.
MIYAKE, S., and KUBO, M., 1947 a, *J. Phys. Soc. Japan*, **2,** 15 ; 1947 b, *Ibid.*, **2,** 20.
MOLLENSTEDT, G., 1946, *Nachr. Wiss. Göttingen* (No. 1), p. 83.
MUGGE, O., 1903, *Neues Jarbuch für Mineralogie, Beilage-Band*, **16,** 335.
NELSON, H. R., 1937, *J. Chem. Phys.*, **5,** 252.
NEUHAUS, A., 1950–51, *Fortschr. Mineral.*, **29–30,** 136 ; 1952, *Angew. Chem.*, **64,** 158.
NEWMAN, R. C., 1956, *Proc. Phys. Soc.* B, **69,** 432.
NEWMAN, R. C., and PASHLEY, D. W., 1955, *Phil. Mag.*, **46,** 927.
PASHLEY, D. W., 1951 a, *Proc. Phys. Soc.* A, **64,** 1113 ; 1951 b, *Fundamental Mechanisms of Photographic Sensitivity* (London : Butterworth), p. 39 ; 1952 a, *Proc. Roy. Soc.* A, **210,** 355 ; 1952 b, *Proc. Phys. Soc.* A, **65,** 33 ; 1952 c, *Phil. Mag.*, **43,** 1028 ; 1952 d, *Acta Crystallogr.*, **5,** 850.
PIGEON, L., 1890, *C.R. Nebd. Seances Acad. Sci.*, **110,** 79.
PINSKER, Z. G., 1953, *Electron Diffraction* (London : Butterworth).
QUARRELL, A. G., 1941 (see CHALMERS, B., and QUARRELL, A. G., 1941, *The Physical Examination of Metals* (London : Edward Arnold), Vol. II, p. 216).
RAETHER, H., 1946, *Optik*, **1,** 296 ; 1949, *Z. Naturforsch.*, **4a,** 582 ; 1950, *J. Phys. Radium*, **11,** 11 ; 1951, *Ergebn. exakt. Naturw.*, **24,** 54 ; 1952, *Z. angew. Phys.*, **4,** 53.
ROYER, L., 1928, *Bull. Soc. franc. Mineral*, **51,** 7 ; 1932, *C.R. Acad. Sci., Paris*, **194,** 1088 ; 1935, *Ann. Phys.*, **23,** 16 ; 1937, *C.R. Acad. Sci., Paris*, **205,** 1418 ; 1948 a, *Ibid.*, **226,** 95 ; 1948 b, *Ibid.*, **226,** 262 ; 1954, *Bull. Soc. franc. Mineral*, **77,** 1004.
RUDIGER, O., 1937, *Ann. Phys.*, **30,** 505.
SAWKILL, J., 1955, *Proc. Roy. Soc.* A, **229,** 135.
SCHULZ, L. G., 1951 a, *J. Chem. Phys.*, **19,** 504 ; 1951 b, *Acta Crystallogr.*, **4,** 483 ; 1951 c, *Ibid.*, **4,** 487 ; 1952 a, *Ibid.*, **5,** 130 ; 1952 b, *Ibid.*, **5,** 264 ; 1952 c, *Ibid.*, **5,** 266.
SCHWAB, G. M., 1942, *Z. phys. Chem.* B, **51,** 245 ; 1947 a, *Trans. Faraday Soc.*, **43,** 715 ; 1947 b, *Ibid.*, **43,** 733 ; 1947 c, *Proc. Int. Congr. Pure and Appl. Chem.*, **11,** 269.

Seifert, H., 1953 (see Gomer and Smith, 1953, pp. 218–72).
Shirai, S., 1937, *Proc. Phys.-Math. Soc. Japan*, **19,** 937 ; 1938, *Ibid.*, **20,** 855 ; 1939, *Ibid.*, **21,** 800 ; 1941 a, *Ibid.*, **23,** 12 ; 1941 b, *Ibid.*, **23,** 914 ; 1943 a, *Ibid.*, **25,** 168 ; 1943 b, *Ibid.*, **25,** 633 ; 1943 c, *Ibid.*, **25,** 637 ; 1947, *J. Phys. Soc. Japan*, **2,** 81.
Shishakov, N. A., 1952, *Zh. Eksper. Teor. Fiz.*, **22,** 241.
Sloat, A. C., and Menzies, A. W. C., 1931, *J. Phys. Chem.*, **35,** 2005.
Smollett, M., and Blackman, M., 1951, *Proc. Phys. Soc.* A, **64,** 683.
Takagi, M., 1954, *J. Phys. Soc. Japan*, **9,** 359.
Takahashi, N., 1952, *C.R. Acad. Sci., Paris*, **234,** 1619 ; 1953, *J. de Chimie Physique*, **50,** 624 ; 1954, *C.R. Acad. Sci., Paris*, **238,** 462.
Thirsk, H. R., 1950, *Proc. Phys. Soc.* B, **63,** 833.
Thomson, G. P., 1948, *Proc. Phys. Soc.*, **41,** 403.
Thomson, G. P., and Cochrane, W., 1939, *The theory and practice of electron diffraction* (London : Macmillan).
Tolansky, S., 1948, *Multiple beam interferometry* (Oxford : Clarendon Press).
Trillat, J. J., 1951, *C.R. Acad. Sci., Paris*, **233,** 1188 ; 1952, *Acta Crystallogr.*, **5,** 471.
Trillat, J. J., Terao, N., Tertian, L., and Gervais, H., 1955, *C.R. Acad. Sci., Paris*, **240,** 1557.
Tull, V. F. G., 1951, *Proc. Roy. Soc.* A, **206,** 219.
Turnbull, D., 1950, *J. Appl. Phys.*, **21,** 1022.
Usmani, I. H., 1941, *Phil. Mag.*, **32,** 89.
Uyeda, R., 1938, *Proc. Phys.-Math. Soc. Japan*, **20,** 656 ; 1940, *Ibid.*, **22,** 1023 ; 1942, *Ibid.*, **24,** 809.
Uyeda, R., Takagi, S., and Hagihara, H., 1940, *Proc. Imp. Acad. Tokyo*, **16,** 386 ; 1941, *Proc. Phys.-Math. Soc. Japan*, **23,** 1049.
Votava, E., 1953, *Naturwissenschaften*, **40,** 290.
Wakkernagel, F., 1825, *Kastner's Archiv. f. gesammte Naturlehre*, **5,** 293.
Wallerant, F., 1902, *Bull. Soc. franc. Mineral*, **25,** 180.
West, C. D., 1945, *J. Opt. Soc. Amer.*, **35,** 26.
Wilman, H., 1940, *Proc. Phys. Soc.*, **52,** 323 ; 1951, *Ibid.* A, **64,** 329 ; 1955, *Ibid.* B, **68,** 474.
Wood, W. A., 1930, *Proc. Phys. Soc.*, **43,** 138 ; 1935, *Trans. Faraday Soc.*, **31,** 1248.
Yamaguti, T., 1935, *Proc. Phys.-Math. Soc. Japan*, **17,** 443 ; 1938, *Ibid.*, **20,** 230.

# *On the Thermal Conductivity and Thermoelectric Power of Semiconductors*

By D. ter Haar† and A. Neaves‡
Department of Natural Philosophy, St. Salvator's College, St. Andrews

[Received January 31, 1956]

CONTENTS



## § 1. Introduction

Recently there has been shown an increased interest in the thermoelectric properties of semiconductors, partly because of possible technical applications of such new semiconducting materials as InSb (Ross and Saker 1955, Saker, Cunnell and Edmond 1955) and $Bi_2Te_3$ (Goldsmid and Douglas 1954, Goldsmid 1955). It is well known that the theory of these effects is very complicated, even if one considers only the electronic component (compare a forthcoming review article by V. A. Johnson). However, it is impossible to account for the observed steep increase of thermoelectric power at low temperatures, if one considers only this component. In the present paper we are therefore considering the lattice component of the thermoelectric power and at the same time the lattice component of the thermal conductivity which follows from the same equations. In § 2 we discuss the various approximations which are usually made in a discussion of transport properties and from that discussion it is clear that it is well nigh impossible not to make some assumptions. We therefore decided to investigate as comprehensively as

† Present address : The Clarendon Laboratory, Oxford.
‡ Present address : Admiralty Materials Laboratory, Holton Heath, Poole, Dorset.
|| Communicated by the Authors.

possible the various scattering mechanisms, but to neglect the influence of deviations from spherical energy surfaces and many-electron phenomena. We also restrict our discussion to the case where only one type of carrier is present, although it would be straightforward to extend the theory to the case of both hole and electron conduction.

One must consider simultaneously phonon scattering and electron scattering. Following Makinson (1938) we assume electron–phonon scattering to be active at high and electron-impurity scattering to be active at low temperatures, while at low temperatures we consider scattering of phonons by boundaries, electrons, and impurities and at high temperatures by electrons, impurities and phonons. This gives us six temperature ranges to consider for which we give expressions for the thermal conductivity and thermoelectric power (see equations (168) to (179)). Most of the paper is concerned with the derivation of these equations, but the last section is devoted to a discussion of the results obtained and a comparison of these with the scarce experimental material available. It is shown that although qualitative agreement exists between theory and experiment, this is not true quantitatively.

## § 2. General Considerations.

"The quantum theory of solids has the reputation of being rather less respectable than other branches of modern theoretical physics. There is some justification for this view because the dynamics of many-body systems, with which it is concerned, cannot be handled without the use of simplifications, or without approximations which often omit essential features of the problem." These opening sentences of Peierls' recent monograph (1955) indicate the problems which confront us when we try to explain theoretically the properties of solids. Although the Drude–Lorentz theory (Lorentz 1909) as modified by Sommerfeld (1928) and Sommerfeld and Bethe (1933) can account in many cases qualitatively for the observed transport properties of metals and semiconductors, this so-called elementary electron theory (for an account we refer to Wilson 1953 (in the following referred to as TM) Ch. I, Seitz 1940, Ch. IV, ter Haar 1954, Ch. X) cannot quantitatively account for the great diversity of observed transport phenomena.

For our further discussion it is useful to list various assumptions introduced in this theory. They are the following ones :

(i) It is possible to define a relaxation time, $\tau$, or a mean free path, $l$, for the charge carriers ;

(ii) one may neglect the influence of the lattice, apart from the fact that it provides a mechanism by which a finite relaxation time may be realized ;

(iii) if $f_0$ denotes the equilibrium carrier distribution function and $f$ the carrier distribution function in the presence of external fields and/or temperature gradients, $|(f-f_0)/f_0| \ll 1$ ;

(iv) one may treat the carriers as if they were independent, that is, one may use the so-called one-electron approximation ;

(v) the equilibrium distribution function $f_0$ depends on the carrier wave vector $\mathbf{k}$ only through the energy $E$ ;

(vi) the energy surfaces are spherical, that, $E$ depends on $\mathbf{k}$ only through its absolute magnitude $k$.

In the development of the elementary electron theory further assumptions are introduced, such as the degeneracy of the gas of conduction electrons in the case of metals or the ' quasi-free ' approximation (see eqn. (17) below). It is interesting to note that assumptions (i) and (iii) together suffice to prove (compare TM p. 196, Peierls 1955, § 6.1) that one may use for $f$ the usual Lorentz expression (1905, 1909 ; see eqn. (15) below).

Several attempts have been made to consider the influence of removing one or more of the restrictive assumptions, but to remove all, and to take into account as well the recently acquired knowledge about the macroscopic structure of solids, is clearly a Herculean task and it seems that for some time to come one must be satisfied to tackle the problem piecemeal and to investigate the influence of the various factors separately, hoping that cross effects will not seriously upset the conclusions reached by this approach and that one's approximations are at least consistent. That one can easily be led astray was illustrated by Sondheimer (1956) who showed that the work by the present authors (ter Haar and Neaves 1955) on the thermoelectric power of metals suffered from inconsistency in the approximations used.

Various Russian authors have in recent years tried to eliminate assumption (iv), but up to now their theories do not seem to be in a state where quantitative numerical predictions can be made. We refer to survey papers by Anselm (1951) and Wonssowski (1954) for a discussion of these theories, and only mention here that it looks from their work as if this particular assumption does not affect the final results to any great extent (see, however, Bontsch–Brujewitsch 1955 and Pines 1955). One should have expected this, since in the case of metals the Pauli principle will effectively restrict the possible interactions between the conduction electrons, while in semiconductors the carrier density will be small enough for two-carrier processes to be negligible.

An interesting point is in how far assumption (vi), especially when taken in conjunction with the ' quasi-free ' approximation, is justified. It is perhaps surprising that nobody seems to have attempted to introduce the vast amount of results from band theory into a systematic discussion of transport phenomena, apart from introducing an effective mass into the discussion (compare Peckar 1946, James 1949, Slater 1949) and from using a two-band approximation (e.g., TM p. 198, Hung 1950). Recent work on cyclotron resonance in germanium (Dexter *et al.* 1954, Lax *et al.* 1954) has shown the necessity to introduce warped energy surfaces and the

so-called many-valley model is now being investigated (Zeiger 1955, Herring 1955, Zeiger, Lax and Dexter, private communication, Lax and Mavroides, 1955).

The main interest of many recent investigations has been in the discussion of assumptions (i) and (ii) and in the calculation of the relaxation time $\tau$. We refer to TM for an account of this work. The present paper falls into this category and we shall throughout introduce assumptions (iii) to (vi) as well as the ' quasi-free ' approximation. Our investigations were instigated by the experimental results of Frederikse (1953) on the thermoelectric power of germanium at low temperatures. His work was an extension of the measurements by Lark-Horovitz *et al.* (1946) and by Middleton and Scanlon (1953). The latter experiments could readily be explained by using the elementary electron theory (Johnson and Lark-Horovitz 1953, see also Lautz 1953), taking into account that there is both electron and hole conduction and that degeneracy (Johnson and Lark-Horovitz 1947) may occur. However, Frederikse's results could not be explained in that way and he suggested that there might be a contribution from the lattice current, the so-called Gurevich effect (1945) ; the same suggestion has been made independently by Herring (1953, 1954 b ; see also Klemens 1954, Parrott 1954) to explain similar experimental results obtained by Geballe and Hull (1954) and Geballe (1953). In the present paper we discuss the influence of lattice heat current and lattice non-equilibrium on both the thermoelectric power and the thermal conductivity. As in an earlier paper (ter Haar and Neaves 1955, to be referred to as A) we shall use Makinson's method (1938, to be referred to as M) which was an extension of a paper by Wilson (1937) on the second order electrical effects in metals. It will be seen that, indeed, the influence of the lattice is of great importance, especially at low temperatures. A preliminary account of the results of some of our calculations on the thermal conductivity was given at the 1954 Amsterdam Conference (ter Haar and Neaves 1954).

We should at this point make a few remarks about our earlier paper on the thermoelectric power of metals at temperatures around the Debye temperature. In that paper we calculated the Thomson coefficient $\gamma$ which is related to the thermoelectric power $Q$ by the Kelvin relation

$$Q=\int(\gamma/T)\,dT. \quad . \quad . \quad . \quad . \quad . \quad . \quad . \quad . \quad (1)$$

In our calculations we assumed (A, eqn. (25)) that we could neglect the electron non-equilibrium in calculating the lattice distribution function. However, Sondheimer (1956) has pointed out that this assumption leads to a violation of the Onsager relations and that one can thus no longer expect that the expression for $Q$ derived from eqn. (1) will be the same as the one derived directly from the current density $J$ in the presence of an electric field $\mathscr{E}$ and a temperature gradient $dT/dx$,

$$\mathbf{e}J=\sigma[(\mathbf{e}\mathscr{E}+d\zeta/dx)-\mathbf{e}Q\,dT/dx], \quad . \quad . \quad . \quad . \quad . \quad (2)$$

where $\zeta$ is the Fermi-level, $\sigma$ the electrical conductivity and $\boldsymbol{e}$ the charge of the carriers. As a result most of the results of A will be incorrect. Moreover, we should like to express our regret for not having discussed in A. Gurevich's paper, the results of which in many respects agree with ours at least qualitatively.

For an understanding of the physical background of the thermoelectric effect it is illuminating to consider briefly the phenomenological theory of these effects (TM § 8.4, ter Haar 1954, App. II, de Groot 1951, Samoilowitsch and Korenblit 1954). Consider a piece of wire under the influence of an electric field $\mathscr{E}$ and a temperature gradient $dT/dx$. There will be both an electrical current density $J$ and a heat current density $w$ and we have the relations

$$J=A(\boldsymbol{e}\mathscr{E}+d\zeta/dx)+B\,dT/dx, \quad . . . . . (3)$$

$$w=C(\boldsymbol{e}\mathscr{E}+d\zeta/dx)+D\,dT/dx, \quad . . . . . (4)$$

where the gradient of the Fermi-level acts as an electrical field, since the Fermi-level is, indeed, the electrochemical potential (compare the discussion on p. 229 of ter Haar 1954).

If the experimental set-up is such that $J=0$ we get the thermoelectric power $Q$ from eqn. (3),

$$Q=-B/A\boldsymbol{e}. \quad . . . . . (5)$$

If, on the other hand, $dT/dx=0$, we are dealing with the Peltier effect, and the Peltier heat $\Pi$, which is the flow of heat per unit electric current is given by the equation

$$\Pi=C/A. \quad . . . . . (6)$$

Finally, the Thomson coefficient $\gamma$ is defined as the negative of the coefficient of $J(dT/dx)$ in the expression for the rate at which heat accumulates, $dH/dt$, in a unit volume of the wire. Now, we have

$$dH/dt=J\mathscr{E}-dw/dx, \quad . . . . . (7)$$

or eliminating $\mathscr{E}$ from eqns. (3), (4) and (7)

$$dH/dt=J^2/A\boldsymbol{e}-(J/\boldsymbol{e})(d\zeta/dx)-(B/A\boldsymbol{e})J(dT/dx)-J[d(C/A)/dT](dT/dx)$$
$$+(d/dx)[\{(BC-AD)/A\}(dT/dx)], \quad . . . . . (8)$$

or

$$\gamma=B/A\boldsymbol{e}+d(C/A)/dT. \quad . . . . . (9)$$

From eqns. (5), (6) and (9) we see that, if the Onsager relations are satisfied, that is, if

$$BT=-C\boldsymbol{e}, \quad . . . . . (10)$$

eqn. (1) and the other Kelvin relation

$$\Pi=QT \quad . . . . . (11)$$

are realized, and one can thus use any of the three eqns. (5), (6) or (9) to calculate the thermoelectric coefficients.

Before we discuss the results obtained by using Makinson's equations we want to remind the reader that one can obtain from simple kinetic arguments (ter Haar 1956) the following expressions for the thermal conductivity $\kappa$ and for the thermoelectric power $Q$,

$$\kappa = c\, v\, l', \quad \ldots \quad (12)$$

$$eQ = -f(c/n)(l'/l), \quad \ldots \quad (13)$$

where in both equations numerical factors have been omitted, Also $c$ is the specific heat per unit volume which is the electronic specific heat when we are dealing with pure electronic effects and which is the lattice specific heat when the lattice heat current dominates, $l'$ is the mean free path of the heat carriers (electron mean free path or phonon mean free path) and $v$ their mean velocity. In eqn. (23) $n$ is the number density of the charge carriers, $l$ the electron mean free path, and $f$ a factor indicating the efficiency with which the phonons carry the electrons along when we are dealing the contribution to $Q$ due to the lattice heat current. For the electronic thermoelectric power eqn. (3) reduces to

$$eQ = -c/n \quad \ldots \quad (14)$$

(for a thermodynamic derivation of eqn. (14) see Keesom 1913). We may remark here that Joffe (1952) discusses the lattice heat conductivity starting from a formula similar to eqn. (12).

In § 3 we give the relevant transport equations. In § 4 we discuss the effect of the non-equilibrium of the lattice and in § 5 we give expressions for $\kappa$ and $Q$. In § 6 we derive expressions for the electronic contribution to $\kappa$ and $Q$. In § 7 and § 8 we discuss the influence of the departure from equilibrium of the lattice on both the lattice heat current and the electronic heat current. Finally, we discuss in § 9 our results and we compare them with experiments and with the results obtained by other authors. We shall use as far as possible the notation of A or M.

## § 3. The Transport Equation for the Electron Distribution Function

We restrict our discussion to n-type semiconductors and use the model introduced by Wilson (1931, see also TM p. 118). It must be remarked, however, that our considerations can easily be adapted to the cases of hole conduction or of conduction by both holes and electrons.

We shall assume that the (normalized) electron distribution function $f(\mathbf{k})$ differs from its equilibrium value $f_0$ and that we may assume it to be of the form (M 17, A 1)

$$f(\mathbf{k}) = f_0 - (k_1/\boldsymbol{k}T)\, c(\eta)\, (\partial f_0/\partial \eta). \quad \ldots \quad (15)$$

We have assumed that there is present an electric field $\mathscr{E}$ and a temperature gradient $dT/dx$ both in the $x$-direction. In eqn. (15) $\mathbf{k}$ is the electron wave vector and $k_1$ its $x$-component, $\boldsymbol{k}$ is Boltzmann's constant, and

$$\eta = (E - \zeta)/\boldsymbol{k}T, \quad \ldots \quad (16)$$

where $\zeta$ is the Fermi-level and $E$ the electron energy for which we use the ' quasi-free ' expression

$$E=\boldsymbol{h}^2k^2/8\pi^2m, \quad \ldots\ldots\ldots \quad (17)$$

where $\boldsymbol{h}$ is Planck's constant, $k$ the absolute magnitude of $\mathbf{k}$ and $m$ the effective electron mass. For $f_0$ we have now instead of eqn. A 5,

$$f_0=\exp(-\eta). \quad \ldots\ldots\ldots \quad (18)$$

We assume the lattice distribution function $N(\mathbf{q})$ to be given by the equation (M 15, A 2)

$$N_j(\mathbf{q})=N_0-(q_1/\boldsymbol{k}T)b_j(z)(\partial N_0/\partial z), \quad \ldots\ldots \quad (19)$$

where $\mathbf{q}$ is the lattice wave vector, $q_1$ its $x$-component and

$$z=\boldsymbol{h}\nu_q/\boldsymbol{k}T, \quad \ldots\ldots\ldots \quad (20)$$

where $\boldsymbol{h}\nu_q$ is the phonon energy. The index $j$ distinguishes between the three possible modes (one longitudinal and two transverse) and the equilibrium distribution $N_0$ is given by the equation

$$N_0=(e^z-1)^{-1} \quad \ldots\ldots\ldots \quad (21)$$

The functions $c(\eta)$ and $b_j(z)$ in eqns. (15) and (19) must be determined from a set of simultaneous integro-differential equations. The first of these equations has the form (compare M 37 or A 8)

$$-4\Lambda\left(\frac{\boldsymbol{h}^2}{8\pi^2m}\right)^{3/2}\left(\frac{\Theta}{T}\right)^3E^{3/2}\left[A+\frac{E}{T}\frac{dT}{dx}\right]-\int_{-\Theta/T}^{\Theta/T}b_j(|z|)\,\alpha(z)\frac{z^2e^{-z}\,dz}{|1-e^{-z}|}=$$
$$\Lambda M_1\left(\frac{\Theta}{T}\right)^3E^2c(\eta)+\int_{-\gamma}^{+\gamma}[Ec(\eta)-c(\eta+z)\{E+\alpha(z)\}]\frac{z^2e^{-z}\,dz}{|1-e^{-z}|}, \quad \ldots \quad (22)$$

where $\Theta$ is the Debye temperature, $\Lambda$ is given by eqn. M 5 a,

$$\Lambda=(4\pi/3)^{1/3}\,4\,Ma\boldsymbol{k}\Theta/3\boldsymbol{h}^2C^2, \quad \ldots\ldots \quad (23)$$

where $M$ is the mass of an atom in the lattice, $a$ the lattice constant, and $C$ a constant giving the interaction between electrons and lattice. The quantity $M_1$ is inversely proportional to the mean free path $l_r$ for impurity scattering and is given by the equation (compare TM p. 284)

$$M_1=\boldsymbol{h}^2/2\pi^2ml_r. \quad \ldots\ldots\ldots \quad (24)$$

The quantities $A$ and $\alpha(z)$ are given by the equations

$$A=\boldsymbol{e}\mathscr{E}+T[\partial(\zeta/T)(\partial x)], \quad \ldots\ldots\ldots \quad (25)$$

$$\alpha(z)=\tfrac{1}{2}\boldsymbol{k}Tz-Dz^2(T/\Theta)^2, \quad \ldots\ldots\ldots \quad (26)$$

where $D$ is given by equation A 13,

$$D=(6\pi^2)^{2/3}\boldsymbol{h}^2/16\pi^2ma^2. \quad \ldots\ldots\ldots \quad (27)$$

Finally, $\gamma$ is given by the equation

$$\gamma=(2E/D)^{1/2}(\Theta/T). \quad \ldots\ldots\ldots \quad (28)$$

We may draw attention to a few differences between eqn. (22) and the corresponding eqn. A 8 for the case of a metal. First of all, the Fermi distribution A 5 is everywhere replaced by the Boltzmann distribution (18). Secondly, the limits of integration of the integral on the right hand side of eqn. (22) are no longer $\pm\Theta/T$, but $\pm\gamma$, where $\gamma$ is given by eqn. (28). The reasons for this change are discussed by Wilson (TM p. 262, see also Fröhlich 1936 p. 234). The final difference is between eqns. (24) and A 10, but this is only an apparent difference, because eqn. A 10 goes over into eqn. (24) by substituting for the residual resistance $\rho_0$ the expression (see TM p. 285)

$$\rho_0 = 3\boldsymbol{h}^3 / 16\pi m \boldsymbol{e}^2 l_r \zeta. \quad . \quad . \quad . \quad . \quad . \quad . \quad . \quad . \quad (29)$$

It must be added that the concept of a residual resistance has obviously no sense in semiconductor theory since the ordinary resistance increases steeply at low temperatures, instead of decreasing as in the case of a metal.

In writing down eqn. (22) we have made the following additional assumptions. First of all, we have assumed that we can use the Debye approximation for the spectrum of the lattice waves. Secondly, we have assumed that we may neglect electron–electron scattering; electron–boundary scattering can easily be taken into account by suitably changing $l_r$.

In metals $l_r$ is a constant which does not depend on the energy. This is, however, in most cases not true for semiconductors, since most impurity centres will be ionized and thus scattering electrons according to the Rutherford scattering formula. If ionized impurity centres are the only scattering centres, $l_r$ will be given by the equation (Conwell and Weisskopf 1950)

$$l_r = (B/\pi N)\,[\ln(1+Bd^2)]^{-1}, \quad . \quad . \quad . \quad . \quad . \quad . \quad . \quad (30)$$

where $N$ is the number of impurity centres per unit volume which for an impurity semiconductor is temperature dependent and equal to the number of carriers, where $2d$ is the average distance between impurity centres, and where $B$ is given by the equation

$$B = 4\kappa_0^2 E^2 / \boldsymbol{e}^4, \quad . \quad . \quad . \quad . \quad . \quad . \quad . \quad . \quad (31)$$

with $\kappa_0$ the dielectric constant.

If we want to take into account scattering by non-ionized impurity centres, by grain boundaries and by the boundaries of the sample we can replace $l_r$ by $l_r^*$ given by the equation

$$1/l_r^* = 1/l_r + 1/l_0, \quad . \quad . \quad . \quad . \quad . \quad . \quad . \quad . \quad (32)$$

where $l_0$ is the mean free path for scattering by non-ionized impurity centres, grain boundaries and sample boundaries which will be energy independent.

In the following we shall neglect $l_0$ and use eqn. (30) for $l_r$. However, this may introduce serious errors at low temperatures, since then most

impurity centres will be neutral and the number of ionized impurity centres will be small. The mean free path $l_r$ will then be much larger than $l_0$ and $M_1$ becomes energy independent.

## § 4. The Transport Equation for the Lattice Distribution Function

Equation (22) gives us one equation for the two unknown functions $c(\eta)$ and $b_j(z)$. We shall now derive a second equation which is the transport equation for the phonon distribution. This equation is (see M 16)

$$u_0 \frac{q_1}{q} \frac{dN_j}{dT} \frac{dT}{dx} = \left[\frac{\partial N_j}{\partial t}\right]_{\mathrm{sc}}, \quad . \quad . \quad . \quad . \quad . \quad . \quad . \quad (33)$$

where $u_0$ is the lattice wave velocity given by the equation

$$u_0 = 2\pi\nu_q/q = (4\pi/3)^{1/3}\, a\, \boldsymbol{k}\Theta/\boldsymbol{h}, \quad . \quad . \quad . \quad . \quad . \quad . \quad (34)$$

where we have used the Debye approximation which involves the assumption that $u_0$ is independent of $\mathbf{q}$. In eqn. (33) the index ' sc ' refers to the change of the lattice distribution function due to scattering ; in many papers the index ' coll ' is used instead.

The following scattering mechanisms may play a role (see M p. 485, TM p. 292, Frederikse 1953)

(i) phonon–electron scattering,

(ii) phonon–boundary scattering (where boundary includes both grain boundaries and the boundaries of the sample),

(iii) phonon–impurity scattering, and

(iv) phonon–phonon scattering.

We have thus for the right hand side of eqn. (33)

$$[\partial N/\partial t]_{\mathrm{sc}} = [\partial N/\partial t]_{\mathrm{el}} + [\partial N/\partial t]_{\mathrm{b}} + [\partial N/\partial t]_{\mathrm{imp}} + [\partial N/\partial t]_{\mathrm{ph}}. \quad . \quad (35)$$

We shall briefly discuss the four terms on the right hand side of eqn. (35). As far as the phonon–electron scattering is concerned, it is usually assumed that only the longitudinal phonons will play a role. Makinson has, however, pointed out that this is in general not correct and that it is better to assume that transverse and longitudinal waves interact to about the same extent with the electrons. We shall adopt this suggestion and write (M p. 485)

$$C_{\mathrm{T}}^2 = C_{\mathrm{L}}^2 = C_j^2 = \tfrac{1}{3}C^2, \quad . \quad . \quad . \quad . \quad . \quad . \quad . \quad (36)$$

$$N_{\mathrm{L}}(\mathbf{q}) = N_{\mathrm{T}}(\mathbf{q}) = N_j(\mathbf{q}), \quad . \quad . \quad . \quad . \quad . \quad . \quad . \quad (37)$$

$$b_{\mathrm{L}}(z) = b_{\mathrm{T}}(z) = b_j(z), \quad . \quad . \quad . \quad . \quad . \quad . \quad . \quad (38)$$

where the $C$ is eqn. (36) is the same as the one in eqn. (23) and where the indices ' L ' and ' T ' refer to longitudinal and transverse waves respectively. It must be added that since it is very difficult to assign a definite value to $C$, the assumption underlying eqn. (36) is unlikely to affect our discussion greatly.

The first term on the right hand side of eqn. (35) satisfies the equation (compare Sommerfeld and Bethe 1933, p. 546 ; M 18)

$$\left[\frac{\partial N_j}{\partial t}\right]_{\mathrm{el}} = \frac{32\pi^3 q_1 C^2 m^2 a^3}{9\boldsymbol{h}^4 M u_0 (e^z-1)} \int_{-\zeta/\boldsymbol{k}T}^{\infty} \exp(-\eta)\, d\eta \left[\tfrac{1}{2}\left\{1+\frac{4\pi m u_0}{\boldsymbol{h}q}\right\} c(\eta+z) + \tfrac{1}{2}c(\eta) - b_j(z)\right]$$

$$= \frac{32\pi^3 q_1 C^2 m^2 a^3}{9\boldsymbol{h}^4 M u_0 (e^z-1)} \left[\tfrac{1}{2}\int_{-\zeta/\boldsymbol{k}T}^{\infty} \exp(-\eta)\, d\eta \left\{\left[1+\frac{4\pi m u_0}{\boldsymbol{h}q}\right] \times c(\eta+z)+c(\eta)\right\} - \exp(-\zeta/\boldsymbol{k}T)\, b_j(z)\right]. \quad (39)$$

For the scattering of phonons by boundaries we can introduce a mean free path, $l_{\mathrm{b}}$, and we have thus for the second term on the right hand side of eqn. (35)

$$\left[\frac{\partial N_j}{\partial t}\right]_{\mathrm{b}} = -u_0 \frac{N_j - N_0}{l_{\mathrm{b}}} = \frac{q_1 u_0}{\boldsymbol{k}T} \frac{b_j(z)}{l_{\mathrm{b}}} \frac{\partial N_0}{\partial z}. \quad (40)$$

Since $l_{\mathrm{b}}$ is determined by the geometrical configuration of the boundaries. we may take it to be independent of $q$.

For the scattering of phonons by impurities we can also introduce a mean free path, $l_{\mathrm{i}}$, which in this case will not be independent of $q$. but following Peierls (1929) we have

$$l_{\mathrm{i}} = l_{\mathrm{i}}^{(0)} (q_0/q)^4, \quad (41)$$

where $l_{\mathrm{i}}^{(0)}$ is independent of $q$, and where $q_0$ is the maximum value of $q$ given by the equation

$$q_0 = (3/4\pi)^{1/3}(2\pi/a) = 2\pi\boldsymbol{k}\Theta/\boldsymbol{h}u_0. \quad (42)$$

Equation (41) for $l_{\mathrm{i}}$ corresponds to the Rayleigh scattering law ; this means that it will only be valid as long as $2\pi/q$ is large compared to the ' size ' of the impurities. For large values of $q$ $l_{\mathrm{i}}$ will either be proportional to $q$. viz., when $2\pi/q$ is of the order of the impurity size, or be independent of $q$. when $2\pi/q$ is small compared to the size of the impurities (see van de Hulst 1946).

Using eqn. (41) we have for the third term on the right hand side of eqn. (35)

$$\left[\frac{\partial N_j}{\partial t}\right]_{\mathrm{imp}} = -u_0 \frac{N_j - N_0}{l_{\mathrm{i}}} = \frac{u_0 q_1 b_j(z)}{l_{\mathrm{i}}^{(0)} \boldsymbol{k}T} \left(\frac{q}{q_0}\right)^4 \frac{\partial N_0}{\partial z}. \quad (43)$$

We are now left with the last term on the right hand side of eqn. (35). We shall use the considerations of Peierls (1929) and Klemens (1951) (see. however, Herring 1954 a). From their work it follows that the phonon–phonon scattering can also be described by a mean free path, $l_{\mathrm{p}}$, which is independent of $q$, but which depends on $T$ as follows (Peierls 1929. see TM p. 293)

$$l_{\mathrm{p}} = G\Theta/T, \; T \gg \Theta \; ; \; l_{\mathrm{p}} = H \exp(\Theta/2T), \; T \ll \Theta, \quad (44)$$

where $G$ and $H$ may be treated as constants. For a justification of eqns. (44) we refer to Klemens' paper (1951).

Using eqns. (44) we get for the last term on the right hand side of eqn. (35) an equation which is the same as eqn. (40), but with $l_b$ replaced by $l_p$. As far as the determination of the $b_j(z)$ is concerned, we could combine $l_b$ and $l_p$ in the usual manner, but we shall not do this as their temperature dependence is different.

## § 5. The General Expressions for the Thermal Conductivity and the Thermoelectric Power

The electrical current density $J$, the electronic heat current density $w_e$, the lattice heat current density $w_g$ and the total heat current density $w$ are given by the equations (compare eqns. M 35, M 36, M 24, A 14, and A 15†)

$$J=\frac{e\hbar}{12\pi^3 m}\left(\frac{8\pi^2 m}{\hbar^2}\right)^{5/2}\int_{-\zeta/kT}^{\infty} E^{3/2}\,c(\eta)\,\frac{\partial f_0}{\partial \eta}\,d\eta, \qquad (45)$$

$$w_e=\frac{\hbar}{12\pi^3 m}\left(\frac{8\pi^2 m}{\hbar^2}\right)^{5/2}\int_{-\zeta/kT}^{\infty} E^{5/2}\,c(\eta)\,\frac{\partial f_0}{\partial \eta}\,d\eta\,, \qquad (46)$$

$$w_g=\frac{3}{2\pi}\Sigma_{\mathbf{q}}\,N_j(\mathbf{q})\,\hbar q_1 u_0^2=\frac{\hbar u_0^2}{4\pi^3 kT}\int_0^{q_0} q^4 b_j(z)\,\frac{e^z\,dz}{(e^z-1)^2}$$

$$=\frac{6\pi k\Theta}{\hbar a^3}\left(\frac{T}{\Theta}\right)^4\int_0^{\Theta/T} z^4\,b_j(z)\,\frac{e^z\,dz}{(e^z-1)^2}, \qquad (47)$$

$$w=w_e+w_g\,, \qquad (48)$$

where we have used eqns. (37), (30), (34) and (42) and the relation

$$z=\hbar u_0 q/2\pi kT\,, \qquad (49)$$

which follows from eqns. (20) and (34). Since in eqn. (47) we are dealing with phonons only, the limit of integration is here $\Theta/T$ and not $\gamma$.

Once again we write (see eqns. M 38, M 37 a, A 16)

$$c(\eta)=-4A\left(\frac{\hbar^2}{8\pi^2 m}\right)^{3/2}\left(\frac{\Theta}{T}\right)^3\left\{Ac^{(3/2)}(\eta)+\frac{dT}{dx}\left[\frac{c^{(5/2)}(\eta)}{T}+c^{(b)}(\eta)\right]\right\} \qquad (50)$$

with $A$ given by eqn. (25). Furthermore we write

$$w_g=yJ+g\,(dT/dx), \qquad (51)$$

a result derived in § 7. We introduce now the following notation

$$K\,(m,n)=-\tau\int_{-\zeta/kT}^{\infty} E^m\,c^{(n)}(\eta)\frac{\partial f_0}{\partial \eta}\,d\eta\,, \qquad (52)$$

$$L_i=-\tau\int_{-\zeta/kT}^{\infty} E^{i+1/2}\,c^{(b)}(\eta)\frac{\partial f_0}{\partial \eta}\,d\eta, \qquad (53)$$

$$\tau=(8A/3\pi\hbar)(\Theta/T)^3, \qquad (54)$$

† There is a misprint in eqns. (A 14) and (A 15) in the exponent of $8\pi^2 m/\hbar^2$.

and we get from eqns. (45) to (48) and (50) to (54)

$$J=K\left(\tfrac{3}{2},\tfrac{3}{2}\right)\boldsymbol{e}A+\left\{K\left(\tfrac{3}{2},\tfrac{5}{2}\right)\frac{\boldsymbol{e}}{T}+\boldsymbol{e}L_1\right\}\frac{dT}{dx}, \quad \ldots \quad (55)$$

$$w=\left\{-K\left(\tfrac{5}{2},\tfrac{3}{2}\right)+\boldsymbol{e}yK\left(\tfrac{3}{2},\tfrac{3}{2}\right)\right\}A+\left\{-\left[K\left(\tfrac{5}{2},\tfrac{5}{2}\right)/T\right]-L_2 +y\left[K\left(\tfrac{3}{2},\tfrac{5}{2}\right)\frac{\boldsymbol{e}}{T}+\boldsymbol{e}L_2\right]+g\right\}\frac{dT}{dx}. \quad \ldots \quad (56)$$

From eqns. (3), (5) and (55) we get for $Q$ the expression

$$Q=Q_e+Q_g, \quad \ldots \quad (57)$$

$$\boldsymbol{e}Q_e=-\left[K\left(\tfrac{3}{2},\tfrac{5}{2}\right)\Big/ T\,K\left(\tfrac{3}{2},\tfrac{3}{2}\right)\right]+\zeta T. \quad \ldots \quad (58)$$

$$\boldsymbol{e}Q_g=-L_1/K\left(\tfrac{3}{2},\tfrac{3}{2}\right), \quad \ldots \quad (59)$$

where the second term on the right-hand side of eqn. (58) derives from the fact that $A$ of eqn. (25) differs from the expression in brackets on the right-hand side if eqn. (3) by a term $-(\zeta T)(dT\,dx)$. The splitting up of $Q$ into two parts is only done for the sake of convenience. The two simultaneous eqns. (22) and (33) are so complicated that one must introduce simplifications. What we shall do is the following. We shall first of all in § 6 calculate the function $c(\eta)$ from eqn. (22) assuming the $b_j(z)$ to be zero. Then we shall in § 7 calculate the functions $b_j(z)$ using for the $c(\eta)$ the expressions derived in § 6. Finally we shall use the expressions for $b_j(z)$ derived in this way to find the $c^{(h)}(\eta)$. Afterwards we must check whether the expressions for $J$ and $w$ derived in this way are consistent with the Kelvin relations, that is, whether for the total expressions (55) and (56) satisfy eqn. (10), or whether

$$K\left(\tfrac{3}{2},\tfrac{5}{2}\right)+TL_1=K\left(\tfrac{5}{2},\tfrac{3}{2}\right)-\boldsymbol{e}yK\left(\tfrac{3}{2},\tfrac{3}{2}\right) \quad \ldots \quad (60)$$

is satisfied. We shall find that, indeed, this relation is only approximately satisfied, but as we have not been able to solve the simultaneous integro-differential equations and as the difference between the left-hand side and the right-hand side of eqn. (60) is only in the numerical coefficients, we felt that our results could probably still be used to indicate the general behaviour of the thermal conductivity and the thermoelectric power and their dependence on various factors.

The thermal conductivity $\kappa$ follows from eqns. (45) and (56) in the usual manner. The condition $J=0$ is used to eliminate the electric field $\mathscr{E}$ and as $\kappa$ is the coefficient of $-(dT/dx)$ in the expression for $w$ we have

$$\kappa=\kappa_e+\kappa_g+\kappa_{eg}, \quad \ldots \quad (61)$$

$$\kappa_e=\left[K\left(\tfrac{5}{2},\tfrac{5}{2}\right)K\left(\tfrac{3}{2},\tfrac{3}{2}\right)-K\left(\tfrac{3}{2},\tfrac{5}{2}\right)K\left(\tfrac{5}{2},\tfrac{3}{2}\right)\right]/TK\left(\tfrac{3}{2},\tfrac{3}{2}\right), \quad (62)$$

$$\kappa_g=-g, \quad \ldots \quad (63)$$

$$\kappa_{eg}=L_2-L_1K\left(\tfrac{5}{2},\tfrac{3}{2}\right)/K\left(\tfrac{3}{2},\tfrac{3}{2}\right). \quad \ldots \quad (64)$$

We have split up the expression for $\kappa$ into three parts which will be considered respectively in §§ 6, 7 and 8.

At this point we want to discuss briefly a mechanism discussed by Price (1954, 1955, see also Fröhlich and Kittel 1954 and ter Haar 1956) which under certain circumstances may give an important contribution to the thermal conduction and also to the thermoelectric power. Price suggests that there may be an additional term in the heat current due to the fact that the carriers may transport ionization energy. The contribution $\kappa_\Delta$ from this effect to the thermal conductivity is of the form

$$\kappa_\Delta = n(\boldsymbol{k}/\boldsymbol{e})[\mu_1\mu_2/(\mu_1+\mu_2)](\Delta^2/\boldsymbol{k}T), \quad . \quad . \quad . \quad . \quad (65)$$

where $n$ is the number density of the carriers, $\mu_1$ and $\mu_2$ are the mobilities of the holes and electrons, and $\Delta$ is the energy gap, or ionization energy. From eqn. (65) it will be seen that $\kappa_\Delta$ will be equal to zero as soon as one of the mobilities is zero, and hence we should not expect a contribution from this effect for our model. This can also be seen as follows. In terms of the electron distribution function $f$ we have for $w$ and $J$ the equations (compare eqns. (45) and (46))

$$J = -\boldsymbol{e}\int uf\, d\mathbf{c}, \quad . \quad . \quad . \quad . \quad . \quad . \quad . \quad . \quad . \quad . \quad . \quad . \quad . \quad . \quad (66)$$

$$w = \int(\Delta+\tfrac{1}{2}mc^2)uf\, d\mathbf{c} = \Delta\int uf\, d\mathbf{c} + \tfrac{1}{2}m\int uc^2 f\, d\mathbf{c} = -(\Delta/\boldsymbol{e})J + w_e, \quad (67)$$

where $u$ is here the $x$-component of the electron velocity, $c$ its absolute magnitude and $d\mathbf{c}$ a volume element of velocity space. Since in order to find $\kappa_\Delta$ we have the condition $J=0$, we see from eqn. (67) that in our case $\kappa_\Delta=0$. Since neither $J$ nor $\Delta$ are temperature dependent the divergence of the first term on the right-hand side of eqn. (67) will be zero and from eqns. (7) and (1) it follows that there will be no contribution to the thermoelectric power either.

## § 6. The Electronic Contribution to the Thermal Conductivity and Thermoelectric Power

In this section we shall assume $b_j(z)=0$, or, $N(\mathbf{q})=N_0$. This means that we are only considering the terms $Q_e$ and $\kappa_e$ in $Q$ and $\kappa$. In order to evaluate the $K(m, n)$ we must determine the $c^{(n)}(\eta)$ for which we have from eqns. (22) and (50) the following equation

$$E^n = \Lambda M_1\left(\frac{\Theta}{T}\right)^3 E^2 c^{(n)}(\eta) + \int_{-\gamma}^{+\gamma}\left[Ec^{(n)}(\eta) - c^{(n)}(\eta+z)\left\{E+\alpha(z)\right\}\right]\frac{z^2e^{-z}\,dz}{|1-e^{-z}|}. \quad . \quad . \quad . \quad (68)$$

We first of all note that the quantity $\gamma$ given by eqn. (28) will practically always be small compared to unity. In fact, inserting into eqn. (27) numerical values and using $m=m_{\mathrm{el}}$, $a=1$Å we have that $\gamma<1$ as long as

$$T > 3\boldsymbol{k}\Theta^2/D \doteqdot 10^{-4}\Theta^2 \sim 10^{\circ}\mathrm{K}, \quad . \quad . \quad . \quad . \quad . \quad (69)$$

if we take $\Theta = 300°\text{K}$. In deriving inequality (69) we used the fact that we are dealing with a Boltzmann distribution for the electrons so that we may put $E \simeq \frac{3}{2}kT$.

As long as $\gamma$ is smaller than one we can expand the integrand in eqn. (68) in powers of $z$. This is more appropriate since the occurrence of a factor $e^{-z}|1-e^{-z}|^{-1}$ means that small values of $z$ will give the main contribution to the integral. Physically this corresponds to the fact that the main electron–phonon scattering is by low energy, long wavelength phonones (compare TM p. 284).

We now solve eqn. (68) by the method of successive approximations (Wilson 1937) and split the problem into two parts according to whether the temperature is large or small compared to the Debye temperature.

### (*a*) *High temperatures* ($\Theta < T$)

In this case we may neglect the first term on the right-hand side of eqn. (68) and we write

$$c^{(n)}(\eta) = c_0^{(n)}(\eta) + c_1^{(n)}(\eta) + \ldots, \qquad (70)$$

where the expansion is essentially one in powers of $\Theta/T$. Inserting expression (70) into eqn. (68), expanding the integrand in powers of $z$ and retaining only the first non-vanishing term we get, using eqn. (28) for $\gamma$, when we neglect all terms but $c_0^{(n)}$ on the right-hand side of eqn. (70)

$$c_0^{(n)}(\eta) = (2E^n/D\gamma^4)(\Theta/T)^2 = \tfrac{1}{2}DE^{n-2}(T/\Theta)^2. \qquad (71)$$

Substituting now the first two terms of the expansion $c^{(n)}(z)$ into eqn. (68) we get for $c^{(n)}(\eta)$ the equation

$$c_1^{(n)}(\eta) = \tfrac{1}{2}DE^{n-3}\left(\frac{T}{\Theta}\right)^2\left[E - \tfrac{1}{2}D\left(\frac{T}{\Theta}\right)^2 \int_{-\gamma}^{+\gamma} \frac{z^2 e^{-z}\,dz}{|1-e^{-z}|} \times \left\{1-(1+\delta z)^{n-2}\left(1+\tfrac{1}{2}\delta z - 2\frac{\tilde{z}^2}{\gamma^2}\right)\right\}\right], \qquad (72)$$

where we have used eqn. (71) and where in the integral containing $c_1^{(n)}(\eta)$ we have made the same approximations as the ones leading to eqn. (71). In eqn. (72) $\delta$ is given by the equation

$$\delta = kT/E, \qquad (73)$$

and we see that the following relations hold

$$\delta \sim 1, \qquad \gamma\delta \ll 1. \qquad (74)$$

In order to evaluate the integral on the right-hand side of eqn. (72) we expand the integrand in powers of $z$. After integrating we are left with a power series in $\gamma$. The first term cancels against the $E$ inside the square bracket on the right-hand side of eqn. (72) and the second term gives the result

$$c_1^{(n)}(\eta) = \tfrac{1}{2}DE^{n-2}\gamma^2(T/\Theta)^2[\{(-n^2+8n-12)\delta^2/12\} + \{(2n-7)\delta/24\} - (1/18)], \qquad (75)$$

and we can see that, indeed $c_1^{(n)}(\eta)$ is small compared to $c_0^{(n)}(\eta)$, the ratio being of the order of magnitude of $\gamma^2$.

Using eqns. (16) and (18) we have

$$-\int_{-\zeta/\boldsymbol{k}T}^{\infty} E^{p}\frac{\partial f_0}{\partial \eta}d\eta=\Gamma(p+1)(\boldsymbol{k}T)^{p}\exp(\zeta/\boldsymbol{k}T), \quad . \quad . \quad (76)$$

and substituting expressions (70), (71) and (75) into eqn. (52) and using eqns. (18) and (73) we find for $K(m, n)$ the expression

$$K(m, n)=\tfrac{1}{2}\exp(\zeta/\boldsymbol{k}T)\tau D\left(\frac{T}{\Theta}\right)^{2}(\boldsymbol{k}T)^{m+n-2}(m+n-2)!$$

$$\times\left[1+\frac{2\boldsymbol{k}\Theta^{2}}{DT}\left\{\frac{-n^{2}+8n-12}{12(m+n-2)}+\frac{2n-7}{24}-\frac{m+n-1}{18}\right\}\right]. \quad . \quad (77)$$

At this point we draw attention to the fact that in contradistinction to the case of metals we have now that in general

$$K(m, n)\neq K(n, m). \quad . \quad . \quad . \quad . \quad . \quad . \quad (78)$$

This means that at this point already the Onsager relations, in the form of eqn. (60) are violated, and that therefore the numerical coefficients of the last term on the right-hand side of eqns. (79) and (84) are not reliable. However, one must bear in mind that, anyhow, a theory such as the one used in the present paper can never claim to give an accurate quantitative picture, as from the beginning one introduces too many simplifying assumptions.

Substituting expression (77) into eqn. (62) we find†

$$\kappa=\exp(\zeta/\boldsymbol{k}T)\tau D\boldsymbol{k}^{3}T^{2}(T/\Theta)^{2}[1-(71\boldsymbol{k}\Theta^{2}/72DT)]. \quad . \quad . \quad (79)$$

Introducing the carrier density $n$ and the electron–phonon mean free path $l_{\mathrm{ep}}$ by the equations (compare ter Haar 1954, p. 246 and TM p. 265)

$$n=2(2\pi m\boldsymbol{k}T/\boldsymbol{h}^{2})^{3/2}\exp(\zeta/\boldsymbol{k}T), \quad . \quad . \quad . \quad . \quad (80)$$

$$l_{\mathrm{ep}}=\boldsymbol{h}^{2}D\Lambda\Theta/4\pi^{2}mT, \quad . \quad . \quad . \quad . \quad . \quad (81)$$

and using eqn. (54) for $\tau$ we can write eqn. (79) in the form

$$\kappa_{e}=\kappa_{e}^{0}[1-(71\boldsymbol{k}\Theta^{2}/72DT)], \quad . \quad . \quad . \quad . \quad . \quad . \quad (82)$$

where

$$\kappa_{e}^{0}=(32/9\pi)^{1/2}(n\boldsymbol{k})(\boldsymbol{k}T/m)^{1/2}l_{\mathrm{ep}} \quad . \quad . \quad . \quad . \quad . \quad (83)$$

is the expression for the thermal conductivity according to the elementary electron theory (see Tm p. 232). The right-hand side of eqn. (83) is written in such a way that its resemblance to eqn. (12) is immediately clear. Since $\boldsymbol{k}\Theta\ll D$ and since we have been dealing with temperatures above the Debye temperature, the correction term in eqn. (82) is always very small.

---

† The numerical coefficient inside the square bracket is different from the one given in a previous communication (ter Haar and Neaves 1954) which was in error.

Substituting expression (77) into eqn. (58) we get

$$eQ_e=(\zeta/T)-2k+(11k^2\Theta^2/144DT), \quad . \quad . \quad . \quad . \quad (84)$$

where the first two terms on the right-hand side of eqn. (84) are the usual expression for the thermoelectric power of a semiconductor (see e.g. TM p. 232). The last term is a correction term which also here is always small.

We may draw attention to the fact that for semiconductors neither $\kappa$ nor $Q$ are small effects.

### (*b*) *Low temperatures* ($T<\Theta$)

As long as inequality (69) is satisfied we can still evaluate the integral on the right-hand side of eqn. (68) by expanding the integrand in power of $z$. For temperatures below the Debye temperature, the first term on the right-hand side of eqn. (68) is, however, the dominant one and we obtain the zero order approximation to $c^{(n)}(\eta)$ by neglecting the integral.

$$c_0^{(n)}(\eta)=(E^{n-2}/AM_1)(T/\Theta)^3, \quad . \quad . \quad . \quad . \quad . \quad . \quad (85)$$

where we have to bear in mind that $M_1$ is not a constant, but depends on $E$ (see eqns. (24), (30) and (31)). The first approximation is obtained by substituting eqn. (70) in eqn. (68) and neglecting in the integral all terms, but $c_0^{(n)}(\eta)$. The results is

$$c_1^{(n)}(\eta)=-2(T/\Theta)^4(E^{n-2}/A^2M_1^2D). \quad . \quad . \quad . \quad . \quad . \quad (86)$$

In deriving eqn. (86) we have made use of the fact that the term $Bd^2$ under the logarithm sign in eqn. (30) can be written in the form

$$Bd^2=4\kappa_0^2E^2d^2/e^4\simeq 4\times 10^8T^2n_{\text{imp}}{}^{-2/3}, \quad . \quad . \quad . \quad . \quad (87)$$

where we have put $E\simeq\frac{3}{2}kT$, $\kappa_0=10$ e.s.u., $d=n_{\text{imp}}{}^{-1/3}$ ($n_{\text{imp}}$ is the impurity concentration). From eqn. (87) we see that only at the highest impurity concentrations ($n_{\text{imp}}\simeq 10^{18}\text{cm}^{-3}$) and lowest temperatures ($T<5^\circ\text{K}$) $Bd^2$ becomes less than one. At these low temperatures, other scattering mechanisms will take over, and we may take $M_1$ to be constant. Otherwise—and this means for practically all cases of interest we may to a fair approximation neglect the variation of the logarithmic factor with energy, and put under the logarithm $E=\frac{3}{2}kT$. This means that we may assume $M_1$ to be proportional to $E^{-2}$, at any rate in the approximation used here, and we shall write

$$M_1=M_1'(kT/E)^2, \quad . \quad . \quad . \quad . \quad . \quad . \quad (88)$$

$$l_r=l_r'(E/kT)^2, \quad . \quad . \quad . \quad . \quad . \quad . \quad . \quad (89)$$

where we shall take $M_1'$ and $l_r'$ to be independent of energy.

Using eqns. (85), (86) and (88) we get from eqn. (52)

$$K(m,n)=(\tau/AM_1')(T/\Theta)^3(m+n)\,!\,(kT)^{m+n-2}$$
$$\exp(\zeta/kT)[1-(m+n-1)(m+n+2)(l_r'/l_{\text{ep}})], \quad . \quad (90)$$

where we have used eqns. (81), (24), (88 and (89) to write

$$\Lambda M_1' D = 2(l_{ep}, l_r')(T, \Theta). \quad \ldots \quad (91)$$

Substituting eqn. (90) into eqn. (62) we get †

$$\begin{aligned}\kappa_e &= (24\tau/\Lambda M_1')(T/\Theta)^3(\boldsymbol{k}T)^2 \exp(\zeta/\boldsymbol{k}T)\boldsymbol{k}[1-50(l_r'/l_{ep})] \\ &= (512/\pi)^{1/2}(n\boldsymbol{k})(\boldsymbol{k}T/m)^{1/2}l_r'[1-50(l_r'/l_{ep}]. \quad \ldots \quad (92)\end{aligned}$$

If $l_r$ had been energy independent, the numerical constant would have been $(32/9\pi)^{1/2}$ as in eqn. (83). Since we are at temperatures well below the Debye temperature, $l_r' \ll l_{ep}$ (compare the neglect of the integral on the right-hand side of eqn. (68) and the ratio of $c_1^{(n)}(\eta)$ to $c_0^{(n)}(\eta)$ which is according to eqns. (85), (86) and (91) $l_r'/l_{ep}$) the correction term in eqn. (92) will, in general, be small. As soon as it becomes appreciable we can no longer use the approximations applied in this section.

From eqns. (58) and (90) we get for the thermoelectric power

$$eQ_e = (\zeta/T) - 4\boldsymbol{k} + 40\boldsymbol{k}(l_r'/l_{ep}). \quad \ldots \quad (93)$$

It $M_1$ had been energy independent , the term $-4\boldsymbol{k}$ would have been $-2\boldsymbol{k}$ as in eqn. (84). While at high temperatures the first two terms are of the same order of magnitude, at low temperatures the $\zeta/T$ term will dominate. A fortiori, the last term on the right-hand side of eqn. (93) will always be small.

## § 7. The Lattice Contribution to the Thermal Conductivity

In order to evaluate $w_g$ we must know $b_j(z)$ for which we have from eqns. (33), (35), (39), (40) and (43)

$$\begin{aligned}b_j(z) = &\left[\frac{1}{l_b} + \frac{1}{l_p} + \frac{1}{l_i^{(0)}}\left(\frac{T}{\Theta}\right)^4 z^4 + \Phi(1-e^{-z})\exp(\zeta/\boldsymbol{k}T)\right]^{-1} \\ &\times\left[\tfrac{1}{2}\Phi(1-e^{-z})\int_{-\zeta/\boldsymbol{k}T}^{\infty} e^{-\eta}d\eta\left\{\left(1+\frac{4\pi m u_0}{\boldsymbol{h}q}\right)c(\eta+z)+c(\eta)\right\}\right. \\ &\left. - \frac{\boldsymbol{h}u_0}{2\pi T}\frac{dT}{dx}\right], \quad \ldots \quad (94)\end{aligned}$$

where we have used eqns. (49) and (42) to express $q/q_0$ in terms of $z$, and where $\Phi$ is given by the equation

$$\Phi = 32\pi^3 C^2 m^2 a^3 \boldsymbol{k}T/9\boldsymbol{h}^4 M u_0^2, \quad \ldots \quad (95)$$

which by using eqns. (34), (23), (81) and (27) can be written in the form

$$\Phi = 2/9l_{ep} \quad \ldots \quad (96)$$

---

† The difference between eqn. (92) and the equation given in a previous communication (ter Haar and Neaves 1954) is due to the fact that then we assumed $M_1$ to be energy independent as in the case of metals.

Substituting eqns. (94) and (96) into eqn. (47) we have

$$w_0 = \frac{6\pi \boldsymbol{k}\Theta}{\boldsymbol{h}a^3}\left(\frac{T}{\Theta}\right)^4 \int_0^{\Theta/T} \frac{z^4 e^z\, dz}{(e^z-1)^2}\left[\frac{1}{l_b}+\frac{1}{l_p}+\frac{1}{l_i^{(0)}}\left(\frac{T}{\Theta}\right)^4 z+\frac{2}{9l_{ep}}(1-e^{-z})\right.$$
$$\left.\times \exp(\zeta/\boldsymbol{k}T)\right]^{-1}$$
$$\left[\frac{1}{9l_{ep}}(1-e^{-z})\int_{-\zeta/\boldsymbol{k}T}^{\infty} e^{-\eta}d\eta\left\{\left(1+\frac{4\pi m u_0}{\boldsymbol{h}q}\right)c(\eta+z)+c(\eta)\right\}\right.$$
$$\left.-\frac{\boldsymbol{h}u_0}{2\pi T}\frac{dT}{dx}\right]. \qquad \ldots \quad (97)$$

In order to evaluate this expression we must simplify it. We cannot neglect the term with the $c(\eta)$, but we shall assume that in different ranges of temperature one of the scattering mechanisms will dominate and that we may neglect all but the dominant scattering mechanism in each of these temperature ranges. In order of increasing temperature the dominant scattering mechanisms will be (see M): phonon–boundary scattering (range I), phonon–electron scattering (range II), phonon–impurity scattering (range III), and phonon–phonon scattering (range IV). Although the Debye temperature will probably occur somewhere between range II and range IV (see TM p. 294) we shall for ranges II and III consider two cases: IIa and IIIa, assuming the Debye temperature to be higher than the temperatures in those ranges, and IIb and IIIb, assuming the Debye temperature to be lower than the temperatures in these ranges. We shall in the following, with Makinson, neglect the term with $4\pi m u_0/\boldsymbol{h}q$ and we refer to M for a justification.

(i) *Temperature range I*

Since we are at temperatures below the Debye temperature we can use for the $c(\eta)$ the solution given by eqn. (85). We neglect here $c_1^{(n)}(\eta)$ since this only amounts to a small correction as we saw in § 6.

We first of all evaluate the integral over $\eta$ in eqn. (97) and we replace $c(\eta+z)$ by $c(\eta)$ which is allowed since the main contribution to the integral over $z$ will come from small values of $z$. The result is

$$\int_{-\zeta/\boldsymbol{k}T}^{\infty} e^{-\eta}\, d\eta\left[\left(1+\frac{4\pi m u_0}{\boldsymbol{h}q}\right)c(\eta+z)+c(\eta)\right] \simeq$$
$$-\frac{8}{M_1'\boldsymbol{k}^2T^2}\left(\frac{\boldsymbol{h}^2}{8\pi^2 m}\right)^{3/2}\left\{A\int_{-\zeta/\boldsymbol{k}T}^{\infty} E^{3/2}\, e^{-\eta}\, d\eta+\frac{1}{T}\frac{dT}{dx}\int_{-\zeta\boldsymbol{k}/\boldsymbol{T}}^{\infty} E^{5/2} e^{-\eta}\, d\eta\right\}$$
$$=-2l_r'\left(\frac{\boldsymbol{h}^2}{8\pi^2 m\boldsymbol{k}T}\right)^{1/2}\exp(\zeta/\boldsymbol{k}T)\left\{\Gamma\left(\frac{5}{2}\right)A+\boldsymbol{k}\Gamma\left(\frac{7}{2}\right)\frac{dT}{dx}\right\}, \qquad \ldots \quad (98)$$

where $\Gamma\left(\frac{5}{2}\right)=\frac{3}{4}\pi^{1/2}$ and $\Gamma\left(\frac{7}{2}\right)=15\pi^{1/2}/8$ (e.g. Larsen 1948, p. 251).

Substituting expression (98) into eqn. (97) and neglecting in the denominator all terms but $1/l_b$ we get after integration over $z$ for $w_g$ the equation

$$w_g = -\frac{6\pi l_b}{\hbar a^3}\left(\frac{T}{\Theta}\right)^3\left[\left(\frac{\hbar^2 k T}{8\pi m}\right)^{1/2}\frac{l_r'}{12 l_{ep}}\exp(\zeta/kT)\left\{2A+5k\frac{dT}{dx}\right\}I_4(\Theta/T)\right.$$
$$\left.+\frac{\hbar u_0 k}{2\pi}\frac{dT}{dx}J_4(\Theta/T)\right], \quad \ldots\ldots\ldots\ldots\ldots\ldots \quad (99)$$

where we have used eqns. (24), (88) and (89) and where

$$I_n(\Theta/T)=\int_0^{\Theta/T} z^n(e^z-1)^{-1}\,dz, \quad \ldots\ldots \quad (100)$$

$$J_n(\Theta/T)=\int_0^{\Theta/T} z^n e^z(e^z-1)^{-2}\,dz. \quad \ldots\ldots \quad (101)$$

These factors will be approximated by us as follows (see TM p. 336)

$$I_n(\Theta/T)\doteq I_n(\infty)=n!\,\zeta(n+1),\ J_n(\Theta/T)\doteq J_n(\infty)=n!\,\zeta(n),\ \Theta>T, \quad \ldots \quad (102)$$

$$I_n(\Theta/T)\doteq n^{-1}(\Theta/T)^n,\ J_n(\Theta/T)\doteq(n-1)^{-1}(\Theta/T)^{n-1},\ \Theta<T, \quad \ldots \quad (103)$$

where $\zeta(x)$ is Riemann's zeta-function ($\zeta(x)=\Sigma_n n^{-x}$).

We can use eqn. (55) to eliminate $A$ in terms of $J$ and $dT/dx$ and using eqn. (80) for $n$ and (42) for $\Theta$ we find for the coefficients $y_I$ and $g_I(=-\kappa_g$, see eqn. (63))

$$y_I=-nl_b l_r\,k^2T^2I_4/12l_{ep}m^2u_0^3\,eK(\tfrac{3}{2},\tfrac{3}{2}) \quad \ldots \quad (104)$$

$$\kappa_g=-g_I=(3l_b k u_0 J_4/a^3)(T/\Theta)^3, \quad \ldots\ldots \quad (105)$$

where in the last equation we have neglected a term of the order $l_r'/l_{ep}$ as compared to the term retained.

We can rewrite the last equation by introducing the lattice specific heat $c_g$ by the equation (compare Sommerfeld and Bethe 1933, p. 547, we have an extra factor 3 to be taken into account the fact that we assume the two transverse modes and the longitudinal mode to be equivalent)

$$c_g=(3/2\pi)(d/dT)\Sigma_{\mathbf{q}}N(\mathbf{q})\hbar u_0 q=(3\hbar u_0/16\pi^4T)\int_0^{q_0} ze^z q^3(e^s-1)^{-2}\,dq$$
$$=(9k/a^3)(T/\Theta)^3J_4, \quad \ldots\ldots\ldots\ldots\ldots\ldots \quad (106)$$

where we have used eqns. (42). Combining eqns. (105) and (106) we have

$$\kappa_g=\tfrac{1}{3}c_g u_0 l_b. \quad \ldots\ldots\ldots \quad (107)$$

and similarly using eqns. (42), (54), (80), (90) and (106) we find

$$y_I=-(\pi c_g l_b T I_4/144 n l_{ep} e J_4)\exp(\zeta/kT). \quad \ldots \quad (108)$$

(ii) *Temperature range IIa*

We shall still use the result of eqn. (98) and now neglecting all terms in the denominator but the one involving $l_{ep}^{-1}$ we get for $w_g$.

$$w_g=-\frac{27\pi l_{ep}}{\hbar a^3}\left(\frac{T}{\Theta}\right)^3\left[\left(\frac{\hbar^2 kT}{8\pi m}\right)^{1/2}\frac{l_r'}{12l_{ep}}\left\{2A+5k\frac{dT}{dx}\right\}J_4\left(\frac{\Theta}{T}\right)\right.$$
$$\left.+\frac{\hbar u_0 k}{2\pi}\exp(-\zeta/kT)\frac{dT}{dx}K_4\left(\frac{\Theta}{T}\right)\right], \quad \ldots\ldots\ldots \quad (109)$$

where

$$K_n(\Theta/T)=\int_0^{\Theta/T} z^n e^{-z}(1-e^{-z})^{-3}\,dz. \quad \ldots\ldots \quad (110)$$

Eliminating once again $A$ we find now

$$y_{IIa}=-\pi c_g T/32ne, \quad \ldots\ldots\ldots\ldots \quad (111)$$

$$\kappa_g=-g_{IIa}=\tfrac{3}{2}c_g u_0 l_{ep}\exp(-\zeta/kT)\,(K_4/J_4), \quad \ldots \quad (112)$$

when once again we have neglected a term of the order $l_r'/l_{ep}$ in $\kappa$ and where in $y_{IIa}$ we have again simplified the final expression.

(iii) *Temperature range IIIa*

We now retain only the term with $(l_i^{(0)})^{-1}$ in the denominator, and we get for $w_g$, $y_{IIIa}$ and $\kappa_g$,

$$w_g=-\frac{6\pi l_i^{(0)}}{\hbar a^3}\frac{\Theta}{T}\left\{\left(\frac{\hbar^2 kT}{8\pi m}\right)^{1/2}\frac{l_r'}{12l_{ep}}\exp(\zeta/kT)\left[2A+5k\frac{dT}{dx}\right]I_0\left(\frac{\Theta}{T}\right)\right.$$
$$\left.+\frac{\hbar u_0 k}{2\pi}\frac{dT}{dx}J_0\left(\frac{\Theta}{T}\right)\right\}, \quad \ldots\ldots\ldots\ldots \quad (113)$$

$$y_{IIIa}=-(\pi c_g l_1^{(0)}TI_0/144nl_{ep}eJ_4)(\Theta/T)^4\exp(\zeta/kT), \quad \ldots \quad (114)$$

$$\kappa_g=-g_{IIIa}=\tfrac{1}{3}c_g u_0 l_1^{(0)}(\Theta/T)^4(J_0/J_4). \quad \ldots\ldots \quad (115)$$

(iv) *Temperature range IIb*

We now must use for the $c^{(n)}(\eta)$ the $c_0^{(n)}(\eta)$ given by eqn. (71). Using the same approximations as the ones leading to eqn. (98) we have now

$$\int_{-z/kT}^{\infty} e^{-\eta}\,d\eta\left[\left(1+\frac{4\pi mu_0}{\hbar q}\right)c(\eta+z)+c(\eta)\right]\simeq -2l_{ep}\left(\frac{\hbar^2}{8\pi^2 mkT}\right)^{1/2}$$
$$\exp(\zeta/kT)\left\{\Gamma(\tfrac{1}{2})A+k\Gamma(\tfrac{3}{2})\frac{dT}{dx}\right\} \quad \ldots\ldots \quad (116)$$

where $\Gamma(\frac{1}{2})=\pi^{1/2}$, $\Gamma(\frac{3}{2})=\pi^{1/2}/2$ (e.g. Larsen 1948, p. 251).

We can use eqn. (116) and neglecting in the dominator of (97) all terms, but the one involving $l_{ep}^{-1}$ we obtain $w_g$, $y_{IIb}$ and $\kappa_g$,

$$w_g=-\frac{27\pi l_{ep}}{\hbar a^3}\left(\frac{T}{\Theta}\right)^3\left[\frac{1}{9}\left(\frac{\hbar^2 kT}{8\pi m}\right)^{1/2}\left\{2A+k\frac{dT}{dx}\right\}J_4\left(\frac{\Theta}{T}\right)\right.$$
$$\left.+\frac{\hbar u_0 k}{2\pi}\exp(-\zeta/kT)\frac{dT}{dx}K_4\left(\frac{\Theta}{T}\right)\right], \quad \ldots\ldots \quad (117)$$

$$y_{IIb}=-\pi c_g T/4ne, \quad \ldots\ldots\ldots\ldots \quad (118)$$

$$\kappa_g=-g_{IIb}=\tfrac{3}{2}c_g u_0 l_{ep}\exp(-\zeta/kT)(K_4/(J_4), \quad \ldots \quad (119)$$

where now we have used eqn. (77) for the $K(m, n)$ and where in $\kappa_g$ we have neglected a term of the order of magnitude $(\hbar^2/6\pi m k\Theta)^2(n/a)(\Theta/T)$ which for $n<10^{18}$ cm$^{-3}$, $T>\Theta=300$°K, $a=3$Å, $m=m_{el}$ is smaller than 0·08.

(v) *Temperature range IIIb*

We now retain only the term with $(l_i^{(0)})^{-1}$ in the denominator and with the same approximations as in the previous subsections we get for $w_g$, $y_{IIIb}$ and $\kappa_g$,

$$w_g=-\frac{6\pi l_i^{(0)}}{\hbar a^3}\frac{\Theta}{T}\left[\frac{1}{9}\left(\frac{\hbar^2 k T}{8\pi m}\right)^{1/2}\exp(\zeta/kT)\left\{2A+k\frac{dT}{dx}\right\}I_0\left(\frac{\Theta}{T}\right)+\frac{\hbar u_0 k}{2\pi}\frac{dT}{dx}J_0\left(\frac{\Theta}{T}\right)\right], \quad (120)$$

$$y_{IIIb}=-(\pi c_g l_i^{(0)} T I_0/18 n e l_{ep} J_4)(\Theta/T)^4\exp(\zeta/kT), \quad (121)$$

$$\kappa_g=-g_{IIIb}=\tfrac{1}{3}c_g u_0 l_i^{(0)}(\Theta/T)^4(J_0/J_4). \quad (122)$$

(vi) *Temperature range IV*

Finally, we retain the term with $l_p^{-1}$ in the denominator and we now get for $w_g$, $y_{IV}$ and $\kappa_g$,

$$w_g=-\frac{6\pi l_p}{\hbar a^3}\left(\frac{T}{\Theta}\right)^3\left[\frac{1}{9}\left(\frac{\hbar^2 k T}{8\pi m}\right)^{1/2}\exp(\zeta/kT)\left\{2A+k\frac{dT}{dx}\right\}I_4\left(\frac{\Theta}{T}\right)+\frac{\hbar u_0 k}{2\pi}\frac{dT}{dx}J_4\left(\frac{\Theta}{T}\right)\right], \quad (123)$$

$$y_{IV}=-(\pi c_g l_p T I_4/18 n e l_{ep} J_4)\exp(\zeta/kT), \quad (124)$$

$$\kappa_g=-g_{IV}=\tfrac{1}{3}c_g u_0 l_p. \quad (125)$$

## § 8. The Change in the Current Densities due to Lattice Non-equilibrium

We must now evaluate the contributions to $\kappa$ and $Q$ due to $c^{(b)}(\eta)$. We shall assume, as we mentioned earlier, that in evaluating these functions we may use for the $b_j(z)$ the expressions obtained by assuming $c^{(b)}(\eta)$ to be zero. We appreciate fully that we should really obtain solutions of the simultaneous integro-differential equations, but we have not succeeded either in doing this or in estimating the errors made in our calculations. However, for reasons to be gone into at the end of this section we feel that our results are probably not too bad and can be used for comparison with experimental data. We shall again distinguish between the temperature ranges I, IIa, IIIa, IIb, IIIb, IV. In the first three cases, the ratio of the first term in curly brackets on the right-hand side of eqn. (94) to the second term is of the order of $l_r'/l_{ep}$ and thus negligibly small, while in the last three cases its ratio is less than 0·1 for $n<10^{18}$ cm$^{-3}$ (compare the remarks at the end of subsection (iv) of § 7). We shall thus use the following expression for $b_j(z)$ in the present section,

$$b_j(z)=-\frac{\hbar u_0}{2\pi T}\frac{dT}{dx}\left[\frac{1}{l_b}+\frac{1}{l_p}+\frac{1}{l_i^{(0)}}\left(\frac{T}{\Theta}\right)^4 z^4+\frac{2}{9 l_{ep}}(1-e^{-z})\exp(\zeta/kT)\right]^{-1}. \quad (126)$$

We now introduce a quantity $\beta(\eta)$ by the equation (compare eqns. A27 and M37a)

$$\int_{-\Theta/T}^{\Theta/T} b_j(|z|)\alpha(z)\frac{z^2e^{-z}\,dz}{|1-e^{-z}|}=4A\left(\frac{\hbar^2}{8\pi^2m}\right)^{3/2}\left(\frac{\Theta}{T}\right)^3\beta(\eta)\frac{dT}{dx}, \quad . \quad (127)$$

so that $c^{(b)}(\eta)$ is the solution of the equation

$$\beta(\eta)=AM_1\left(\frac{\Theta}{T}\right)^3E^2c^{(b)}(\eta)+\int_{-\gamma}^{+\gamma}\left[Ec^{(b)}(\eta)-c^{(b)}(\eta+z)\{E+\alpha(z)\}\right]\frac{z^2e^{-z}\,dz}{|1-e^{-z}|}. \quad . \quad . \quad . \quad (128)$$

For temperatures above the Debye temperatures we may neglect the first term on the right-hand side of eqn. (128) and we get after the usual expansion in powers of $z$ the integral sign and the neglecting of all but the dominant term (compare the derivation of eqn. (71))

$$c^{(b)}(\eta)=\tfrac{1}{2}D(T/\Theta)^2E^{-2}\beta(\eta). \quad . \quad . \quad . \quad . \quad . \quad . \quad . \quad (129)$$

For temperatures below the Debye temperatures, the integral can be neglected and we get, using eqn. (91),

$$c^{(b)}(\eta)=(AM_1E^2)^{-1}(T/\Theta)^3\beta(\eta)=\tfrac{1}{2}D(T/\Theta)^2(\boldsymbol{k}T)^{-2}(l_r'/l_{ep})\,)\beta(\eta). \quad . \quad (130)$$

We can now consider the six temperature ranges. We use eqn. (64) for $\kappa_{eg}$, (59) for $Q_g$ and (53) for the $L_i$. In the temperature ranges I, IIa, IIIa we use eqn. (90) for the $K(m,n)$ and (130) for $c^{(b)}(\eta)$, and in the other three temperature ranges we use eqn. (77) for the $K(m,n)$ and (129) for $c^{(b)}(\eta)$, in both cases neglecting the correction terms in the expressions for the $K(m,n)$. Finally we only retain the term with $l_b^{-1}$ in the denominator in eqn. (126) in temperature range I, only the term with $l_{ep}^{-1}$ in ranges IIa and IIb, only the term with $(l_i^{(0)})^{-1}$ in ranges IIIa and IIIb, and only the term with $l_p^{-1}$ in range IV. We then get for $\beta(\eta)$, $c^{(b)}(\eta)$, $L_i$, $\kappa_{eg}$ and $Q_g$ in these six cases the following expressions, where in eqn. (127) we have neglected the first term in $\alpha(z)$ in accordance with inequality (69).

(i) *Temperature range I*

$$\beta(\eta)=\frac{\hbar u_0\,l_b\,D}{40\pi TA}\left(\frac{8\pi^2m}{\hbar^2}\right)^{3/2}, \quad . \quad . \quad . \quad . \quad . \quad . \quad . \quad . \quad . \quad . \quad . \quad (131)$$

where we have neglected terms of the order $(T/\Theta)^5$.

$$c^{(b)}(\eta)=\frac{\hbar u_0\,l_b\,D^2\,l_r'}{80\pi TA\boldsymbol{k}^2\,\Theta^2\,l_{ep}}\left(\frac{8\pi^2m}{\hbar^2}\right)^{3/2}, \quad . \quad . \quad . \quad . \quad . \quad . \quad . \quad . \quad . \quad (132)$$

$$L_i=\frac{c_g\,l_b}{180\,J_4}\left(\frac{2}{m\boldsymbol{k}T}\right)^{1/2}\left(\frac{\Theta}{T}\right)^5\exp(\zeta/\boldsymbol{k}T)\frac{l_r'}{l_{ep}}\Gamma(i+3/2)(\boldsymbol{k}T)^{i-1}, \quad (133)$$

$$\kappa_{eg}=-\frac{c_g\,l_b}{160\,J_4}\left(\frac{2\pi\boldsymbol{k}T}{m}\right)^{1/2}\frac{l_r'}{l_{ep}}\left(\frac{\Theta}{T}\right)^5\exp(\zeta/\boldsymbol{k}T), \quad . \quad . \quad . \quad . \quad . \quad (134)$$

$$eQ_g=-\frac{\pi c_g}{1920J_4}\frac{l_b}{l_{ep}}\left(\frac{\hbar^2}{2\pi m\boldsymbol{k}T}\right)^{3/2}\left(\frac{\Theta}{T}\right)^5. \quad . \quad . \quad . \quad . \quad . \quad . \quad . \quad (135)$$

(ii) *Temperature range IIa*

$$\beta(\eta)=\frac{9\boldsymbol{h}\,u_0\,l_{\rm ep}\,D}{16\pi\,T\,\Lambda}\left(\frac{8\pi^2 m}{\boldsymbol{h}^2}\right)^{3/2}\left(\frac{T}{\Theta}\right)^5\exp\,(-\zeta/\boldsymbol{k}T)\,(2J_4+I_4)\,, \quad . \quad (136)$$

$$c^{(b)}(\eta)=\frac{9\boldsymbol{h}\,u_0\,l_{\rm r}'\,D^2}{32\pi\,\Theta\,\Lambda\,\boldsymbol{k}^2\,\Theta^2}\left(\frac{8\pi^2 m}{\boldsymbol{h}^2}\right)^{3/2}\left(\frac{T}{\Theta}\right)^3\exp\,(-\zeta/\boldsymbol{k}T)\,(2J_4+I_4), \quad . \quad (137)$$

$$L_i=\frac{c_g\,l_{\rm r}'}{8\,J_4}\left(\frac{2}{m\boldsymbol{k}T}\right)^{1/2}(2J_4+I_4)\Gamma(i+3/2)(\boldsymbol{k}T)^{i-1}, \quad . \quad . \quad . \quad . \quad (138)$$

$$\kappa_{eg}=-\frac{9c_g\,l_{\rm r}'}{64\,J_4}\left(\frac{2\pi\boldsymbol{k}T}{m}\right)^{1/2}, \quad . \quad . \quad . \quad . \quad . \quad . \quad . \quad . \quad . \quad . \quad (139)$$

$$\boldsymbol{e}Q_g=-\left[2+\frac{I_4}{J_4}\right]\frac{3\pi c_g}{128n}. \quad . \quad . \quad . \quad . \quad . \quad . \quad . \quad . \quad . \quad . \quad (140)$$

(iii) *Temperature range IIIa*

$$\beta(\eta)=\frac{\boldsymbol{h}\,u_0\,l_{\rm i}^{(0)}\,D}{8\pi T\Lambda}\left(\frac{8\pi^2 m}{\boldsymbol{h}^2}\right)^{3/2}, \quad . \quad . \quad . \quad . \quad . \quad . \quad . \quad . \quad . \quad (141)$$

$$c^{(b)}(\eta)=\frac{\boldsymbol{h}\,u_0\,l_{\rm i}^{(0)}\,D^2\,l_{\rm r}'}{16\pi\,T\,\Lambda\,\boldsymbol{k}^2\,\Theta^2\,l_{\rm ep}}\left(\frac{8\pi^2 m}{\boldsymbol{h}^2}\right)^{3/2}, \quad . \quad . \quad . \quad . \quad . \quad . \quad (142)$$

$$L_i=\frac{c_g\,l_{\rm i}^{(0)}}{36\,J_4}\left(\frac{2}{m\boldsymbol{k}T}\right)^{1/2}\left(\frac{\Theta}{T}\right)^5\frac{l_{\rm r}'}{l_{\rm ep}}\exp\,(\zeta/\boldsymbol{k}T)\Gamma(i+3/2)(\boldsymbol{k}T)^{i-1}, \quad . \quad . \quad . \quad (143)$$

$$\kappa_{eg}=-\frac{c_g\,l_{\rm i}^{(0)}}{32\,J_4}\left(\frac{2\pi\boldsymbol{k}T}{m}\right)^{1/2}\frac{l_{\rm r}'}{l_{\rm ep}}\left(\frac{\Theta}{T}\right)^5\exp\,(\zeta/\boldsymbol{k}T), \quad . \quad . \quad . \quad . \quad (144)$$

$$\boldsymbol{e}Q_g=-\frac{\pi c_g}{384\,J_4}\left(\frac{\boldsymbol{h}^2}{2\pi m\boldsymbol{k}T}\right)^{3/2}\frac{l_{\rm i}^{(0)}}{l_{\rm ep}}\left(\frac{\Theta}{T}\right)^5. \quad . \quad . \quad . \quad . \quad . \quad . \quad . \quad (145)$$

(iv) *Temperature range IIb*

$$\beta(\eta)=\frac{9\boldsymbol{h}\,u_0\,l_{\rm ep}\,D}{8\pi\,T\,\Lambda}\left(\frac{T}{\Theta}\right)^5\left(\frac{8\pi^2 m}{\boldsymbol{h}^2}\right)^{3/2}\exp\,(-\zeta/\boldsymbol{k}T)\,J_4, \quad . \quad (146)$$

where we have neglected a term of the order of $\Theta/T$,

$$c^{(b)}(\eta)=\frac{9\boldsymbol{h}\,u_0\,l_{\rm ep}\,D^2}{16\pi\,T\,\Lambda\,E^2}\left(\frac{T}{\Theta}\right)^7\left(\frac{8\pi^2 m}{\boldsymbol{h}^2}\right)^{3/2}J_4\exp\,(-\zeta/\boldsymbol{k}T), \quad . \quad (147)$$

$$L_i=\frac{1}{8}\,c_g l_{\rm ep}(\tfrac{1}{2}m\boldsymbol{k}T)^{-1/2}\Gamma(i-\tfrac{1}{2})(\boldsymbol{k}T)^{-1}, \quad . \quad . \quad . \quad . \quad . \quad . \quad (148)$$

$$\kappa_{eg}=-\frac{3}{8}\,c_g(\pi\boldsymbol{k}T/2m)^{1/2}l_{\rm ep}, \quad . \quad . \quad . \quad . \quad . \quad . \quad . \quad . \quad . \quad . \quad (149)$$

$$\boldsymbol{e}Q_g=-\frac{3\pi\,c_g}{16n}. \quad . \quad . \quad . \quad . \quad . \quad . \quad . \quad . \quad . \quad . \quad . \quad (150)$$

(v) *Temperature range IIIb*

$$\beta(\eta)=\frac{\hbar u_0 l_i^{(0)} D}{4\pi \Theta \Lambda}\left(\frac{8\pi^2 m}{\hbar^2}\right)^{3/2} I_0, \quad \ldots\ldots\ldots \quad (151)$$

$$c^{(b)}(\eta)=\frac{\hbar u_0 l_i^{(0)} D^2}{8\pi T \Lambda E^2}\left(\frac{T}{\Theta}\right)^3\left(\frac{8\pi^2 m}{\hbar^2}\right)^{3/2} I_0, \quad \ldots\ldots\ldots \quad (152)$$

$$L_i=\frac{c_g l_i^{(0)}}{36}\left(\frac{2}{mkT}\right)^{1/2}\left(\frac{\Theta}{T}\right)^4 \frac{I_0}{J_4}\exp(\zeta/kT)\,\Gamma(i-\tfrac{1}{2})(kT)^{i-1}, \quad (153)$$

$$\kappa_{eg}=-\frac{c_g l_i^{(0)}}{12}\left(\frac{\pi kT}{2m}\right)^{1/2}\frac{I_0}{J_4}\exp(\zeta/kT), \quad \ldots\ldots \quad (154)$$

$$eQ_g=-\frac{\pi c_g l_i^{(0)}}{48 l_{ep}}\left(\frac{h^2}{2\pi m kT}\right)^{3/2}\left(\frac{\Theta}{T}\right)^4\frac{I_0}{J_4}. \quad \ldots\ldots\ldots \quad (155)$$

(vi) *Temperature range IV*

$$\beta(\eta)=\frac{\hbar u_0 l_p D}{4\pi T \Lambda}\left(\frac{8\pi^2 m}{\hbar^2}\right)^{3/2}\left(\frac{T}{\Theta}\right)^5 I_4, \quad \ldots\ldots\ldots \quad (156)$$

$$c^{(b)}(\eta)=\frac{\hbar u_0 l_p D^2}{8\pi T \Lambda E^2}\left(\frac{T}{\Theta}\right)^7\left(\frac{8\pi^2 m}{\hbar^2}\right)^{3/2} I_4, \quad \ldots\ldots\ldots \quad (157)$$

$$L_i=\frac{c_g l_p}{36}\left(\frac{2}{mkT}\right)^{1/2}\frac{I_4}{J_4}\exp(\zeta/kT)\,\Gamma(i-\tfrac{1}{2})(kT)^{i-1}, \quad (158)$$

$$\kappa_{eg}=-\frac{c_g l_p}{12}\left(\frac{\pi kT}{2m}\right)^{1/2}\frac{I_4}{J_4}\exp(\zeta/kT) \quad \ldots\ldots\ldots \quad (159)$$

$$eQ_g=-\frac{\pi c_g l_p}{48 l_{ep}}\left(\frac{\hbar^2}{2\pi m kT}\right)^{3/2}\frac{I_4}{J_4}. \quad \ldots\ldots\ldots \quad (160)$$

Before we start the discussion of our results, we want to report briefly the results obtained for the case of metals, and also we wish to see whether or not eqn. (60) is approximately satisfied. This equation is not satisfied in the case of metals, since to the approximation used in our present paper $y=0$ for metals, while $L_i=0$ and $K(m,n)=K(n,m)$. We give therefore our results for metals including only an approximate value for the numerical coefficients involved. Our results were

$$eQ_g=-0{\cdot}3(c_g/n)(l_b/l_{ep}), \quad \ldots\ldots\ldots \quad \text{(range I)} \quad (161)$$

$$eQ_g=-0{\cdot}3c_g/n, \quad \ldots\ldots\ldots \quad \text{(range IIa)} \quad (162)$$

$$eQ_g=-0{\cdot}002(c_g/n)(l_i^{(0)}(l_{ep})(\Theta/T)^4, \quad \ldots\ldots \quad \text{(range IIIa)} \quad (163)$$

$$eQ_g=-0{\cdot}3c_g/n, \quad \ldots\ldots\ldots \quad \text{(range IIb)} \quad (164)$$

$$eQ_g=-0{\cdot}1(c_g/n)(l_i^{(0)}(l_{ep})(\Theta/T), \quad \ldots\ldots \quad \text{(range IIIb)} \quad (165)$$

$$eQ_g=-0{\cdot}05(c_g/n)(l_p/l_{ep})(\Theta/T). \quad \ldots\ldots \quad \text{(range IV)} \quad (166)$$

We may draw attention to the fact that eqns. (162) and (164) are, indeed, similar to the expressions derived in A, apart from the numerical factor and the sign. The different numerical factor arises from using Wilson's method of integration instead of the approximate one used in A and the different sign arises from our use of the Thomson coefficient instead of $Q$ (see Sondheimer 1956). The results are not sufficiently reliable for comparison with experimental data. As far as eqn. (60) is concerned, to a fair approximation $K(m, n)=K(n, m)$ as we saw in § 6 so that we must check whether or not

$$\mathrm{TL}\simeq -\boldsymbol{e}yK(\tfrac{3}{2}, \tfrac{3}{2}), \quad \text{or} \quad Q_g\simeq y/T. \quad . \quad . \quad . \quad . \quad (167)$$

Comparing the results of the present section with those of § 7, we see that eqn. (167) is, indeed, to a first approximation satisfied, apart from the occurrence of factors $(\Theta/T)$ in the low temperature cases I and IIIa. There are indications that these factors should not be present in a more satisfactory theory and we have therefore discarded them for the discussion in § 9.

## § 9. Discussion

We can now put all our results together using eqn. (61) for $\kappa$ and eqn. (57) for $Q$. We first of all notice that the expressions for $\kappa$ derived in § 8 are all of the same order of magnitude as the terms neglected in § 7, that is, they are small compared to the main contribution to $\kappa$. We shall therefore neglect $\kappa_{eg}$ in our discussion. As far as $\kappa_e$ and $Q_e$ are concerned, the correction terms are small compared to the main term in all cases of interest so that we shall also neglect those in the present section. We can now combine the results of §§ 6 to 9 as follows.

$$\kappa=10(n\boldsymbol{k})(\boldsymbol{k}T/m)^{1/2}l_{\mathrm{r}}'+0{\cdot}3c_gu_0l_{\mathrm{b}}, \quad . \quad . \quad . \quad . \quad . \quad \text{(range I)} \quad (168)$$

$$\kappa=10(n\boldsymbol{k})(\boldsymbol{k}T/m)^{1/2}l_{\mathrm{r}}'+1{\cdot}5c_gu_0l_{\mathrm{ep}}\exp(-\zeta/\boldsymbol{k}T), \quad . \quad \text{(range IIa)} \quad (169)$$

$$\kappa=10(n\boldsymbol{k})(\boldsymbol{k}T/m)^{1/2}l_{\mathrm{r}}'+0{\cdot}01c_gu_0l_i^{(\mathrm{av})}, \quad . \quad . \quad . \quad . \quad \text{(range IIIa)} \quad (170)$$

$$\kappa=(n\boldsymbol{k})(\boldsymbol{k}T/m)^{1/2}l_{\mathrm{ep}}+2{\cdot}3c_gu_0l_{\mathrm{ep}}\exp(-\zeta/\boldsymbol{k}T)(T/\Theta), \quad \text{(range IIb)} \quad (171)$$

$$\kappa=(n\boldsymbol{k})(\boldsymbol{k}T/m)^{1/2}l_{\mathrm{ep}}+0{\cdot}3c_gu_0l_{\mathrm{i}}^{(0)}, \quad . \quad . \quad . \quad . \quad . \quad \text{(range IIIb)} \quad (172)$$

$$\kappa=(n\boldsymbol{k})(\boldsymbol{k}T/m)^{1/2}l_{\mathrm{ep}}+0{\cdot}3c_gu_0l_{\mathrm{p}}, \quad . \quad . \quad . \quad . \quad . \quad . \quad \text{(range IV)} \quad (173)$$

$$\boldsymbol{e}Q=(\zeta/T)-4k-0{\cdot}001(c_g/n)(l_{\mathrm{b}}/l_{\mathrm{ep}})\exp(\zeta/\boldsymbol{k}T), \quad . \quad . \quad \text{(range I)} \quad (174)$$

$$\boldsymbol{e}Q=(\zeta/T)-4k-0{\cdot}2(c_g/n), \quad . \quad . \quad . \quad . \quad . \quad . \quad . \quad \text{(range IIa)} \quad (175)$$

$$\boldsymbol{e}Q=(\zeta/T)-4k-0{\cdot}001(c_g/n)(l_{\mathrm{i}}^{(\mathrm{av})}/l_{\mathrm{ep}})\exp(\zeta/\boldsymbol{k}T), \quad . \quad \text{(range IIIa)} \quad (176)$$

$$\boldsymbol{e}Q=(\zeta/T)-2k-0{\cdot}6(c_g/n) \quad . \quad . \quad . \quad . \quad . \quad . \quad . \quad \text{(range IIb)} \quad (177)$$

$$\boldsymbol{e}Q=(\zeta/T)-2k-0{\cdot}6(c_g/n)(l_{\mathrm{i}}^{(0)}/l_{\mathrm{ep}})\exp(\zeta/\boldsymbol{k}T), \quad . \quad \text{(range IIIb)} \quad (178)$$

$$\boldsymbol{e}Q=(\zeta/T)-2k-0{\cdot}1(c_g/n)(l_{\mathrm{p}}/l_{\mathrm{ep}})\exp(\zeta/\boldsymbol{k}T)(\Theta/T), \quad . \quad \text{(range IV)} \quad (179)$$

where we have only given approximate values of the numerical coefficients and where in eqns. (174) and (176) we have dropped the extra factors $\Theta/T$ in accordance with what we said at the end of § 8. In eqns. (170) and (176) $l_{\mathrm{i}}^{(\mathrm{av})}$ is the average phonon–impurity mean free path given by the equation

$$l_{\mathrm{i}}^{(\mathrm{av})}=l_{\mathrm{i}}^{(0)}(\Theta/T)^4. \quad . \quad . \quad . \quad . \quad . \quad . \quad (180)$$

First of all, we shall study the general temperature dependence of the various expressions. Assuming the number of impurities to be proportional to $n$, $l_r'$ is proportional to $T^2$, while $l_{ep}$ is proportional to $T^{-1}$ (see eqns. (89) and (81)). As long as we are not at too low temperatures, $n$ and $\zeta/T$ are practically constant. It follows that below the Debye temperature $\kappa_e$ is proportional to $T^{5/2}$ and above the Debye temperature $\kappa_e$ is proportional to $T^{1/2}$, while $Q_e$ varies only slowly with temperature (for its temperature variation we can refer to the papers by Johnson and Lark-Horovitz (1953), Lautz (1953) and Fukuroi and Tanuma (1952) and also a forthcoming survey article by Johnson). To study the temperature dependence of the lattice contributions we take $l_b$, $l_i^{(0)}$ and $u_0$ to be constant, $l_p$ and $l_{ep}$ to be proportional to $T^{-1}$, $c$ to be proportional to $T^3$ below $\Theta$ and to be constant above $\Theta$, $n$ and $\zeta/T$ to be connected through eqn. (80), and $n$ to be approximately constant. If we write $\kappa_g$ proportional to $T^r$ and $Q_g$ proportional to $T^s$ we get for $r$ and $s$ in the six temperature ranges under consideration

$$r_{\mathrm{I}}=3,\quad r_{\mathrm{IIa}}=7/2,\quad r_{\mathrm{IIIa}}=-1,\quad r_{\mathrm{IIb}}=3/2,\quad r_{\mathrm{IIIb}}=0,\quad r_{\mathrm{IV}}=-1\ ; \qquad (181)$$

$$s_{\mathrm{I}}=5/2,\ s_{\mathrm{IIa}}=3,\quad s_{\mathrm{IIIa}}=-3/2,\ s_{\mathrm{IIb}}=0,\quad s_{\mathrm{IIIb}}=-\tfrac{1}{2},\ s_{\mathrm{IV}}=-5/2. \qquad (182)$$

From eqns. (181) and (182) we see that both $\kappa_g$ and $Q_g$ should show a maximum and this has, indeed, been observed (see Rosenberg 1954, 1955, Estermann and Zimmerman 1952, Goff and Keesom 1954, and Frederikse 1953 for $\kappa_g$ [compare also Goldsmid 1956] and Frederikse 1953, Geballe and Hull 1954, 1955, Mooser and Woods 1955, Fukuroi *et al.* 1949 for $Q$). It is of interest to note that Rosenberg in a very high purity sample of germanium finds, indeed, an exponent larger than the usual 5/2, although the value of 4·4 found by him is much larger than any of the exponents mentioned in eqn. (181). Another point of interest in this connection is the dependence of $\kappa$ on $n$ : it is found to decrease with increasing number of carriers in accordance with eqn. (169). The region where the dependence on $n$ occurs is the same as the region where the maximun of $Q_g$ seems to occur and may thus well correspond to our temperature range IIa. This point needs further investigation, however, as in the case studied $n$ is so small as to practically exclude the possibility of phonon–electron scattering. We may refer to a paper by Ziman (1956). As far as the order of magnitude of $\kappa_g$ is concerned, using $\Theta=362°\mathrm{K}$ (Keesom and Pearlman 1953) and $a=3\text{Å}$, we find that at $20°\mathrm{K}$ for $n=10^{16}\,\mathrm{cm}^{-3}$ $l_{ep}$ should be $10^{-5}$ cm which does not seem to be unreasonable. At $20°\mathrm{K}$ we find that $\kappa_g/\kappa_e$ is of the order of 10 for $n=10^{16}\,\mathrm{cm}^{-3}$ and of the order of 1000 for $n=10^{15}\,\mathrm{cm}^{-3}$.

As to the thermoelectric power, we also find there an increase with decreasing $n$ as is to be expected. The qualitative agreement with the experimental data is quite satisfactory, but quantitatively, eqn. (175) gives values for $Q_g$ which are too large by about two orders of magnitude. At temperatures below $\Theta$, $Q_g$ dominates, but above $\Theta$, $Q_e$ is the larger, which is satisfactory since, as we mentioned earlier, at high temperatures

the theory of $Q_e$ can satisfactorily explain the observed behaviour of the thermoelectric power.

In conclusion we should like to discuss briefly the relation between the theory developed in the present paper and those of other authors. The theories of Klemens (1954) Parrott (1954) and MacDonald (1954) are qualitative and more closely related to a kinetic discussion (ter Haar 1956). Gurevich (1945) only deals with metals and with $Q_g$. He considers four temperature regions, two below and two above the Debye temperature and finds the exponent $s$ to have the values 1, 3, 1, $-1$ respectively while we find 4, 3, 0, $-1$ in rough agreement with his results, but not exactly the same. Our results are in direct contradiction to the opinion expressed by Pikus (1951) who claims that $Q_g$ will always be much smaller than $Q_e$. As his conclusion is based on some unpublished calculations according to which $l_{ep} \gg l_p$ it is difficult to see where Pikus' calculations go wrong, since they must have gone wrong somewhere as the experimental data indicate $l_{ep} \ll l_p$ at low temperatures, while Pikus claims $l_{ep} \gg l_p$ for $T > 3°K$.

Finally, we must say a few words about Herring's theory (1954). In his very elaborate analysis Herring uses what he calls the $\Pi$-approach, where one calculates the Peltier heat rather than the Seebeck effect. It seems to us that his approach does not satisfy the Onsager relations, as he assumes implicitly (e.g. on p. 1170) that one may use the equilibrium lattice distribution function in calculating the non-equilibrium carrier distribution function. He uses the quasi-free model, but discusses in an appendix some of the consequences of the many-valley model. It is difficult to make a closer comparison between his and our theories as he, of necessity, introduces a number of simplifying assumptions which are partly different from the simplifications introduced by us. One of his results, however, seems to be to us incorrect, namely, that the increase of $Q_g$ at about 20°K would not depend on $n$. This seems to us to be both in disagreement with Frederikse's experimental results and with the result obtained from a kinetic argument and we feel that our result (175) in the neighbourhood of the maximum—at any rate in so far as its dependence on $n$ is concerned—should be more reliable. His analysis goes much further than ours in also considering degenerate semiconductors, but our analysis is more elaborate, we feel, in its discussion of the various scattering mechanisms.

After this paper was written, Dr. V. A. Johnson of Purdue University kindly sent us a preprint of a review article on the Seebeck effect in semiconductors which will be published shortly. Her approach is more closely related to that by Herring than to ours ; moreover, she is mainly concerned with $Q_e$.

ACKNOWLEDGMENTS

We should like to express our thanks to Dr. H. P. R. Frederikse for drawing our attention to this problem and putting his experimental data at our disposal prior to publication, to Dr. K. Lark-Horovitz for discussions and information about the work of the Purdue Semiconductor Group,

to Dr. E. H. Sondheimer for comments on our theory and for communicating to us his considerations on the Kelvin relations before publication, to Dr. H. J. Zeiger for informing us about the work in progress at M.I.T. on the many-valley semiconductors, and to the Department of Scientific and Industrial Research for the award of a maintenance grant to one of us (A. N.).

## References

Anselm, A. I., 1951, *J. Tech. Phys. U.S.S.R.*, **21,** 489.
Bontsch-Brujewitsch, W. L., 1955, *Fortschr. Phys.*, **3,** 408.
Conwell, E., and Weisskopf, V. F., 1950, *Phys. Rev.*, **77,** 388.
Dexter, R. N., Zeiger, H. J., and Lax, B., 1954, *Phys. Rev.*, **95,** 557.
Estermann, I., and Zimmerman, J. E., 1952, *Bull. Inst. Internat. Froid*, p. 33.
Frederikse, H. P. R., 1953, *Phys. Rev.*, **92,** 248.
Fröhlich, H., 1936, *Elektronentheorie der Metalle* (Berlin : Springer).
Fröhlich, H., and Kittel, C., 1954, *Physica*, **20,** 1086.
Fukuroi, I., and Tanuma, S., 1952, *Sci. Rep. Res. Inst. Tôhoku Univ.*, **A4,** 353.
Fukuroi, I., Tanuma, S., and Tobisawa, S., 1949, *Sci. Rep. Res .Inst. Tôhoku Univ.*, **A1,** 373.
Geballe, T. H., 1953, *Phys. Rev.*, **92,** 857.
Geballe, T. H., and Hull, G. W., 1954, *Phys. Rev.*, **94,** 1134 : 1955, *Ibid.*, **98,** 940.
Goff, J., and Keesom, P. H., 1954, *Purdue University Semi-conductor Group, Final Report* (unpublished).
Goldsmid, H. J., 1955, *Journ. Electronics*, **1,** 218 : 1956, *Proc. Phys. Soc.* B, **69,** 203.
Goldsmid, H. J., and Douglas, R. W., 1954, *Brit. J. Appl. Phys.*, **5,** 386, 458.
Groot, S. R. de, 1951, *Thermodynamics of irreversible processes* (Amsterdam : North Holland Publishing Co.).
Gurevich, L., 1945, *J. Phys. U.S.S.R.*, **9,** 477.
Haar, D. ter, 1954, *Elements of statistical mechanics* (New York : Rinehart) ; 1956, *Physica*, **22,** 61.
Haar, D. ter, and Neaves, A., 1954, *Physica*, **20,** 995 ; 1955, *Proc. Roy. Soc.* A, **228,** 568.
Herring, C., 1953, *Phys. Rev.*, **92,** 857 ; 1954 a, *Ibid.*, **95,** 954 ; 1954 b, *Ibid.*, **96,** 1163 ; 1955, *Bell Syst. Tech. J.*, **34,** 337.
Hulst, H. C. v. d., 1946, *Recherches Astron. de l'Observ. d'Utrecht*, **11,** no. 1.
Hung, C. S., 1950, *Phys. Rev.*, **79,** 727.
James, H. M., 1949, *Phys. Rev.*, **76,** 1611.
Joffe, A. F., 1952, *Dokl. Acad. Nauk, U.S.S.R.*, **87,** 369.
Johnson, V. A., and Lark-Horovitz, K., 1947, *Phys. Rev.*, **71,** 374 ; 1953, *Ibid.*, **92,** 226.
Keesom, P. H., and Pearlman, N., 1953, *Phys. Rev.*, **91,** 1347.
Keesom, W. H., 1913, *Leiden Commun.*, Suppl. 30b.
Klemens, P. G., 1951, *Proc. Roy. Soc.* A, **208,** 108 ; 1954, *Austral. J. Phys.*, **7,** 520.
Lark-Horovitz, K., Middleton, A. E., Miller, P. E., Scanlon, W. W., and Walerstein, I., 1946, *Phys. Rev.*, **69,** 259.
Larsen, H. D., 1948, *Rinehart mathematical tables, formulas and curves* (New York : Rinehart).
Lautz, G., 1953, *Z. Naturforsch.*, **8a,** 361.
Lax, B., Zeiger, H. J., and Dexter, R. N., 1954, *Physica*, **20,** 818.

Lax, B., and Mavroides, J. G., 1955, *Phys. Rev.*, **100**, 1650.
Lorentz, H. A., 1905, *Arch. Néerl. Sci.*, **10**, 336 ; 1909, *The theory of electrons* (Leipzig : Teubner).
MacDonald, D. K. C., 1954, *Physica*, **20**, 996.
Makinson, R. E. B., 1938, *Proc. Camb. Phil. Soc.*, **34**, 474.
Middleton, A. E., and Scanlon, W. W., 1953, *Phys. Rev.*, **92**, 219.
Mooser, E., and Woods, S. B., 1955, *Phys. Rev.*, **97**, 1721.
Parrott, J. E., 1954, *Proc. Phys. Soc.* B, **67**, 587.
Peckar, S., 1946, *J. Phys. U.S.S.R.*, **10**, 431.
Peierls, R. E., 1929, *Ann. Phys.*, **3**, 1055 ; 1955, *Quantum theory of solids* (Oxford : University Press).
Pikus, G. E., 1951, *J. Exp. Theor. Phys. U.S.S.R.*, **21**, 852.
Pines, D., 1955, *Adv. Solid State Phys.*, **1**, 368.
Price, P. J., 1954, *Phys. Rev.*, **95**, 596 ; 1955, *Phil. Mag.*, **46**, 1192.
Rosenberg, H. M., 1954, *Proc. Phys. Soc.* B, **67**, 587 ; 1955, *Proc. Paris Low Temp. Con.*, No. 89.
Ross, I. M., and Saker, E. W., 1955, *Journ. Electronics*, **1**, 223.
Saker, E. W., Cunnell, F. A., and Edmond, J. T., 1955, *Brit. J. Appl. Phys.*, **6**, 217.
Samoilowitsch, A. G., and Korenblit, L. L., 1954, *Fortschr. Phys.*, **1**, 486.
Seitz, F., 1940, *The modern theory of solids* (New York : McGraw-Hill).
Slater, J. C., 1949, *Phys. Rev.*, **76**, 1592.
Sommerfeld, A., 1928, *Z. Phys.*, **47**, 1.
Sommerfeld, A., and Bethe, H. A., 1933, *Handb. Phys.*, **24** (2), 333.
Sondheimer, E. H., 1956, *Proc. Roy. Soc.* A, **234**, 391.
Wilson, A. H., 1931, *Proc. Roy. Soc.* A, **133**, 458 ; 1937, *Proc. Camb. Phil. Soc.*, **33**, 371 ; 1953, *The theory of metals* (Cambridge : University Press), 2nd Edn.
Wonssowski, S. W., 1954, *Fortschr. Phys.*, **1**, 239.
Zeiger, H. J., 1955, *Phys. Rev.*, **98**, 1560.
Ziman, J. M., 1956 *Phil. Mag.*, **1**, 191.

Fig. 5

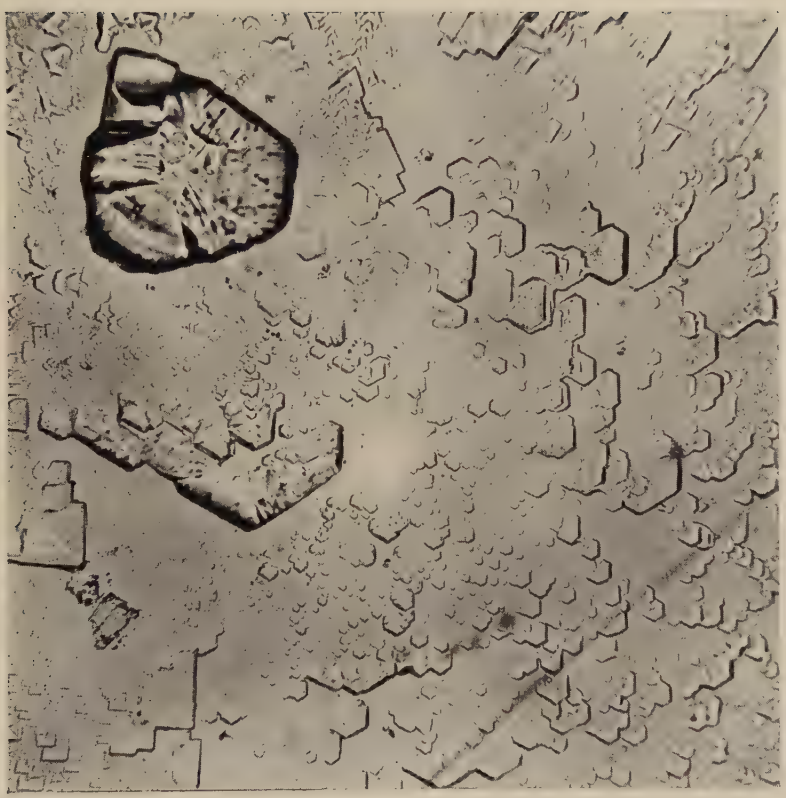

Oriented hexagonal-based crystallites of sodium chloride upon mica.

Fig. 6

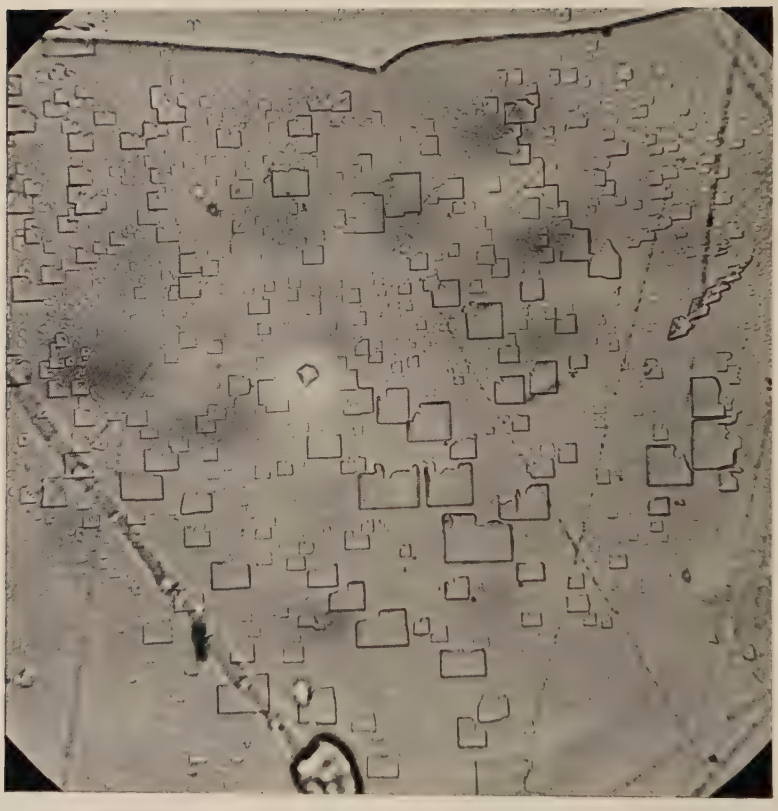

Oriented square-based crystallites of potassium bromide upon mica.

Fig. 11

Oriented silver bromide upon a silver (111) surface. Asymmetrical intensity distribution about central line indicates pronounced single positioning. Ag [$1\bar{1}0$] azimuth.

Fig. 13

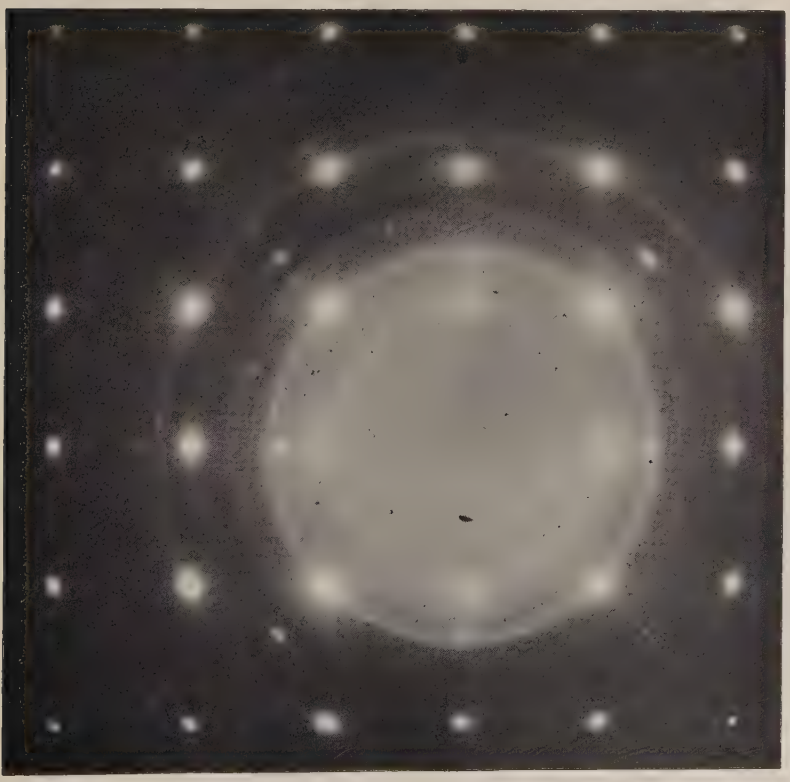

Pattern from a (100) film of silver chloride showing the formation of oriented silver during electron bombardment.

Fig. 17

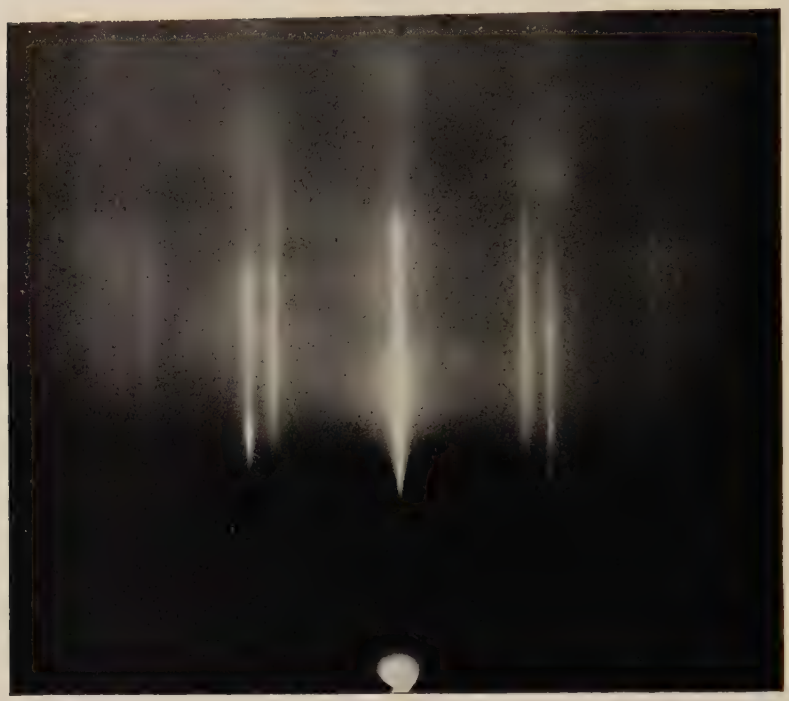

A layer of about 2 Å of lead on an atomically flat (111) silver surface. Ag [110] azimuth.

Fig. 18

A layer of about 2 Å of copper on an atomically flat (111) silver surface. Ag [1$\bar{1}$0] azimuth. Diffuse copper spots appear just outside vertical streaks due to silver.

Fig. 19

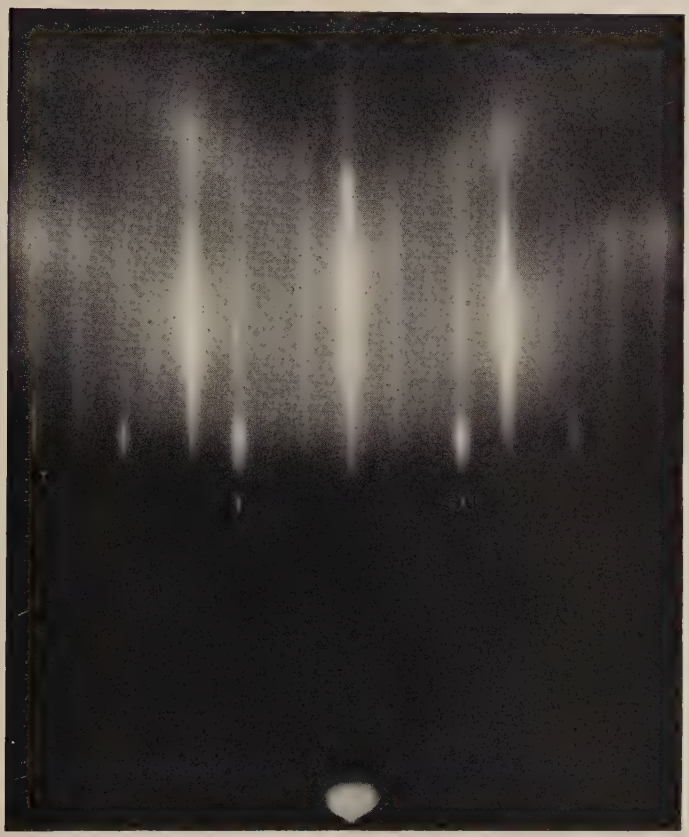

A layer of about 2 Å of silver bromide on an atomically flat (111) silver surface. Ag [$1\bar{1}0$] azimuth. Spots due to bromide ; vertical streaks due to silver and to secondary diffraction.

Fig. 21

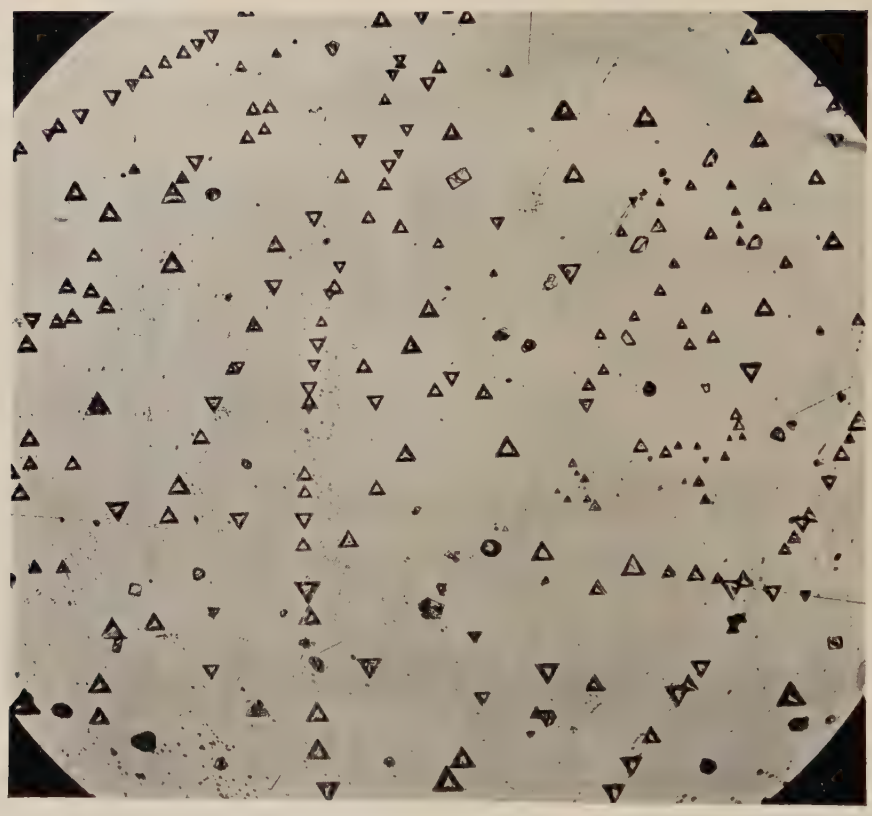

Oriented triangular-based pyramids of ammonium iodide upon mica.

Fig. 22

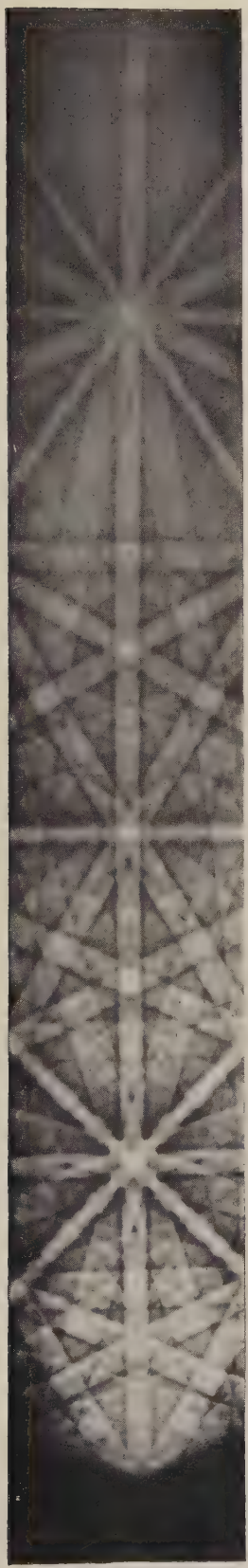

High angle Kikuchi line pattern from an oriented silver layer on mica.
Mica [100] azimuth.

Fig. 23

Silver bromide layer on a (110) silver surface. AgBr [1$\bar{1}$0] azimuth.

Fig. 24

As for fig. 23 except AgBr [001] azimuth.

Fig. 29

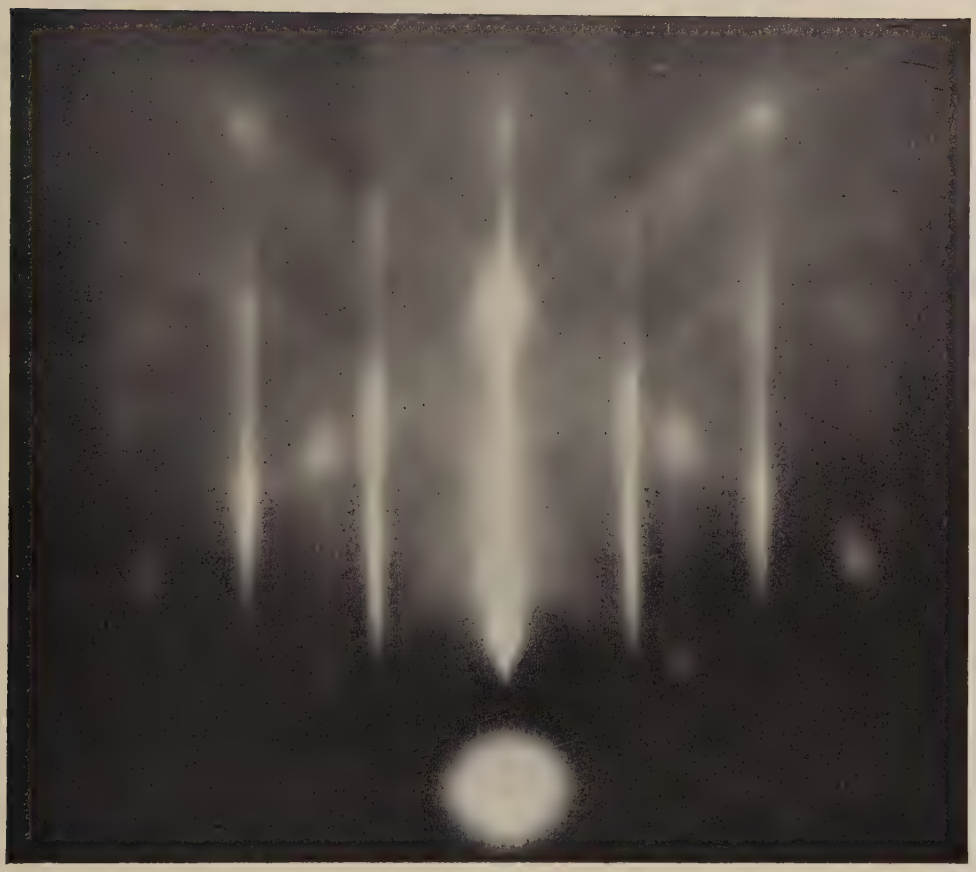

A layer of about 2 Å of silver on a heated rocksalt surface. NaCl [011] azimuth.

Fig. 30

As for fig. 29 except silver thickness of about 20 Å.

Fig. 31

As for fig. 30 except silver thickness of about 150 Å.

# *Journal of Fluid Mechanics*



## *Contents of July, 1956*



**Price per part £1**

**Price per annum £5 10s. post free**

*Printed and Published by*

TAYLOR & FRANCIS LTD

RED LION COURT, FLEET STREET, LONDON, E.C.4

# *The Philosophical Magazine*

**First Published in 1798**

*Editor:*
PROFESSOR N. F. MOTT, M.A., D.Sc., F.R.S.

*Editorial Board:*
SIR GEORGE THOMSON, M.A., D.Sc., F.R.S.
PROFESSOR A. M. TYNDALL, C.B.E., D.Sc., F.R.S.
SIR LAWRENCE BRAGG, O.B.E., M.C., M.A., D.Sc., F.R.S

## *Contents of June, 1956*



**Price per part 15s.**
**Price per annum £8 post free**

*Printed and Published by*

TAYLOR & FRANCIS LTD

**RED LION COURT, FLEET STREET, LONDON, E.C.4**

## *Contents of July, 1956*



**Subscription price per volume £3 10s. post free,** *payable in advance*

4 parts per volume—£1 per part

Printed and Published by

TAYLOR & FRANCIS LTD

RED LION COURT, FLEET STREET, LONDON, E.C.4

# *Journal of Electronics*

**A Philosophical Magazine Associated Journal**

***Devoted to Electron Sciences***



## *Contents of May, 1956*



**Price per part £1**

**Price per annum £5 10s. post free**

*Printed and Published by*

TAYLOR & FRANCIS LTD

RED LION COURT, FLEET STREET, LONDON, E.C.4

# Annals of Science

A QUARTERLY REVIEW OF THE HISTORY OF SCIENCE SINCE THE RENAISSANCE





# THE MATHEMATICAL WORKS OF JOHN WALLIS, D.D., F.R.S.

*by*

## J. F. SCOTT, Ph.D., B.A.

"His work will be indispensable to those interested in the early history of The Royal Society. I commend to all students of the Seventeenth Century, whether scientific or humane, this learned and lucid book."—Extract from foreword by Prof. E. N. da C. Andrade, D.Sc., Ph.D., F.R.S.

**Recommended for publication by University of London**

**12/6** net


*Printed and Published by*

**TAYLOR & FRANCIS, LTD.**

RED LION COURT, FLEET STREET, LONDON, E.C.4.

# Early Scientific Publications


## DIARY OF ROBERT HOOKE, M.A., M.D., F.R.S.
1672-1680

Edited by **H. W. ROBINSON** and **W. ADAMS**
**Recommended for publication by the Royal Society, London**

**25/-**
net

"This vivid record of the scientific, artistic and social activities of a remarkable man during remarkable years has too long remained in obscurity."—Extract from foreword by Sir Frederick Gowland Hopkins, O.M., President of the Royal Society.

## MATHEMATICAL WORK OF JOHN WALLIS, D.D., F.R.S.

By **J. F. SCOTT, Ph.D., B.A.**

**12/6**
net

"His work will be indispensable to those interested in the early history of The Royal Society. I commend to all students of the Seventeenth Century, whether scientific or humane, this learned and lucid book."—Extract from foreword by Prof. E. N. da C. Andrade, D.Sc., Ph.D., F.R.S.
**Recommended for publication by University of London**

## CORRESPONDENCE AND PAPERS OF EDMOND HALLEY

Arranged and Edited by **EUGENE FAIRFIELD MACPIKE**

**21/-**
net

First published on behalf of The History of Science Society by Oxford University Press. Now re-issued by Taylor & Francis, Ltd.

## MEMOIRS OF SIR ISAAC NEWTON'S LIFE

**5/-**
net

By **WILLIAM STUKELEY, M.D., F.R.S., 1752**
From an Original Manuscript
Now in the possession of the Royal Society, London

## HEVELIUS, FLAMSTEED AND HALLEY

**12/6**
net

Three Contemporary Astronomers and their Mutual Relations
By **EUGENE FAIRFIELD MACPIKE**
**Published by arrangement with The History of Science Society**

Established
over 150 years

**TAYLOR & FRANCIS, LTD.**
**RED LION COURT, FLEET ST., LONDON E.C.**
**PRINTERS & PUBLISHERS OF SCIENTIFIC BOOKS**